Crystallographic Studies on Integral Membrane Light Harvesting Complexes From Photosynthetic Bacteria

Karen McLuskey

Submitted in part fulfilment for the degree of Doctor of Philosophy

Department of Chemistry

University of Glasgow

January 1999

ProQuest LLC.
789 East Eisenhower Parkway
P.O. Box 1346
Ann Arbor, MI 48106 – 1346

What doesn't kill me makes me stronger

Frederick Nietzeche (1844-1900)

This thesis is dedicated to my parents, James and Annette;

My first and lasting inspiration.

ABSTRACT

The three dimensional crystal structure of the B800-820 light harvesting complex, an integral membrane pigment-protein complex, from the photosynthetic bacterium *Rhodopseudomonas acidophila* strain 7050, has been determined to a resolution of 2.8Å.

This thesis outlines the processes by which the structure was solved; gives an initial comparison between it and the crystal structure of the B800-850 LH complex from *Rhodopseudomonas acidophila* strain 10050[1]; and suggests reasons for the observed spectroscopic differences between the two complexes.

Additionally, biochemical investigations performed on a further three light harvesting complexes are described, and a novel spectroscopic method for monitoring the purity of the complexes is introduced.

Acknowledgements

I would like to begin by thanking my supervisors Neil Isaacs and Richard Cogdell. Together they have provided me with a great deal of support, faith, encouragement and the infectious enthusiasm and calming influence that every Ph. D. student should have. I would also like to thank Neil for allowing me to torment him with the crystallography questions that tormented me; for arranging the final stages of my thesis so quickly; and for looking as if he believed me every time I set myself a new deadline. I am also very grateful to Richard for "pulling" me through the times when the bugs were misbehaving and for reading through the rough, no the ragged drafts of this manuscript; no supervisor deserves that.

Along with Neil and Richard I am deeply grateful to "my post-doc" Stephen Prince. Steve provided many of the ideas behind this work (after numerous attempts to make me think for myself) and has taught me a great deal, with enormous patience, not only about this project, but about various aspects of science in general.

I am also very much indebted to "Young" John Mclean, who may take offense as not being referred to as "Lard" when reading this (I didn't think it was appropriate). John is my crystallography hero! Without his support and endless patience I might have broken as many computers as I did fish tanks (a story for another time perhaps); he has answered manymanymany questions (not always different); responded to my whingeing with do-nuts; and turned a conundrum of scientific words into what has now become this thesis.

I would also like to thank Dina Fotinou for her overwhelming generosity. Dina has freely shared a huge amount of her time and knowledge, and has offered me much encouragement and support throughout this project. Along with Dina, I would like to thank Paul Emsley for his part in my "Editorial support team" and for dragging me slightly further away from my Windows environment. Together Dina and Paul have supplied me with numerous meals and have provided a top quality bed and breakfast service on many occasions, that I highly recommend. I would also like to say thank you to Tina Howard for reading through some of the initial drafts of this work, for listening to my many ramblings and for, being able to, keep me calm.

I would also like to express my sincere appreciation to Gerry McDermott, who introduced me

to the project and is partly responsible for where I am now. Gerry has been a constant mentor from a distance of two, and now six thousand miles, proving that you can run but you just can't hide from questions about the bugs.

Along with the people mentioned above I am in debt to a huge amount of people in Glasgow for their friendship and support throughout this project. These people have helped me and provided me with numerous things ranging from inspiration to food supplies at 1.30 am. They are (in no order at all): Peter, Chris E, Stuart M, Paulene, Andy, Adrian, Aleks, Isobel, Russell, Jeremy, Katherine, John Coggins, Gordon, Lindsay, Joanne, Jennifer, Iain, Tino, Evelyn, Stuart B, Niall, Chris L, Tanweer, Marie, Neil H, Wille, Betty, Derek, James, Margaret, Paul and probably many others that I have forgotten, sorry.

Out with work I would just like to thank a few special people, without whom I would have been far less sAnE today, they are: Maria McGraw, Tracy Devlin, Lesley McDermott, Lorraine Gibson and Roisin Lochrin. These 'guys' have been there for me unconditionally over the last few years; I hope they know what they mean to me and I'd just like to say how much I appreciate them. I'd also like to thank Phil for being a star and for putting up with me over the last few months (and for not running away screaming!).

I'd also like to thank the brother-thing (James) for the beer he WILL be buying me and "my wean" the sister-thing (Claire) for putting up with all my horrible ways; I realise I'm not the easiest person to live with. Finally, I'd like to thank my parents for all of their love, support and guidance throughout my academic career. I couldn't have started this without them and I most certainly wouldn't have finished it. Unfortunately, I can't promise that I'll get a "real" job now!

Contents

Abbreviations

Å	Angstrom 10^{-10} m
Ac	Acetate
AML	Artificial Mother Liquor
AMS	Ammonium Sulphate
B	Bulk (with reference to bacteriochlorophyll pigments)
BA	Benzamadine hydrochloride
BChl	Bacteriochlorophyll
β-OG	β-octyl-glucopyranoside
CCP4	Collaborative Computational Project number 4
CMC	Critical Micelle Concentration
CSD	Cambridge Structural Database
FPLC	Fast Liquid Protein Chromatography
LH	Light Harvesting
LH1	Core light harvesting complex
LH2	Peripheral light harvesting complex
LDAO	Lauryl-DimethylAmine N-Oxide
*k*D	kiloDaltons
KP_i	di-Potassium hydrogen phosphate
MR	Molecular Replacement
MS	Mass Spectrometry
NCS	Non Crystallographic Symmetry
NIR	Near Infra Red
ps	pico-second (10^{-12})
OD	Optical Density
RpalG	Rhodopinal glucoside
RpG	Rhodopin glucoside
RC	Reaction Centre
Rb.	*Rhodobacter*
Rps.	*Rhodopseudomonas*
Rs.	*Rhodospirillum*
Tris	Tris-hydroxymethyl-aminomethane

1. INTRODUCTION.

1.1 Photosynthesis

We obtain all of our energy from the plant kingdom, either directly or through herbivorous animals. Plants in turn obtain all of their energy directly from sunlight. Sunlight is a pure but not very useful form of energy; it cannot be eaten, it cannot be used to drive mechanical processes and it cannot be stored for later use. In order to make use of this energy source the sunlight must be converted into other forms. The transformation of this energy into useful products occurs by photosynthesis in which sunlight provides the energy to convert carbon dioxide and water into oxygen and carbohydrates. Plants use the energy stored in these carbohydrates as a food source and are consequently known as autotrophs or self-feeders. Autotrophs are also found in the bacterial kingdom.

The basic reaction for plant photosynthesis is frequently written as:

$$6H_2O + 6CO_2 + light \rightarrow C_6H_{12}O_6 + 6O_2 \tag{1.1}$$

because glucose, a six carbon sugar, is often an intermediate product of the photosynthetic reactions. This process is the net result of an oxidative and a reductive process: water is oxidised and electrons are transferred along with the hydrogen ions to the carbon dioxide, reducing it to sugar.

The above equation is deceptively simple and photosynthesis is usually described as two separate processes: the *photo* process, known as the light reactions, and the *synthesis* process, known as the dark reactions (or the Calvin cycle). The light reactions are responsible for the capture and storage of light energy (producing oxygen gas as a by-product). Energy is stored in the form of chemical bonds in molecules such as the reduced form of nicotinamide adenine dinucleotide phosphate (NADPH) and energy rich adenosine triphosphate (ATP). These molecules transfer their high energy cargo on to the Calvin cycle and complement each other: NADPH serves as a source of energised electrons (providing "reducing power" for the Calvin cycle) whilst ATP provides a rich source of chemical energy.

During the Calvin cycle chemical energy is stored in the form of carbohydrates and is later utilised by higher organisms in the food chain. The Calvin cycle or the dark reactions do not require the presence of light to proceed but require both ATP and NADPH produced by the preceding light reactions.

The photosynthetic light reactions excel in speed and efficiency and there is the potential to use knowledge gained from these primary reactions in the development of highly efficient man-made solar energy systems. The reason for this is that although the overall photosynthetic process generally stores only 8% of the light absorbed as chemical energy, the early steps which involve the capture and transfer of the solar energy are highly efficient with a quantum yield of 90% or higher[2]. If this light harvesting system could be mimicked outwith nature the potential for using solar energy on a large scale would be enormous.

1.2 Photosynthetic bacteria

Photosynthetic bacteria are widely used in photosynthetic research because the processes which occur within them broadly correspond to parallel processes in higher plants, but their photosynthetic machinery is simpler than the corresponding apparatus in higher plants.

Photosynthetic bacteria can be divided into 4 different groups: the cyanobacteria, the purple bacteria, the green bacteria and the heliobacteria. However, it is only the cyanobacteria which have the ability to evolve oxygen like their higher plant relatives. Such bacteria are thought to have existed for over 3 billion years, making them the first oxygen evolving organisms on earth[3]. Other types of photosynthetic bacteria are incapable of extracting electrons from H_2O and are thus known as anoxygenic phototrophs. They use light energy to extract electrons from organic or inorganic electron donors (including elemental hydrogen). Where the electron donor is an organic compound it may serve as the carbon source. A comparison of bacterial and plant photosynthesis lead to C. B. van Neil proposing the generalised equation for photosynthesis[4]:

$$2H_2A + CO_2 + light \rightarrow (CH_2O) + 2A + H_2O \tag{1.2}$$

Where H_2A is the electron donor.

1.2.1 Purple bacteria

The photosynthetic apparatus and reactions of the purple bacteria have been studied more extensively than those of any other species of photosynthetic bacteria[5]. The purple bacteria are divided into two separate groups: the sulphur bacteria (Chromatiaceae) which have the ability to use sulphur as the primary electron donor; and the non-sulphur bacteria (Rhodospirillaceae) which lack this ability. The purple non-sulphur bacteria typically use an organic electron donor, such as succinate or malate, and in contrast to the sulphur bacteria they have the interesting ability to survive aerobically in the dark by respiration[6]. However, as the cells become anaerobic they switch to their

photosynthetic mode of growth and their cell membranes become extensively infolded into the cytoplasm. The structure of the invaginations varies, and has been used as a basis for classification of the bacteria[7].

All of the equipment required for the light reactions of photosynthesis are found in and along these invaginated membrane structures[8]. The membrane infolds are thought to provide a large surface area to volume ratio, which allows the membrane to accommodate the extra components required for photosynthesis[8]. In photosynthetic bacteria, pigment molecules act as both energy and electron carriers and are bound to protein structures through highly specific binding sites, which moderate the rate and pathway of the transfers involved[6]. More specifically, there are two functionally distinct types of integral membrane pigment-protein complexes which comprise the so-called photosynthetic unit (PSU) of purple bacteria:

- **The Reaction Centre** (RC):which carries out photochemical redox reactions by functioning as a light-driven electron pump across the photosynthetic membrane.
- **Light Harvesting antenna complexes** (LH complexes): which capture and transfer solar radiation to the reaction centre.

1.3 The bacterial reaction centre

In 1985 the publication of the X-ray crystallographic structure of the reaction centre from the bacterium *Rhodopseudomonas viridis*[9] gave photosynthesis a new and exciting dimension. Researchers now had a model with which to interpret a large body of existing experimental data and an entity which would allow them to begin explaining mechanism and function in relation to the structure. Along with its importance in photosynthesis, this structure was a landmark event in the field of protein crystallography and resulted in Deisenhofer, Michel and Huber being awarded the Nobel prize for chemistry in 1988. In a series of published Nobel lectures Johann Deisenhofer and Hartmut Michel describe in detail various aspects of the importance of the reaction centre structure[10]. These lectures are on a range of related topics such as the crystallisation, structure determination and structure-function relationship of the RC, the relationship to Photosystem II, and various other aspects of membrane protein crystallisation. This section aims to give a brief

overview of the reaction centre complex.

1.3.1 Structural aspects

The reaction centre from *Rps. viridis* (Figure 1.1) consists of a series of pigment molecules within three protein subunits: the light (L), the medium (M) and the heavy (H) chains (so called because of their apparent molecular weights as determined by gel electrophoresis[11]). The apoproteins bind two bacteriochlorophyll *b* (Bchl *b*) which make up the so-called "special pair", a further two "accessory" Bchl *b*, two bacteriopheophytin *b* (Bphe *b*), two quinones (Q_A and Q_B), one non-heme iron and a carotenoid molecule[9]. In this species of bacteria the reaction centre also has a tightly bound molecule of cytochrome c.

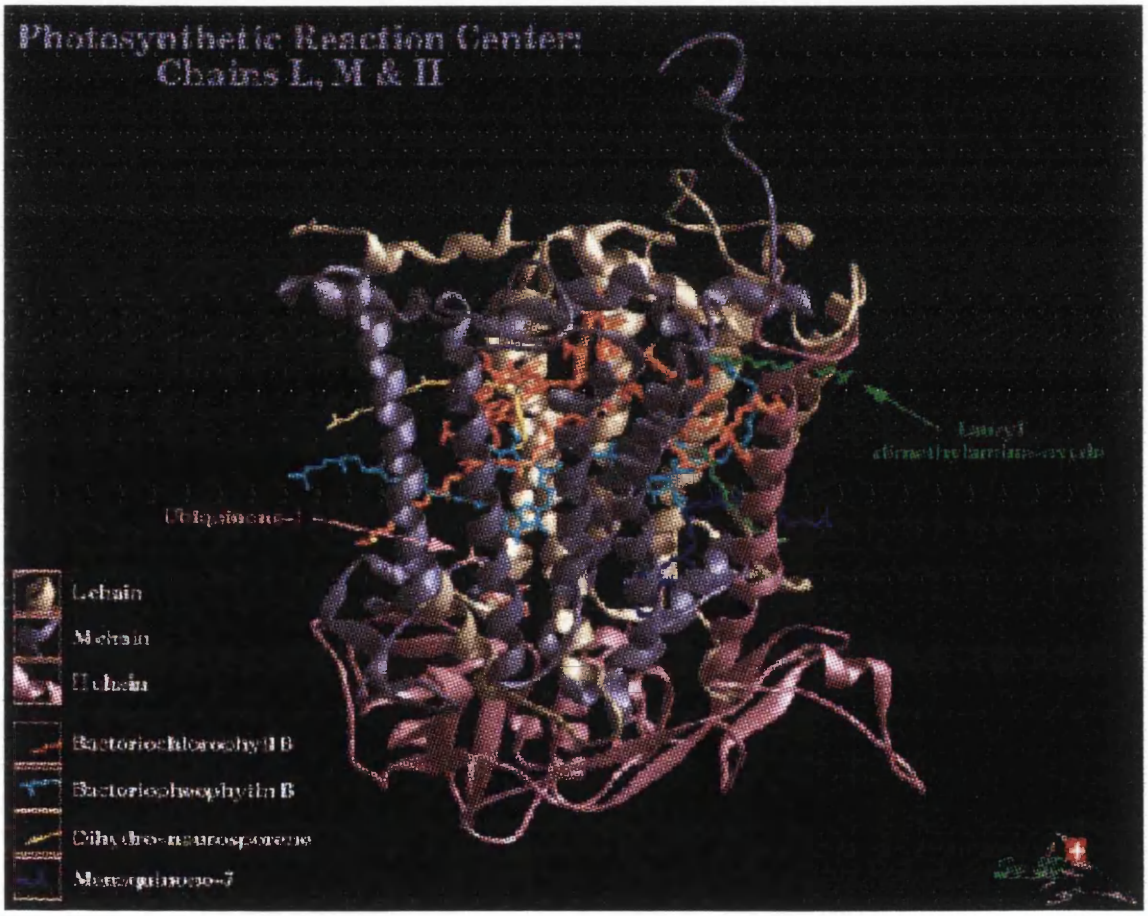

Figure 1.1: The photosynthetic reaction centre from *Rps.viridis*[9]

The pigments are found within a protein cage composed of the L and M subunits, each of which contains a 5 α-helical transmembrane domain. The H subunit contains a single membrane spanning helix and is not involved directly in the accommodation of the pigment molecules. It is instead thought to maintain stability and keep the RC in the proper functional orientation in the membrane[12]. The chromophores are arranged in two symmetrical arms within the protein cage with only the carotenoid molecule breaking the pseudo two fold symmetry (Figure 1.2). Although the two arms appear symmetric, electron transfer is known only to proceed along one branch branch, which comprises one half of the special pair, one accessory Bchl *b*, one Bphe *b* and Q_A. The reason for the functionally redundant pigments is unclear and the phenomenon has been the subject of much study to date, using both site directed mutagenesis and crystallography.

1.3.2 Function and mechanism

The reaction centre functions as a light-driven proton pump, creating a proton gradient across the cell membrane, with the special pair of Bchl *b* molecules providing the starting point for the process. The energy pathway has been detailed by Deisenhofer & Michel[13] and will only be covered briefly. Initial energy is absorbed by the exciton coupled special pair of Bchl *b* molecules and an electron is transferred from these molecules to a neighbouring acceptor Bchl *b* molecule. Subsequent electron transfer reactions proceed down one arm of the reaction centre resulting in the reduction of Q_A, before the electron crosses onto Q_B which resides on the other pigment branch. The process is complete after the second of two electron transfers results in the formation of doubly reduced Q_B. This molecule then picks up protons from the cytoplasm and is released from the reaction centre into the surrounding membrane, with the site being refilled from a pool of dissolved quinones in the membrane. The net effect of the entire light-driven electron flow is the generation of a proton gradient across the membrane by the net movement of two protons from the cytoplasm to the periplasm.

1.4 Bacterial light harvesting

Photosynthetic light harvesting complexes are the pigment-protein complexes responsible for gathering the solar energy required by the reaction centre. In purple bacteria, the minimal size

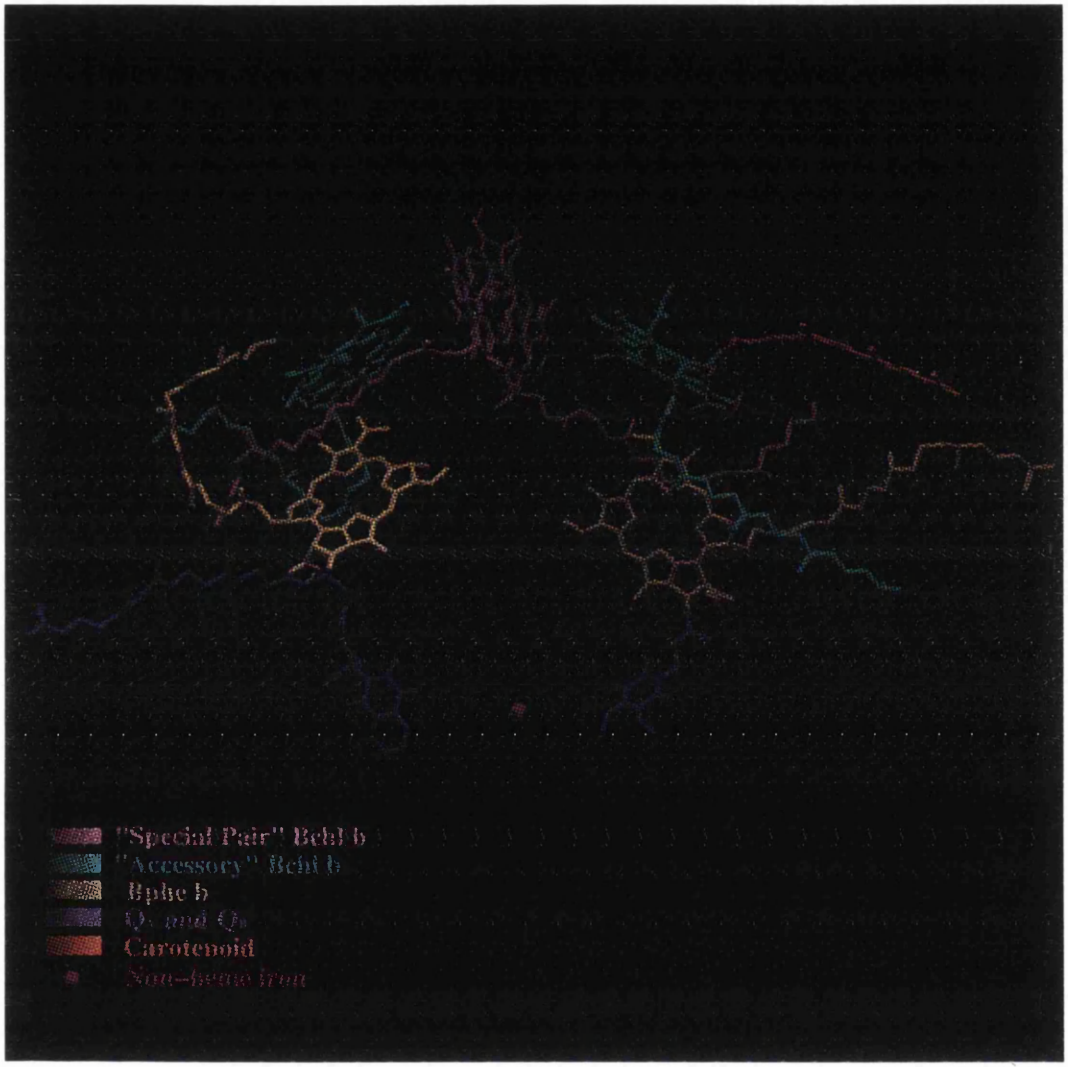

Figure 1.2: The pigment arrangement in the photosynthetic reaction centre from *Rps.viridis*

of the of PSU is that of the reaction centre and the core light harvesting (LH1) complex which is present in all species of bacteria. This basic unit comprises the so-called "core" complex of the PSU. In species such as *Rhodospirillum rubrum* and *Rps. viridis*, LH1 is the sole LH complex synthesised[5]. However, in most species of purple bacteria an additional light harvesting (LH2) complex is produced to increase the light harvesting potential[5]. LH2 is often called the "peripheral" light harvesting complex as it is found around the periphery of the core complex. Together, these pigment-protein complexes function as a regulated energy uptake and transfer system[14].

1.4.1 Structural similarities

The light harvesting antenna complexes of purple bacteria have been extensively characterised by a variety of spectroscopic and biochemical methods (see Zuber[15] for a review) with the results showing that light harvesting complexes are based on the same modular principle and exhibit a set of general features[15, 5]:

- All types of light harvesting complex are composed of two[i] low molecular weight apoproteins (with molecular weights in the region of 5 to 7 kDa[17]), denoted α and β[18].
- The analogous apoproteins in LH1 and LH2 exhibit sequence homology and are structurally related.
- All of the apoproteins contain a central hydrophobic span of about 20-23 amino-acids that form α-helices with hydrophilic N- and C-terminal domains.
- The hydrophobic domain of the apoproteins is predicted to constitute the membrane spanning region.
- The apoproteins non-covalently and stoichiometrically bind the pigment molecules Bchl *a* and carotenoid.
- The intact antenna complexes are oligomers of the apoprotein pairs with their associated pigment moieties.

[i] In some species of bacteria, LH2 complexes are found to contain multiple types of α- & β-polypeptide[16].

1.4.2 Light harvesting pigments

In the light harvesting complexes of purple bacteria the pigment molecules Bchl *a* and carotenoid are both found. The major function of the pigments is as light harvesters: collecting the required solar energy and rapidly transferring it to the reaction centre. Bchl *a* is the major light harvesting pigment with the carotenoids participating in light harvesting whilst providing other additional functions.

1.4.2.1 The carotenoids

The carotenoids in purple bacteria (especially those found in LH2) are responsible for the range of distinctive colours found throughout the various strains and species. They have a long conjugated double bond system of with the general structure being a symmetrical tetraterpene skeleton formed by tail to tail linkage of two C_{20} units (see Figure 1.3, for an example). The extended conjugation is responsible for the carotenoids absorbing light in the blue-green spectral region (450-570 nm) and hence accounts for their strong absorption properties. Absorption of photons by the carotenoids is followed by rapid energy transfer to neighbouring Bchl *a* molecules, the efficiency of which varies according to the carotenoid present[18].

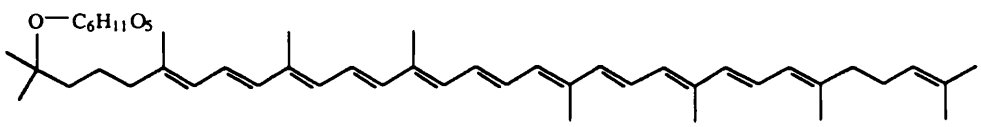

Figure 1.3: The carotenoid Rhodopin glucoside

A vital additional function of the carotenoid is to act as a photo-protective agent, suppressing photo-oxidative reactions caused by the presence of singlet oxygen. Singlet oxygen is created when triplet-state excited Bchl *a* sensitises molecular oxygen, which is such a powerful oxidant that cells exposed to high concentrations die rapidly[19, 20]. This was demonstrated using the R26

mutant of *Rhodobacter* (*Rb.*) *sphaeroides* which lacked carotenoid; when this organism was illuminated in the presence of oxygen it sensitised its own death[22]. The photo-protective mechanism involves triplet-triplet energy transfer from the Bchl *a* to the carotenoid[23].

A third and often neglected function of the carotenoid is that of maintaining the structural stability of the complex: the absence of carotenoids in the LH2 complex from *Rb. sphaeroides* was shown to cause the apoproteins to rapidly turn over in the membrane[24].

1.4.2.2 Bacteriochlorophyll a

Bacteriochlorophyll *a* (Bchl *a*) molecules function as the major light harvesting pigment in purple bacteria with the ratio of Bchl *a* to reaction centre varying between 30 and 250[25]. These are large macrocyclic pigments with a complex porphyrin-type conjugated "head" group, which carries a magnesium ion at its centre. The "tail" of the molecule is an extended unsaturated hydrocarbon structure, known as the phytyl chain. The large π-electron system gives the molecule a large molar extinction coefficient making it particularly suitable for energy absorption. Bchl *a* are also sensitive to their local environmental which allows them to absorb over a rather large spectral range.

The asymmetric conjugated π system gives the molecules two principal absorption characteristics arising from the characteristic Q_y and Q_x transition dipoles[26] (see Figure 1.4). Q_y is the Bchl *a* absorption maximum; it occurs in the near infra-red (NIR) and is the result of a transition dipole lying within the plane of the bacteriochlorin system and along the longer (Y) axis. Q_x runs perpendicular to Q_y and results in a weaker Bchl *a* absorption band in the visible spectral range. A third band, the Soret, is observed in the blue region and arises from the overlap of several bands which correspond to electronic transitions at higher energy levels[26].

It is the Bchl *a* absorption maximum in the NIR (from Q_y) which displays the greatest sensitivity to environmental changes. In an organic solvent such as acetone, monomeric Bchl *a* absorbs in the NIR at a wavelength of 772 nm[27]. However, when the molecules are bound in a reaction centre or light-harvesting complex, this peak is strongly red-shifted to between 800 and 900 nm[28]. LH1 has a single Bchl *a* absorption maximum (Q_y band) which is found to occur between 870 and 890 nm (generalised as absorbing at 875 nm). Bchl *a* molecules within LH2 are divided into two

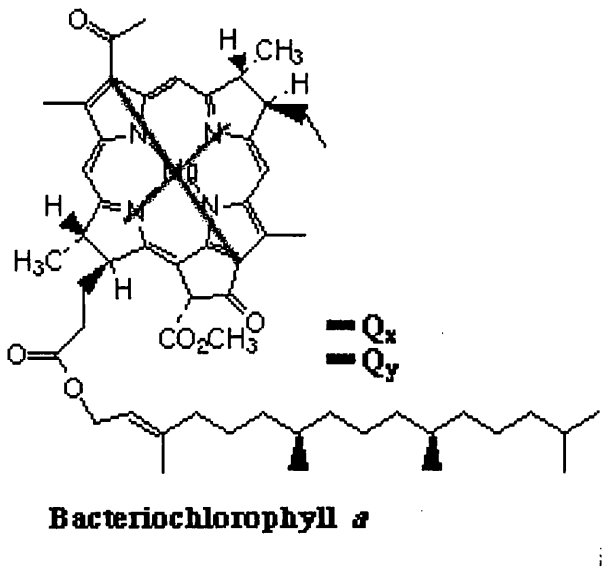

Figure 1.4: Bacteriochlorophyll *a* and its Q_x and Q_y transition dipoles.

spectrally distinct forms whose absorption maxima occur at ~800 and ~850 nm, respectively.

1.4.3 Nomenclature

The nomenclature of both LH complexes and the individual populations of their bacteriochlorophylls is primarily based on the Bchl *a* absorption maximum[18]. The prefix B (for bulk bacteriochlorophyll) is followed by the approximate wavelength of the Bchl *a* absorption maxima. Hence LH1 is also known as a B875 complex and LH2 is also known as the B800-850 LH complex; with the two groups of 800 and 850 nm absorbing Bchl *a* molecules being known as B800 and B850 molecules, respectively. In addition to this the B850 molecules are co-ordinated through their central Mg ions to Histidine residues on either the α- or β-apoprotein. The B850 molecule co-ordinated to His31 on the α-apoprotein (αHis31) is termed αB850 and the other, co-ordinated to βHis30, is known as βB850.

1.5 The peripheral light harvesting complex

The peripheral light harvesting complex (LH2) increases the light-harvesting capacity of the intramembrane light harvesting system. The amount of LH2 surrounding the reaction centre varies

under differing environmental growth conditions[5, 29], and it is this variability which accounts for the stoichiometric differences in the amounts of in the Bchl *a* which surround the reaction centre. LH2 transfers energy to the reaction centre via LH1.

1.5.1 LH2 absorption spectra

As a result of the bound pigment moieties, LH2 displays a highly characteristic absorption profile in both the visible and the NIR region (Figure 1.5) which can be used to monitor the complex for impurities and denaturation[18] (see Sections 2.6.1 and 3.2.3). The absorption at ~280 nm is from the aromatic residues of the apoproteins; at ~370 nm, ~580 nm and ~800 - 860 nm the absorption is from the Soret, Q_x and Q_y bands from bound Bchl *a* molecules, respectively (described in Section 1.4.2.2); and the three "fingers" in the 450-570 nm spectral region are characteristic of the type of carotenoid present (here rhodopin glucoside).

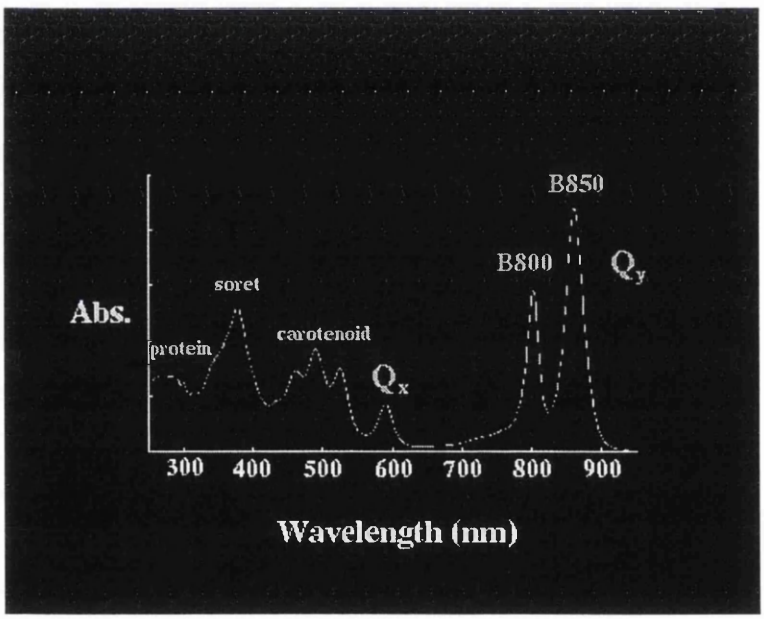

Figure 1.5: The absorption spectrum of the B800-850 LH complex from *Rps. acidophila* strain 10050.

1.5.2 Structural aspects

To date, the three dimensional crystal structures of two LH2 complexes are available from *Rps. acidophila* strain 10050[1] and *Rhodospirillum* (*Rs.*) *molischianum*[30] have been determined using X-ray crystallography. The structure from *Rs. molischianum* was solved by Molecular Replacement (MR) using the coordinates of the LH2 structure from *Rps. acidophila* strain 10050 as a search model. Both similarities and differences were found in the architecture of these proteins, with the most notable difference being the oligomeric state of the two complexes: the crystal structure of LH2 from *Rps. acidophila* revealed a nonameric arrangement whereas the *Rs. molischianum* complex was found to be an octamer.

The amino-acid sequences of the apoproteins from the two complexes are very similar in the transmembrane region, with all the major differences found at the N- and C-termini[30]. This is where the α- and β-apoproteins interact and it was presumed that the oligomeric state may be a function of the primary sequence in this area[31]. Other differences in the two complexes lie within the B800 molecules. Firstly, the B800 ligation sites are different in the two complexes. In both complexes the B800 molecules are ligated through their central Mg ions. However, in the LH2 complex from *Rps. acidophila* the B800 ligand is a formylated Met at position 1 on the α-apoprotein (fMet α1) as opposed to the Asp α6 ligand found in the *Rs. molischianum* structure. Also, the bacteriochlorin ring of the B800 molecules of the *Rs. molischianum* structure lie tilted at approximately 45° to the equivalent molecules of the *Rps. acidophila* structure. A more indepth comparison can be found in Koepke *et al.*[30].

The crystal structure of LH2 from *Rps. acidophila* strain 10050 is now described because of its relevance to this thesis. This LH2 has a nonameric arrangement of protomer complexes within which the spectrally distinct B800 and B850 molecules could be clearly divided into two discrete groups: the B800 molecules as a group of nine monomeric pigment molecules with their porphyrin head groups lying almost parallel to the membrane surface; and the B850 molecules as a closely interacting ring of eighteen pigments whose head groups lie almost perpendicular to the membrane surface. The nine carotenoid molecules span the entire depth of the complex. Figure 1.6 shows the assembly of the apoproteins and the Bchl *a* molecules.

Individual protomers consist of an inner (α) and outer (β) apoprotein which enclose:

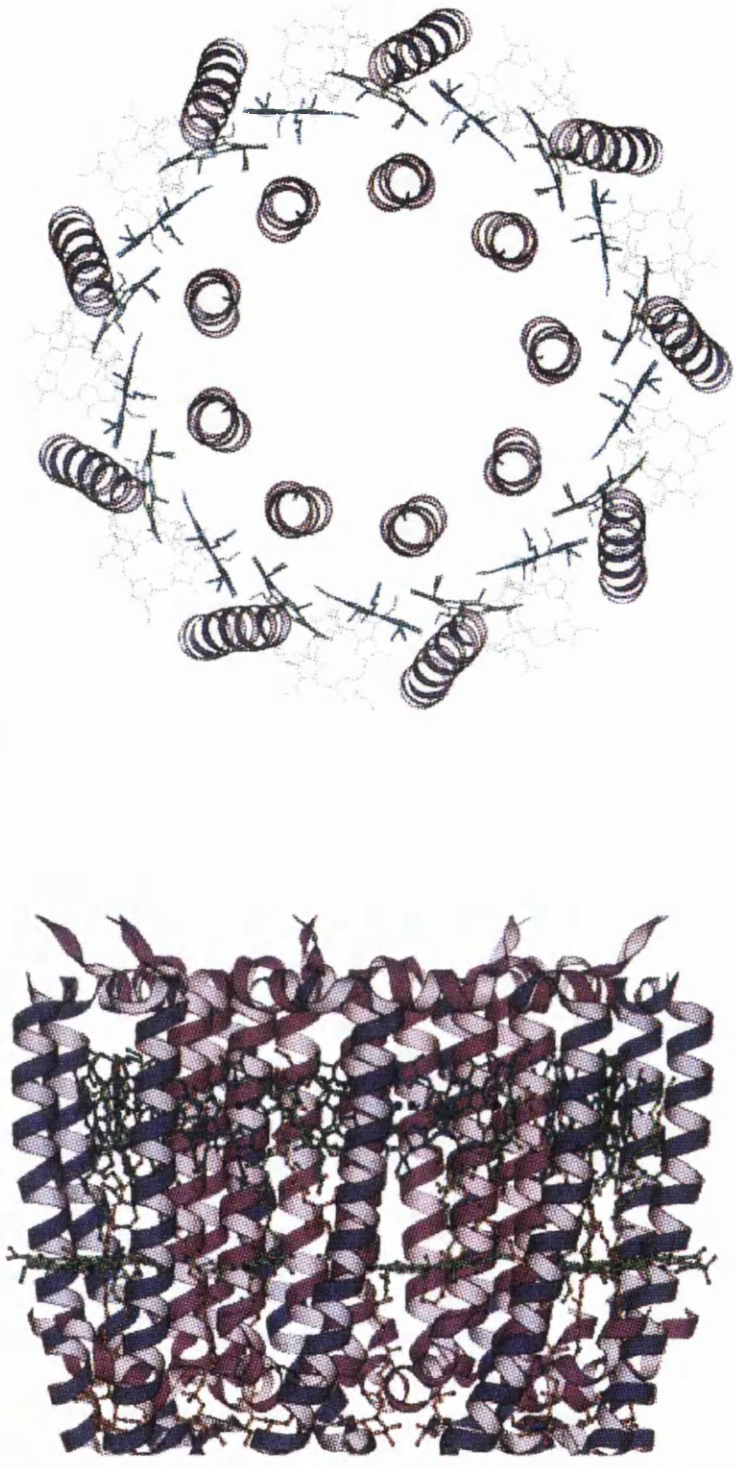

Figure 1.6: The arrangement of the Bchl *a* molecules and the apoproteins of LH2, viewed from above the membrane surface (top) and perpendicular to it.

- Two 850nm absorbing Bchl *a* molecules (B850).
- One 800nm absorbing Bchl *a* molecule (B800).
- The carotenoid rhodopin glucoside.

A protomer of the B800-850 LH complex from *Rps. acidophila* strain 10050 is shown in Figure 1.7.

1.6 The photosynthetic unit

A crystal structure of the complete photosynthetic unit has not yet been determined. However, with the wealth of structural and biochemical information now available, it is now possible to model the entire photosynthetic unit from purple bacteria[32, 33].

1.6.1 The core light-harvesting complex

LH1 is the direct donor of energy to the reaction centre and is thought to encircle it[34, 35].Recently, an 8.5 Å electron microscopy projection map of LH1, from *Rs. rubrum* was determined from a two dimensional crystal of the re-constituted[ii] complex[37]. The projection map showed LH1 as a ring of 16 subunits; each subunit apparently corresponding to an αβ-heterodimer (Figure 1.8). The ring has a diameter of 116 Å with a 68 Å hole in the centre large enough to incorporate a reaction centre. This result, in conjunction with the recent report of an electron micrograph of a two dimensional crystal of the core complex, confirms the location of the reaction centre in the middle of the LH1 ring[38].

1.6.2 Three dimensional structural representation of LH1

An illustrative model of the LH1 complex has been constructed using the 8.5Å resolution projection map described previously[32, 39](Figure 1.9 shows the LH1 model with the reaction centre placed in the centre.)

Since the primary sequences of the LH1 and LH2 are generally very similar[5], a 16-fold replication of the LH2 αβ-heterodimer was assembled to approximate to the contour peaks of the

[ii] In LH1, the complex can be reversibly dissociated into the constituting subunits by the addition of detergent[36]

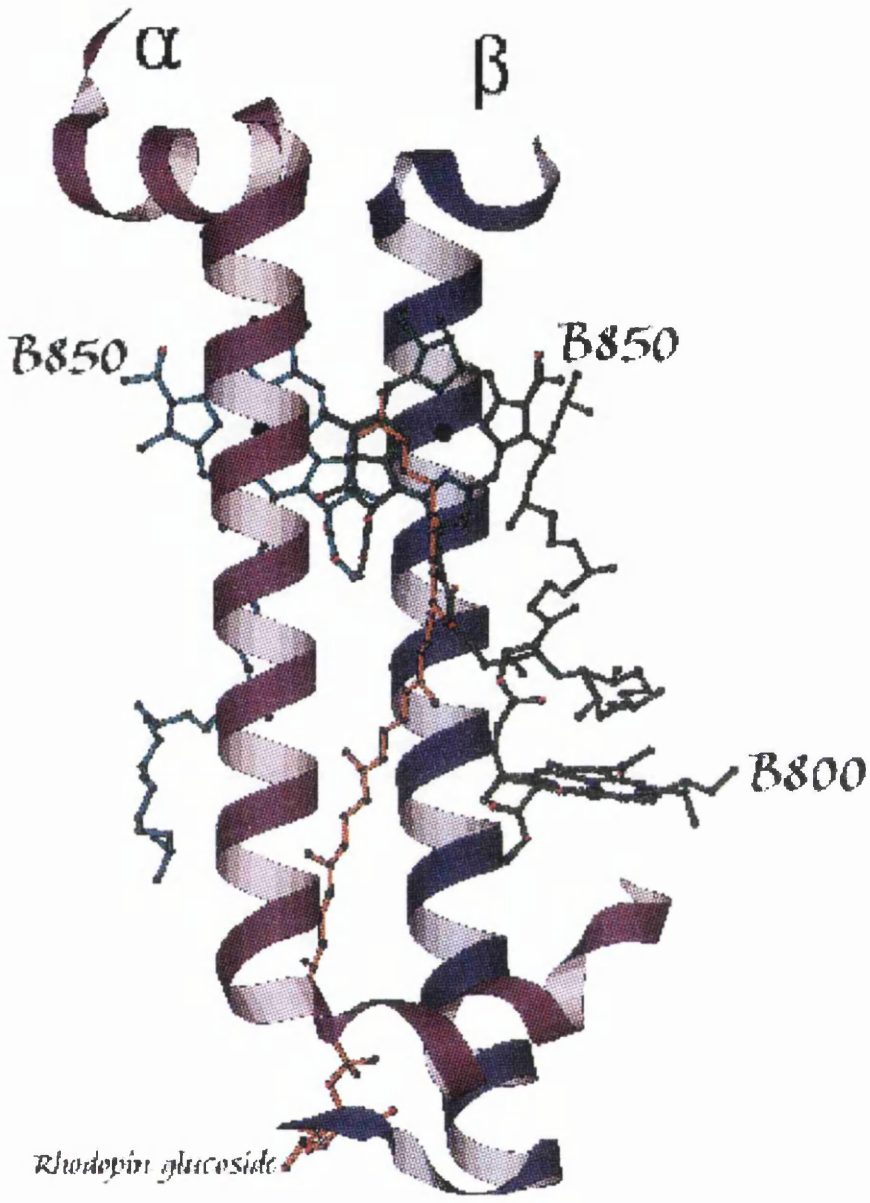

Figure 1.7: The individual protomer of the B800-850 LH complex from *Rps. acidophila* strain 10050 viewed perpendicular to the membrane surface.

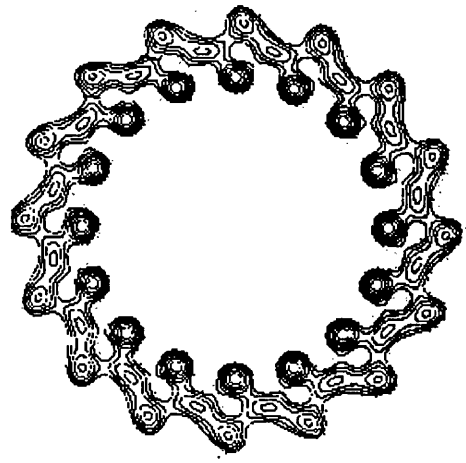

Figure 1.8: The 16-fold rotationally filtered image which was extracted from the LH1 projection map.

projection map. From the map it was also possible to see a ring of peaks between the helices which were assumed to represent a ring of B875 molecules (see Figure 1.8).

These pigments can be structurally equated to the B850 molecules in LH2, as the Bchl *a* co-ordinating histidines[iii] on the α- and β-polypeptides[5] of both complexes are at the same position. This allowed the B875 molecules to be placed at the same "depth" in the membrane as B850 molecules and moreover the LH2 co-ordinate system to be used to build the LH1 model[32].

1.6.3 A model of the PSU

The model of LH1 and the crystal structures of LH2 and the reaction centre can now be integrated: by placing the reaction centre structure[40] at the centre of the LH1 model and placing several LH2 complexes at the circumference of LH1 a complete representation of the bacterial photosynthetic unit is created[32]. This type of model has shown that it is possible to pack a maximum of eight LH2 rings closely around LH1 (Figure 1.10) and would suggests that a RC would be surrounded by a total of 248 Bchl *a* molecules *i.e.* 32 Bchl *a* from LH1 and 216 Bchl *a* from eight LH2 complexes. However, to approach this situation practically it would be necessary to grow cells at very low-light intensities, to obtain the maximum size of the PSU (~250 Bchl *a* per RC)[31].

[iii] Resonance Raman spectroscopy identified the histidine molecule which co-ordinated the Mg^{2+} ion at the centre of the B875 bacteriochlorin rings.[41]

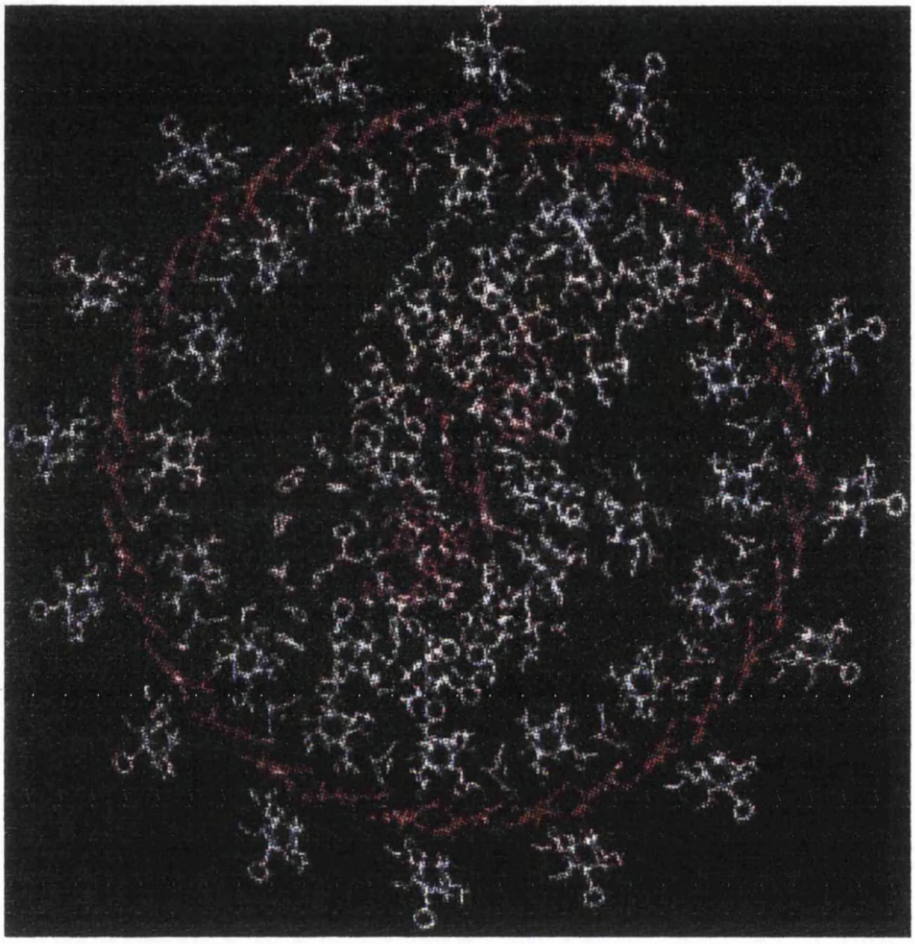

Figure 1.9: A model of LH1 constructed using the co-ordinates of LH2; the reaction centre from *Rhodobacter sphaeroides*[40] has been placed in the centre

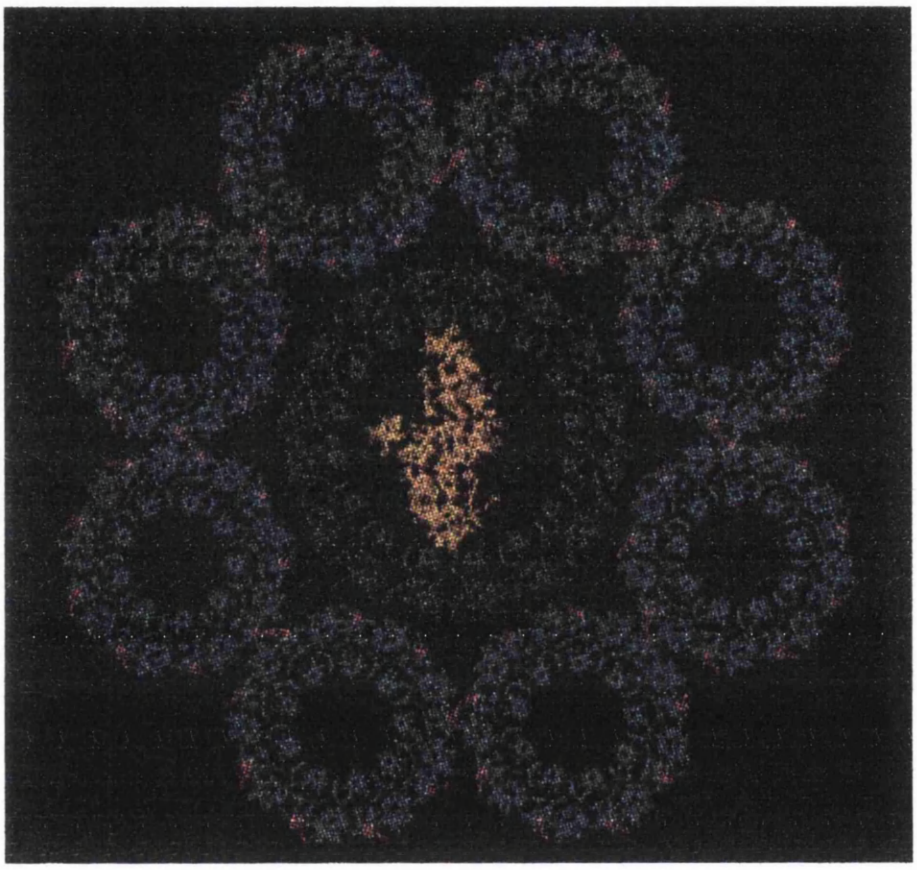

Figure 1.10: A proposed model of the photosynthetic unit in purple bacteria[32].

1.6.4 The light harvesting funnel

The purpose of the whole light-harvesting array is to provide a unidirectional energy gradient to the reaction centre, with maximum efficiency and minimum energy loss[2], and the ability of the antenna apoproteins to modulate the long wavelength absorption maxima of Bchl *a* is of fundamental importance to this process. The bacteria modify the absorption properties of their chromophores such that the spectrum available to them *in vivo* is maximised and the absorbed energy productively transferred and made available for photochemistry.

Energy corresponding to photons absorbed by any of the light harvesting pigment molecules is transferred down an energetically favourable gradient from pigment molecules in high energy states (low wavelength) to those of a lower energy. Consequently, all the pigment molecules in LH2 rapidly transfer energy to the coupled ring of B850 molecules at the top of the complex, which then transfer the energy onto the B875 molecules in LH1 and subsequently into the reaction centre. This provides a funnel of absorbed light energy from the light-harvesting apparatus to the reaction centre.

1.7 The B800-820 LH complex

Depending on their growth conditions certain species and strains of bacteria are able to produce a second form of LH2 which has different spectral characteristics. These bacteria are grown and have the ability to survive under what are generally classed as "stressed" conditions (see Section 1.7.1); and in doing so they produce this spectrally distinct form of LH2. This complex has Bchl *a* absorption maxima at approximately 800nm and 820nm and is hence referred to as the B800-820 light harvesting complex (or occasionally LH3[30]). The absorption spectrum of the B800-820 LH complex is shown in Figure 1.11. In order to make best use of the light available to the bacteria this complex is a more efficient light-harvester than its B800-850 counterpart. The rate of transfer of energy into the reaction centre is very similar[42] but the equilibrium of energy within this system is shifted so that back transfer from the LH1-RC core is much more restricted in the presence of the B800-820 LH complex[43, 42]. This makes the overall energy funnelling system much sharper.

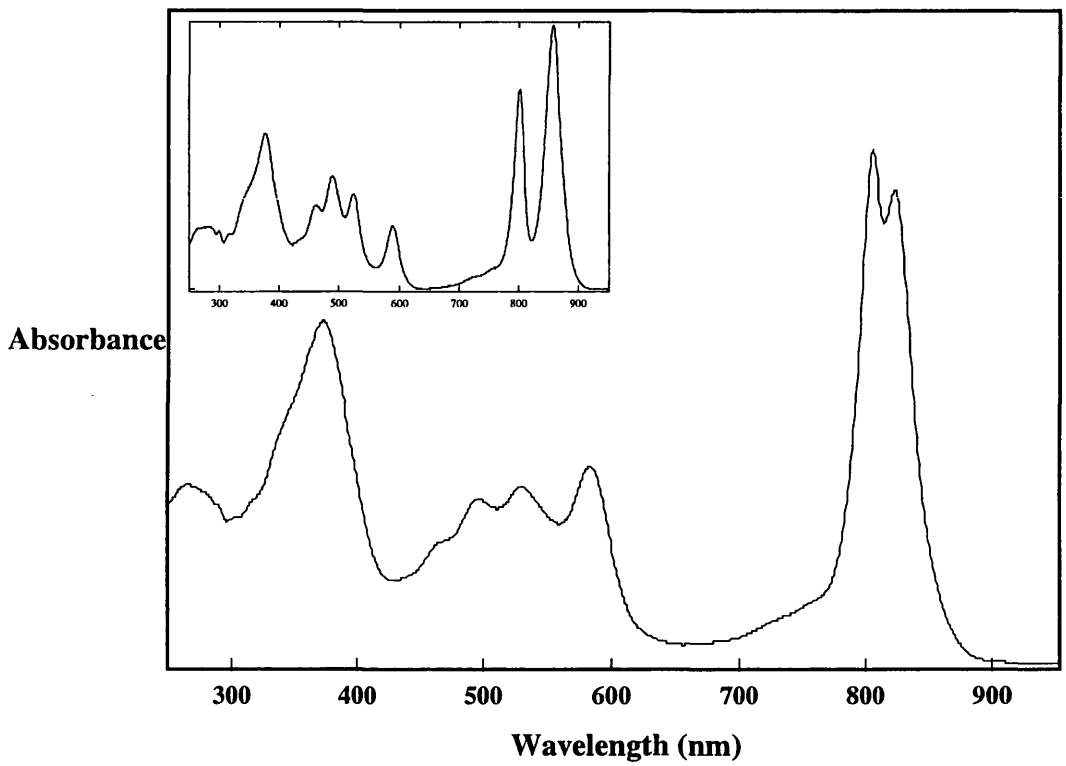

Figure 1.11: The main figure shows an absorption spectrum for a B800-820 LH complex.

For a comparison the insert shows the equivalent spectrum of a B800-850 complex.

Additionally, this form of LH2 is produced in greater stoichiometric abundance with respect to the core complex, than the B800-850 LH complex. As many as 250 Bchl *a* molecules can be found to surround the core complex compared to 30 Bchl *a* molecules when the B800-850 LH complex is present. Also, the carotenoid composition often differs significantly within the B800-850 and the B800-820 complexes from the same species of bacteria. This often results in the production of a more efficient carotenoid to LH2 energy transfer system[2].

1.7.1 Production of the complex

Most commonly, and perhaps most understandably, reduced light intensity causes certain species of bacteria to synthesise a B800-820 complex before they would produce a B800-850 complex[44], and this can perhaps be explained by the bacteria making better use of the light available to them. However, the growth temperature has also been reported to affect the type of LH2 complex produced by the bacteria: reducing the growth temperature of *Rps. acidophila* strain 7750 cells causes growth of the B800-820 complex to predominate[44]. Other environmental parameters, such as the nature of the carbon source supplied for the growth medium, and varying oxygen levels, have also been reported to affect the type of complex produced, but these observations have not yet been subjected to systematic study[29].

1.7.2 Suggested reasons for the spectral shift

The B800-820 LH complexes are thought to be built on the same modular principle as B800-850 LH complexes with the changes in their absorption spectra being linked to differences in the amino acid sequences of the apoproteins[45]. If this is the case then the antenna polypeptides are of functional significance with regard to the adaptation of antenna complexes to their environment[14]. A comparison of the amino-acid sequences from the B800-850 and the B800-820 LH complexes from *Rps. acidophila* identified certain conserved residues in B800-850 LH complexes which are consistently different in the B800-820 LH complexes[45] (See Figure 1.12).

Brunisholz and Zuber proposed that the replacement of the conserved residues Tyr44 and Trp45 on the α-apoprotein (Tyr α44, Trp α45, respectively) of the B800-850 LH complexes was directly correlated to the spectral shift[45]. It has since been shown that a blue shift in the spec-

		31	32	33	34	35	36	37	38	39	40	41	42	43	44	45	46	47	48	49	50	51	52	53
10050	B800-850	**H**	L	A	I	L	S	H	T	T	W	F	P	A	Y	W	Q	G	G	V	K	K	A	A
7050	**B800-820**	**H**	A	A	V	L	T	H	T	T	W	Y	A	A	F	L	Q	G	G	V	K	K	A	A
7050	B800-850	**H**	A	A	V	L	S	H	T	T	W	F	P	A	Y	W	Q	G	G	L	K	K	A	A
7750	B800-850	**H**	L	A	I	L	S	H	T	T	W	F	P	A	Y	W	Q	G	G	V	K	K	A	A
7750	**B800-820**	**H**	L	A	V	L	T	H	T	T	W	F	P	A	F	T	Q	G	G	L	K	K	A	A

Figure 1.12: Primary sequence of the C-termini of the α-apoproteins from *Rps. acidophila*, shown from the conserved Bchl *a* binding Histidine residue at position 31. Highlighted section shows the residues conserved in the B800-850 complexes and differing in the B800-820 complexes, proposed to be associated with the spectral shift[45].

trum is induced by mutation of the residues at these positions on the α-apoprotein of the LH2 complexes from *Rb sphaeroides*[46]. Site directed mutagenesis was used to replace two tyrosine residues with phenylalanine and leucine (Tyr α44, Tyr α45→ Phe α44, Leu α45), which are the two residues present in the B800-820 LH complex from *Rps. acidophila* strain 7050. In this genetically modified complex the 850 nm absorption band blue-shifted to 826 nm whereas in the B800-820 complex from *Rps. acidophila* strain 7050 this absorption peak is found at 823 nm.

From the mutagenesis, it was suggested that the loss of two hydrogen bonds from Tyr α44 and Tyr α45 to an acetyl carbonyl oxygen of the B850 molecule, and the strengthening of another to a B850 keto carbonyl group , were responsible for the blue shift in the absorption spectrum[47]. However, in the structure of the B800-850 complex from *Rps. acidophila* strain 10050[1] it was found that while the residues αTyr44 and αTrp45 do form hydrogen bonds to acetyl oxygens there is no hydrogen bonding to keto carbonyl groups on any of the B850 molecules[48]. From the structure it can be seen that the environment of the chromophores is governed by the protein, providing conditions which determine the nature of the pigments and modulate their absorption spectra. However, this relationship is not a simple one[48] and the elucidation of the crystal structure of a B800-820 LH complex is vital to determine the precise role that the protein plays in modulating the long wavelength absorption band of Bchl *a*.

1.8 Membrane protein crystallogenesis

1.8.1 Introduction

Today there are available around 7,000 X-ray crystallographic structures of soluble proteins. This implies that even though the crystallisation process is not yet fully understood, there are various straightforward and reliable methodologies which have proved successful in obtaining X-ray quality crystals of soluble proteins. However, although it is almost two decades since the first reports of integral membrane protein crystals[49, 50] the number of 3D membrane protein crystal structures available is still below 20. The majority of integral membrane protein crystals have been obtained using standard protein crystallisation conditions and methodologies[51]. However, there are a variety of conceptual and practical problems which are specific to working with and crystallising integral membrane proteins and as a consequence the "Art of crystallising membrane proteins[52]" is still some distance from being reduced to a few general and well defined scientific steps..

The last three years have provided several new integral membrane protein structures including: two bacterial LH complexes[1, 30]; bacterial and mitochondrial cytochrome *c* oxidase[53, 54]; α-hemolysin[55]; bacteriorhodopsin[56]; and the potassium channel from *Streptomyces lividans*[57]. All of these structures give researchers a long-awaited bank of data to analyse and learn from. As for all crystallographic systems, obtaining well ordered crystals is one of the major rate-limiting steps in integral membrane protein structure determination; as indeed was found in the current structure determination of a B800-820 light harvesting complex.

1.8.2 Biological membranes and membrane proteins

Many fundamental biological processes occur in or on the cell membrane: the control of nutrients, waste products and ions flowing in and out of a cell, the receipt and transduction of signals, and biological energy conversion are all membrane-mediated processes. The membrane is generally composed of a heterogeneous mixture of lipids and protein. The fluid mosaic model of the biological membrane (Figure 1.13) describes membrane lipids arranged in a bilayer structure[58].

Here the polar head groups are aligned to form two continuous hydrophilic surfaces, which are in contact with an aqueous environment. The non-polar lipid "tails" are located between these

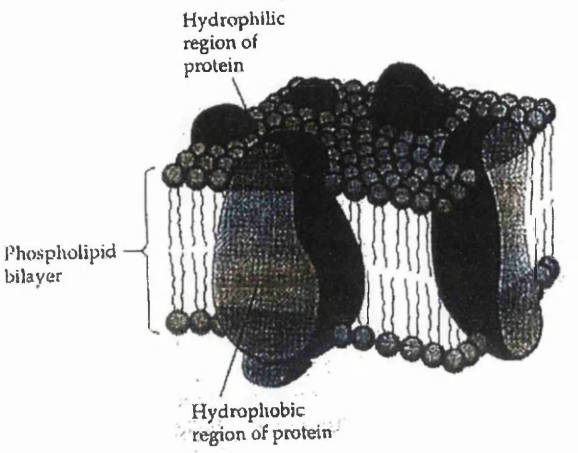

Figure 1.13: The fluid mosaic model of the cell membrane.

two surfaces, creating in effect a hydrophobic filling in a hydrophilic sandwich. The membrane proteins only interact specifically with a small number of the lipids and are generally free to diffuse laterally through the membrane. Functionally, the lipid components form a permeability barrier necessary for organising processes into different compartments while specific proteins, which are found in or on this barrier, mediate nearly all other cell functions.

1.8.2.1 Membrane protein classification

Membrane proteins are generally divided into two groups[58]: extrinsic or *peripheral* and intrinsic or *integral* membrane proteins. These are classed on how tightly they are connected to the cell membrane. Peripheral membrane proteins are only weakly associated with the cell membrane. They are essentially localised within the hydrophilic section of the bilayer and their mode of adherence to the membrane is generally ionic, although in some cases they are attatched to the membrane via a hydrophobic anchored region. Consequently, peripheral membrane proteins can be dissociated from the membrane relatively easily and free of lipid components[58] and once removed from the membrane they are generally soluble in aqueous solutions.

Conversely, integral membrane proteins are tightly associated with the bilayer and are exposed to a section of the membrane interior. Therefore integral membrane proteins are hydrophobically integrated into the membrane and can only be dissociated from it by adopting relatively aggressive

methods[58]. Also, as a result of their location integral membrane proteins are generally of an amphipathic nature. The section of the protein immersed in the non-polar membrane interior has a predominately hydrophobic surface, whereas the portion which extends into the aqueous environment (or that is in contact with the polar head groups), is largely sheathed with polar residues. A consequence of this is that once these proteins are removed from the membrane they are rendered mainly insoluble in both aqueous and apolar media. This attribute of integral membrane proteins stops them forming the monodisperse solutions which are usually required as a starting point for crystal growth.

In general it is "integral membrane protein" which is implied by generic references to "membrane protein" and this category of protein can be further subdivided: Proteins which are exposed to a specific membrane surface (while being partially buried in the interior) are generally known as *inner* or *outer* integral membrane proteins and others which span the entire depth of the membrane are known as *trans-membrane* proteins.

1.8.3 Detergent solubilised systems

Like the phospholipids, which compose the cell membrane, detergents are amphiphilic molecules made up of a hydrophobic "tail" section and hydrophilic "head" group. However, detergent molecules have an ability that the phospholipids do not posses: they can form micelles in solution. Micelles are thermodynamically stable colloidal aggregates which form in solution above a certain threshold monomer concentration known as the *critical micelle concentration* (CMC). The hydrophobic interactions responsible for micelle formation are very similar to the interactions responsible for the assembly of lipid bilayers[59]. In general, integral membrane proteins are extracted from the membrane and kept soluble in aqueous solution using detergents.

1.8.3.1 Solubilisation

The use of detergents is a general and efficacious way to dissociate integral membrane proteins from the membrane whilst (with the correct conditions) allowing protein stability and integrity to be maintained. To keep trans-membrane proteins soluble the detergent is assumed to bind to the hydrophobic torso of the protein and the polar head groups point towards the aqueous solution[60].

When the detergent is added to an aqueous solution of biological membranes, it initially binds to the membrane. As this concentration is increased the membrane will eventually fragment and ideally result in protein with bound detergent distributed around the hydrophobic area in a uniform mass.

A schematic and simplistic view of solubilisation as a function of detergent concentration is presented in Figure 1.14.

This is the theoretical situation and in reality it is seldom so simple. The ability of detergent to solubilise effectively a protein does not rely solely on detergent concentration but instead depends on the type of protein, detergent and lipids involved and on the complex interactions between them. Complete delipidation may not be possible as tightly bound phospholipids can resist extraction by detergents and adding a sufficient amount of detergent does not guarantee single copies of the protein surrounded by the associated detergent micelle.

1.8.3.2 Protein crystallisation

Protein molecules in a vast array of shapes and sizes have now been crystallised and the majority of the problems encountered when attempting to obtain X-ray quality crystals arise more because of their strange physico-chemical properties than their shape. Their specific functionality makes them greatly sensitive to their environment and their optimal stability in aqueous media is often restricted to a very narrow temperature and pH range. This means that "severe" conditions can often denature or degrade proteins in a manner that would diminish any hope of crystal formation. In addition, there is a huge number of biological parameters which affect the crystallisation of macromolecules[61].

The crystallisation of protein molecules is not a fundamentally different process to that of small molecules[62], but the kinetic and thermodynamic parameters which govern these process are quite distinct[63, 64].

1.8.3.3 Crystal growth

Like the growth of crystals from small molecules, protein crystal growth is a result of three classical steps: nucleation, growth and termination:

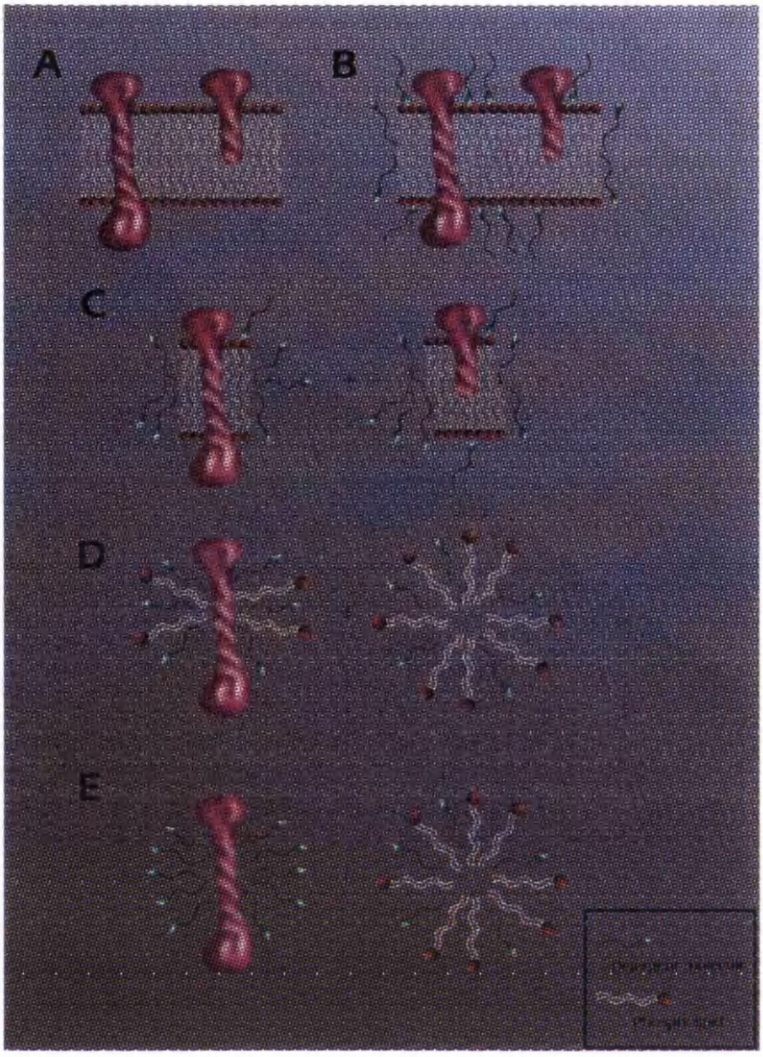

Figure 1.14: Solubilisation of membrane proteins; the detergent concentration increases from Part A to E.

Diagram courtesy of Drs Paul Emsley and Dina Fotinou.

Part A: *Intact membrane*

Part B: *Binding* and incorporation of the detergent molecules to the membrane occurs at very low concentrations of detergent to protein.

Part C: *Lysis* occurs as the concentration increases; producing segments of membrane which incorporate detergent molecules.

Part D: *Solubilisation* of the protein into individual lipid-protein-detergent complexes occurs next, along with the formation of lipid-detergent micelles.

Part E: *Delipidation* should eventually be achieved at much higher concentrations of detergent to protein giving protein-detergent complexes and lipid-detergents micelles.

- *Nucleation* is the association of just enough protein molecules to form the smallest, thermodynamically stable, ordered aggregates of the crystal; the nucleus.

- *Growth* of the crystal occurs at the surface of the nuclei by the incorporation of molecules into the crystalline lattice.

- *Termination* of growth can occur for several reasons, these include: the depletion of macromolecules from the solution; destabilisation of the lattice as a result of growth defects; poisoning of the crystal faces by impurities and ageing and/or denaturation of the molecules.

Both the nucleation and growth of protein crystals occur in supersaturated solutions where the concentration of the protein exceeds its solubility. Supersaturation is a function of both the concentration of the protein and the parameters that affect its solubility, and is often expressed as: C/C_s, where C is the concentration of the protein before crystallisation and C_s is the solute equilibrium concentration. Supersaturated solutions are thermodynamically metastable and equilibrium is generally restored to the system by the formation of macromolecular precipitants, some of which can be crystalline. The region of solution parameter space which is suitable for crystallisation is often represented by a solubility curve (Figure 1.15). For crystallisation to occur the protein must lie within the metastable region, since at any point below the solubility curve the protein remains soluble and at any point above the precipitation curve the protein will precipitate immediately. However, the growth of a seed crystal need not take place at the same level of supersaturation needed to induce nucleation: crystal growth occurs at a level of supersaturation lower than is required to produce nuclei. Therefore the supersaturated region can be divided into two distinct zones, known as the labile and the metastable region, which are separated by a supersolubility curve. In the labile region both growth and nucleation can take place whereas in the metastable region only crystal growth is sustained.

1.8.3.4 Solubility parameters

In order to crystallise, a protein solution must be guided extremely slowly towards supersaturation. The reason for this is that protein crystals are generally nucleated at extremely high levels of supersaturation, compared to small molecules[65], and this makes the formation of amorphous

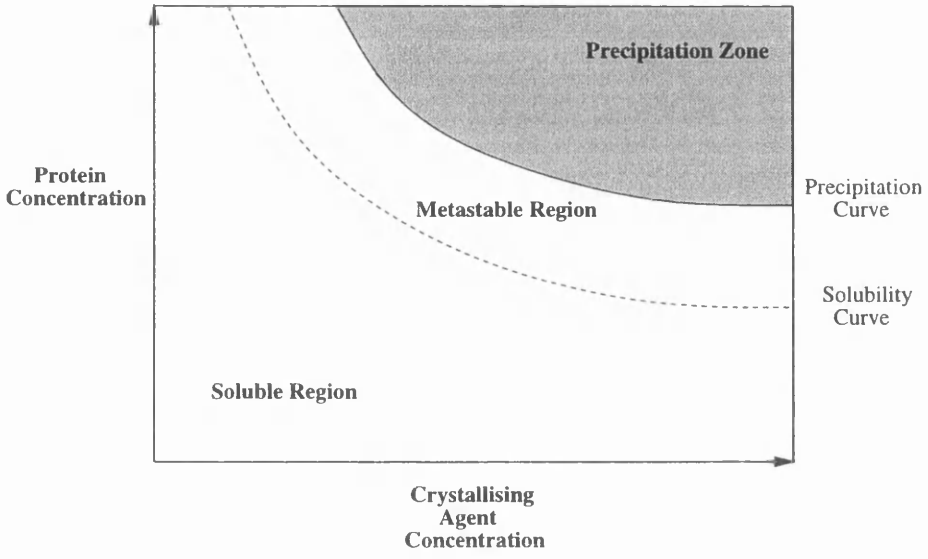

Figure 1.15: Phase diagram for protein in solution.

precipitate a real possibility. Slowly reaching supersaturation is achieved by gradually altering parameters which will reduce the solubility of the protein by depriving it of sufficient ions or water molecules to maintain hydration. There are four general parameters which are used to modify the solubility of a solution of protein molecules: the temperature; the pH; the ionic strength and the organic content of the solution[51].

Precipitants

Changing the ionic strength or the organic content of the system is most commonly achieved by the modifying the properties of the solvent through equilibrium with precipitating agents. Precipitants would be more correctly known as solubility-influencing agents since precipitation is only one possible outcome of the system. These additives alter the charges on the surface of the protein or disturb the interactions between the protein and bulk solvent water molecules, to promote associations that may lead to crystal growth. The traditional precipitating agent is ammonium sulphate, although many other salts, alcohols, polymers and detergents have all been found successful in crystallisation trials[66]. The methods by which the majority of proteins are induced out of solution relies on the property of almost all proteins to "salt-in" or "salt-out"[51].

- *Salting-in* occurs when the solubility of the protein increases as the ionic strength of the solution increases. The initial solution contains a small number of ions which increase the potential for favourable interactions between protein and water molecules, thus making it more soluble. Conversely, as these ions are removed from the solution the protein molecules tend to satisfy their electrostatic requirements through interactions with themselves.

- *Salting-out* occurs when the solubility of the protein decreases as the ionic strength of the solution increases. The protein is exposed to increasing concentrations of precipitants and competition between the protein and the precipitant for the water molecules renders the protein insoluble. This technique was used to crystallise the B800-850 LH complex from *Rps. acidophila* strain 10050.

pH

The pH of a protein solution is possiblythe most important consideration in crystallisation trails after precipitant concentration. The aggregation state and hence the solubility of the protein depend on net charge and the ionisation state of the amino-acids; both of which change with pH. It is usual for proteins to be least soluble near their pI[iv] and as a result of this they can often denature or aggregate when working close to this value. Also, when working near the pK of a large number of similarly charged residues the solubility change can be extremely rapid, making the pH a very sensitive parameter. Consequently, it is worthwhile to test the behaviour of a "new" protein as a function of pH in order to assess the suitability of pH as a crystallisation parameter.

Temperature

Temperature of a protein solution affects the solubility of the protein and in general an increase in solubility is observed with increasing temperature[67]. However, proteins in high salt concentrations are found to be more soluble at lower temperatures and conversely those soluble in low salt or precipitant concentrations generally precipitate more easily at cold temperatures[68]. It follows that by varying the temperature it is theoretically possible to control the protein nucleation rate. However, it is more general to work within a constant temperature range and it is important to

[iv] The pI of a protein is the pH at which the overall net charge is zero.

However, it is more general to work within a constant temperature range and it is important to remember that the rate at which equilibrium is reached is slower in the cold causing precipitation or crystal growth to take longer.

1.8.3.5 Crystallisation methods

When searching for the optimal conditions for the nucleation and growth of protein crystals it is important to remember that conditions which are suitable using one crystallisation method may not be as effective using another. Consequently, crystallisation strategies often include a variation in methods and a few of the more general methods are described below.

Batch crystallisation

Batch crystallisation is the simplest method used for the crystallisation of proteins. It requires only that all of the components (including the precipitating agent) are placed in a single solution and left undisturbed. The initial solution must be sufficiently supersaturated for nucleation to be achieved, which theoretically results in a system which appears less than ideal as nucleation would be assumed to occur too rapidly. However, changes in the protein concentration as a result of the formation of nuclei or precipitates, and the resulting depletion of molecules from the solution, make it possible to obtain fairly large crystals when working close to the metastable region. The general theory behind this method is applicable to most other crystallisation techniques: high levels of supersaturation are achieved initially with lower, crystal growth facilitating levels being reached at some later time.

Vapour diffusion

Today micro-methods, especially vapour diffusion and dialysis, are the most commonly used techniques[69]. Vapour diffusion techniques, as the name suggests, rely on the diffusion of water or solvent molecules through air to bring the protein solution slowly towards a state of supersaturation. Typically, a droplet of protein solution containing precipitant (and other additives) is equilibrated against a reservoir containing a solution of precipitating agent at a higher concentration. Vapour diffusion occurs until the vapour pressure in the droplet equals that of the reservoir, with the aim being to reduce the volume of the protein solution, through dehydration, until it reaches

the required level of supersaturation to facilitate the formation of nuclei. At this stage the reservoir no longer acts to concentrate the drop but only maintains a constant vapour pressure. The three methods by which the vapour diffusion technique is most commonly applied are hanging drop, sitting drop and sandwich drop systems.

Dialysis

Dialysis is again based on the same general principle but is actually one of the more versatile methods. The protein solution is altered by the diffusion of the precipitant through a semipermeable membrane. This allows the composition of the protein solution to be modified accurately any number of times.

Seeding

The final technique described here is seeding which is becoming increasingly more common (especially for increasing crystal size). Although there are various types of seeding procedures[70] the basic idea behind each is the same and in contrast to the above, this technique utilises the fact that rates of nucleation and growth generally have different dependencies on protein supersaturation. Seeding aims to achieve separate optimisations of both procedures by transferring crystals from nucleating conditions into those which support crystal growth.

1.8.4 Availability of membrane proteins

One of the major problems when working with membrane proteins is that they are found in the cells at very low levels. Although there have been recent attempts to overexpress and engineer[71] membrane proteins, producing large amounts of most membrane proteins is still difficult to achieve. Also, while refolding of recombinant protein from inclusion bodies often works well for soluble proteins it is still a large problem when over-expressing membrane proteins. However, there have recently been reports of successful over-production of a membrane protein, and of the refolding of membrane proteins from inclusion bodies[72]. Consequently, the development of standard procedures for obtaining sufficient amounts of membrane proteins for use in structural studies is extremely important to the field. Fortunately, working with proteins found in photosynthetic membranes meant that the membrane proteins have been cultured and isolated from natural sources.

These proteins are therefore available in copious amounts and are generally structurally well characterised.

1.8.5 The crystallisation of membrane proteins

In the last twenty years several methods have been proposed for the crystallisation of membrane proteins, each of which has seen limited success and applicability. These include the use of proteolysis to form crystallisable species[73]; solubilisation and crystallisation in organic solvents[74] and solubilisation in detergent followed by detergent removal[75]. More recently techniques have been developed specifically for the crystallisation of membrane proteins. The first of these was the F_v fragment-mediated crystallisation of bacterial cytochrome c oxidase[53]. This technique increased the extramembranous polar region, by the addition of a F_v fragment, to extend the surface available to form crystal contacts. Another novel technique was the crystallisation of bacterio rhodopsin by the use of lipidic cubic phases[56]. This method was devised to enable the protein to remain in a quasisolid membranous environment throughout crystallisation. Bicontinuous lipidic phases were chosen to provide nucleation sites and to allow protein growth to be supported by lateral diffusion of the protein molecules. Lipidic phases look promising for the crystallisation of membrane proteins although the crystallisation of other proteins in these phases are still required to prove this theory. Currently, lipidic cubic phases have produced crystals of a reaction centre complex and are being tested on the B800-850 complex from *Rps. acidophila* strain 10050[76].

However, the majority of X-ray quality crystals have been grown from preparations of detergent solubilised protein, where the heterogeneous membrane lipids are replaced with homogeneous detergent molecules. This system provides a general and effective means of working with membrane proteins once they are removed from their native environment. Many of the early developments in membrane protein crystallisation were a result of the awareness of the role that detergents play in the solubilisation and crystallisation of membrane proteins[52]. Whilst detergent solubilised systems have undoubtedly yielded the best results in crystallisation trials, a poor choice of such a system can often lead to metastable solubilisation and subsequent non-specific aggregation[77]. Recognising that the protein-detergent aggregate is the species that actually crystallises makes it obvious why it is so important to understand the characteristics and behaviour of

the detergent layer.

1.8.5.1 Crystal formation

According to Michel[78] there are two basic types of membrane protein crystals, where the original hydrophobic regions of the protein are counterbalanced in different ways: Type I and Type II crystals (Figures 1.16 and 1.17).

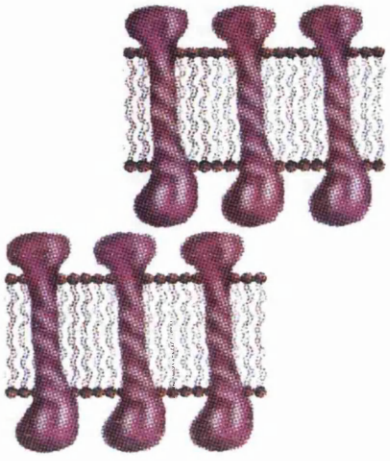

Figure 1.16: Membrane protein crystals: Type I

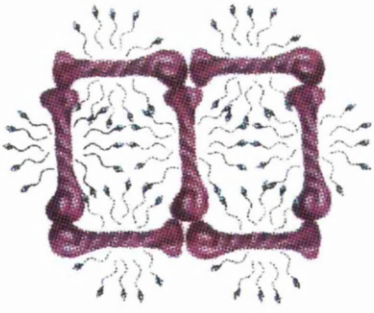

Figure 1.17: Membrane protein crystals: Type II

Type I crystals are not formed from protein with the associated detergent micelle but instead

rely on the hydrophobic interactions between protein, lipid and protein to compensate for the hydrophobicity, in the same way as is found in the cell membrane. These are basically 2D crystals, formed in the plane of the membrane and then stacked in an ordered way. The formation of such crystals is possible e.g. solubilised purple membranes were crystallised in such a way by gradually removing the detergent at high salt concentrations[75]. These crystals are held together by hydrophobic and polar interactions and the attractive forces of both these of these have to be increased during a crystallisation experiment. While crystals of this type are possible the overwhelming majority of membrane protein crystals belong to type II. Type II crystals are a result of crystallising the proteins from within their detergent micelles; they are held together mainly by polar interactions from the protein, although the possibility of micelle-micelle and micelle-protein contacts are now being considered[79]. At the moment the success of producing X-ray quality crystals seems to lie with producing type II crystals. To obtain these crystals the membrane protein surrounded by its detergent 'belt' is treated as a soluble protein, using standard crystallisation procedures. However, the presence of the detergent means that there are a variety of conceptual and practical problems which must be considered.

1.8.5.2 Detergent effects

The size and shape of the detergent micelles depend on the type, size and stereochemistry of the monomer and changes in these affect the size and shape of the detergent layer on the protein. This layer is important as the Type II crystal lattice is established through polar contacts from the protein regions extending out of the detergent micelle. Therefore this micelle must be compact enough to fit into the crystal lattice. However, neutron diffraction studies on the reaction centre from *Rps. viridis*[79] and on OmpF porin from *Escherichia coli*[80], suggested that the detergent-detergent interactions may also play a role in stabilising the crystal lattice. Work on the reaction centre revealed that the detergent layer extended beyond the protein surface adjoining neighbouring detergent layers and protein in the crystal. Whilst the main contacts were protein-protein (and the detergent-detergent contacts found in the OmpF porin were more subtle) it was suggested that changes in the detergent composition could affect and perhaps even disrupt the crystal packing.

This theory has experimental backing as described by Ostermeier and Michel[81] who reported

small differences in the detergent to cause essential differences in protein crystallisation behaviour. Examples were given on how minor changes in the alkyl chain length produced dramatically different effects on the crystal systems. These results suggested that for membrane protein crystallisation there is an optimal chain length for the chosen detergent for the crystallisation of any particular system of protein-detergent molecules[81]. However, this is not the case for the B800-850 light harvesting complex from *Rps. acidophila* strain 10050 and the reaction centre from *Rhodobacter sphaeroides*[82]. Both of these proteins have been crystallised using a variety of detergent systems and the light harvesting complex is reported to produce more than one crystal form.

1.8.5.3 Solubilisation conditions

Choosing a suitable type and concentration of detergent for the solubilisation of a membrane protein depends on its ability remove the protein from the membrane while maintaining native structure and function; its effectiveness in delipidating the protein; its capacity for maintaining the protein in a stabilised state; and the eventual effect it has on the crystallisation system[52].

The overall aim is to effect solubilisation so that integral membrane proteins are capable of being purified and characterised by conventional means. To achieve this, the protein environment is maintained at a concentration of detergent high enough to keep the protein soluble[83] (slightly above the CMC of the detergent usually suffices[84]). When attempting to obtain the maximum amount of protein from the membrane it is not enough to add a large excess of detergent to a solution of dilute membranes, as this can potentially denature the protein[85]. However, when the protein concentration is high the detergent to protein concentration becomes an important consideration as the optimal amount of detergent (i.e. the concentration which effectively recovers the maximum amount of protein) required increases as the concentration of the protein increases[59]. Incomplete delipidation of membrane proteins and hence the presence of heterogeneous lipids can also be detrimental to the production of well ordered crystal forms.

1.8.5.4 Phase separation

Along with the size and shape of the detergent monomers, detergent solutions have colloidal properties, which add yet another dimension to the complexity of membrane protein crystallisation.

Micellarisation of monomeric detergent is an example of a phase transition which occurs in an aqueous solution of detergent molecules and in general protein-detergent complexes are continuously in association and dissociation with free detergent monomers[86]. However, other phase changes which involve micelles can actually create nonisotropic solutions and mesophases. At a certain temperature, called the *cloud point*, the solution turns turbid as it quickly passes through a phase boundary and results in what is commonly know as *phase separation*[v][87]. This results in a micelle rich phase which is rich in detergent but contains little of the precipitant ions; and a micelle depleted phase which is rich in ions.

Phase separation is a major obstacle in crystallisation of membrane proteins and, because protein-detergent complexes behave essentially like detergent micelles[88], the phase transition is generally formed by a shift in temperature or the addition of precipitants to the solution. The variation of temperature often has opposite effects on protein solubility and phase transitions; phase transition shifts to a higher precipitant concentration with increasing temperature whereas protein solubility in high salt generally increases with decreasing temperature.

Micelles develop attractive interactions in the presence of salt and the strength of these interactions increases with decreasing temperature, so that phase separation theoretically would occur on lowering the temperature. The attractive forces which cause free micelles in solution to aggregate are thought to be the same as the attractive polar interactions between the protein bound detergent micelles, thought to be helpful in stabilising the crystal lattice. This would explain why many membrane proteins have been reported to crystallise near to or within the phase separation boundary[84]. There have been reports where X-ray quality crystals have formed in this phase[84, 49, 87]. However, it is more usual for the protein to denature rapidly when exposed to such an excess of detergent or to result in the growth of microcrystals[89]. Phase separation is generally considered detrimental to a crystallisation experiment and difficult to control, and systematic work to elucidate the mechanism of these phase changes is lacking. However, there have been several observations reported by a variety of researchers[84, 89] :

- Phase separation is reduced when ammonium sulphate is used as the precipitant as opposed to potassium or sodium phosphate.

[v] The phase separation phenomena is extensively covered by Zulauf 1991

- Phase separation can be shifted to higher salt concentrations with the use of certain additives, e.g. glycerol.

- The use of small amphiphiles such as dimethylamineoxides shift the phase transition to higher precipitant concentrations (in some cases the transition disappears altogether).

- The phase separation conditions are specific for the detergent-precipitant system and not the protein i.e. when one detergent is exchanged for another crystallisation conditions may change despite the protein to be crystallised being the same.

The specific properties of detergents depend primarily on the chemical structures of their monomers, but they are also affected by experimental conditions such as temperature, pressure, pH and ionic strength. As yet no global explanation for the interaction of detergents with biomacromolecules exists and as a result the task of finding the best detergent is essentially left to trial and error. The suitability of a detergent is generally added to the list of parameters that are to be tested in crystallisation trials and the use of detergent screening procedures have made testing various detergents a more attainable task.

1.8.6 The role of the small amphiphile

In 1983 Hartmut Michel reported the crystallisation of membrane proteins after a "long period of fruitless attempts"[78]. In obtaining X-ray quality crystals, the use of both detergents and small amphiphilic molecules were found to be essential. Both types of molecules are often used in the crystallisation of membrane proteins and whilst detergents are seen as a fundamental part of the system the necessity and the function of the small amphiphile is still unclear.

Small amphiphilic molecules are differentiated from detergents by their inability to form micelles. The behaviour of the detergent is significantly affected by the addition of such additives as they interact directly with the micelles by partitioning into the detergent layers[90] thus affecting the CMC, micelle size and phase transitions of the detergent. Sensible use of amphiphiles can allow suppression of detergent phase separation and hence be beneficial to the crystallisation process[91]. One mode of action suggested for these molecules was that they acted to reduce the radius of the micelle belt thereby removing steric hindrance in the formation of the crystal lattice. Since

then it has been shown that the insertion of the small amphiphilic molecule, of heptan-1-2-3-triol reduces the apparent mass and size of both LDAO[92] and β-OG[93] host micelles while increasing their curvature. However, as yet their function has not been adequately explained.

Several drawbacks of adding small amphiphiles to a protein-detergent solution have also been observed. They must be added at relatively high concentrations (typically 1% to 5%) to have an influence on the detergent phase transitions. At these concentrations "side-effects" include protein denaturation, irreproducible nucleation and crystal metastability although their general efficacy may also depend on the precipitant used[81]. Interestingly, the reaction centre from *Rps. viridis* has been the only reported case where crystals could not be grown in the absence of small amphiphilic additives, although there have been many cases where the crystal quality has been improved by their presence[84]. While the additives are thought to be useful in crystallisation of membrane proteins, they are not thought to be essential but rather should be used to "fine-tune" existing crystallisation conditions[91].

A summary list of published crystallisation conditions for membrane proteins including choices for, detergent, amphiphiles, precipants, pH and temperature has been produced by Howard *et al.*[82].

2. BIOCHEMICAL METHODS AND MATERIALS

2.1 Introduction

Throughout the duration of this project, work was carried out on four light harvesting (LH) complexes from purple non-sulphur photosynthetic bacteria of the genera *Rhodopseudomonas* (*Rps.*). Both the B800-820 and B800-850 LH complexes from *Rps. cryptolactis* were studied, along with a further two B800-820 LH complexes from *Rps. acidophila*; from each of the strains 7050 and 7750. The basic biochemical procedures were similar for each complex and this chapter gives an overview of the methods and materials involved. Differences in optimal cell culture and specific experimental details on the isolation, purification and crystallisation of the individual complexes can be found in Chapters 3 and 4.

2.2 Cell culture

The media in which the cells were grown contained all of the nutrients required by the bacteria and was specific to each type. All cultures of *Rps. acidophila* were grown anaerobically in PFENNIGS media[94], an acidic growth medium which contains succinate as the carbon source. Cells of *Rps. cryptolactis* were grown anaerobically in THERMED media[95] (at pH 6.8) which utilises pyruvate as the carbon source.

Initially, cells were streaked out onto agar plates and incubated anaerobically for 2-3 days. Once grown, single colonies were selected and transferred freshly prepared agar, which contained the required growth media. The cells were then allowed to grow anaerobically in the agar for 3 - 4 days, at room temperature, after which time liquid "starter" cultures were prepared by the addition of 15 ml of growth media. The cultures were either grown at room temperature or placed in temperature regulated water baths, which were kept isolated from excess light in order to control the light intensity available to the bacteria. Both the light intensity and the temperature used were

dependant on the type of light harvesting (LH) complex required and on the species of bacteria being grown. The light intensity was controlled by placing the bacteria at various distances from rows of incandescent light bulbs.

Once the starter cultures had grown to a sufficient density (1-4 days) the cells were used to inoculated fresh growth media and again the cells grown under the required conditions. This procedure was repeated until 500 ml flat-sided bottles contained grown bacteria, which were then harvested or kept at 4°C until required. All inoculations were carried out in aseptic conditions in a laminar air-flow cabinet.

2.3 Cell harvesting

In an average purification protocol, six litres of grown bacteria were harvested by centrifugation at 3500 rpm for 20 minutes at 4°C. (Fison MSE Coolspin centrifuge). From six litres of grown bacteria, the general yield from a purification run, which involved separating the B800-850 LH complex from the B800-820 LH complex, was approximately 2.5 mg of protein. After centrifugation, the supernatant was discarded and the pelleted cells were resuspended in the minimum amount of 20mM Tris-HCl, pH 8.00 (at this stage cells that were not required immediately were stored at -20°C). To break the cell walls and release the membranes, the harvested cells were mechanically disrupted by two passages through a French pressure cell, at a pressure of 154 Mpa.

2.4 Solubilisation

The LH complexes were released from the cell membrane and kept soluble using the detergent lauryl-dimethylamine N-oxide (LDAO). The conditions used to solubilise the different LH complexes varied although the general procedure was the same. The starting conditions for solubilisation were based on those used to solubilise the B800-850 LH complex from *Rps. acidophila* strain 10050[96]. These conditions are given below:

- Protein solution : Optical Density at 850 nm[i] (OD_{850}) = 25 cm^{-1}

[i] Optical density was generally used as a measure of protein concentration with an OD of 100 cm^{-1} being equal to ~5mg/ml of protein.

- Detergent concentration: 2% (v/v) LDAO
- Incubation time: 3 hours

Using the above conditions, solubilisation of the cell membranes would be achieved as follows: broken cells were adjusted with 20 mM Tris-HCl, pH 8.0 to a concentration which gave an $OD_{850/820}$ of 25 cm^{-1}. To this, 2% LDAO (v/v) was then added and the solution incubated for 3 hours at 4°C. After incubation the solubilised membranes were centrifuged at 15,000 g for 20 minutes at 4°C to remove any unsolubilised material. The supernatant containing the solubilised complexes was then collected and the pellet containing the unsolubilised material was discarded.

2.5 Isolation of the peripheral LH complex

The peripheral LH complexes (LH2) were isolated from the core light harvesting complex (LH1) and the reaction centre (RC) by the use of discontinuous sucrose density gradients[29].

The gradients were composed of 0.2, 0.4, 0.6 and 0.8 M sucrose solutions, which were prepared in 20 mM Tris-HCl, pH 8.0 and contained 0.1% (v/v) LDAO. Starting with the highest concentration of sucrose, 6.5 ml of each solution was sequentially poured into a 30 ml polycarbonate centrifuge tube, creating the discontinuous gradient. 4 ml of the solubilised complexes were layered on top of the sucrose and the gradients spun in an ultra-centrifuge at 45,000 rpm for 16 hours, at 4°C.

On removing the gradients from the centrifuge it could be seen that the complexes had resolved into two distinct pigmented bands. The lower band comprised the core complex (LH1 & RC) and the upper band contained the LH2 complexes (See Figure 2.1). The LH2 band was easily removed from the gradient, using a pipette.

2.6 Purification

2.6.1 Spectrophotometric estimation of purity

Throughout a purification run, the integrity of the complex and the purity of the preparation were monitored by measuring the ratio of the absorbance at ~820 nm (or ~850 nm) to that at ~280

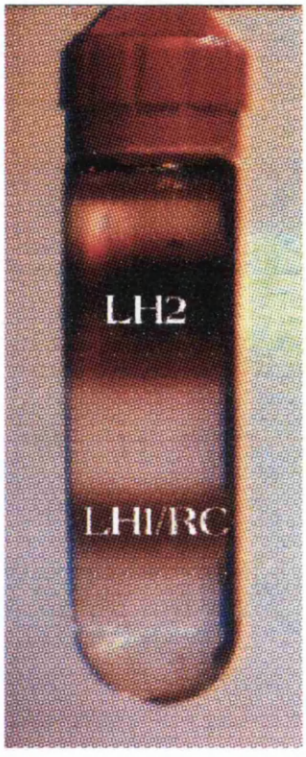

Figure 2.1: Sucrose gradient containing solubilised complexes from *Rps. acidophila* strain 7050.

nm[18] (See Figure 2.2 for a representative absorption spectrum). The bacteriochlorophyll *a* (Bchl *a*) molecules only absorb at 820 nm when stoichiometrically bound to the apoprotein. Therefore, any reduction in this ratio indicates either an decrease in bound pigments, from denatured complexes, or extraneous protein contaminants. This ratio shall be termed as the integrity ratio (I_r) throughout this thesis and typically acceptable values were $I_r \geq 3$.

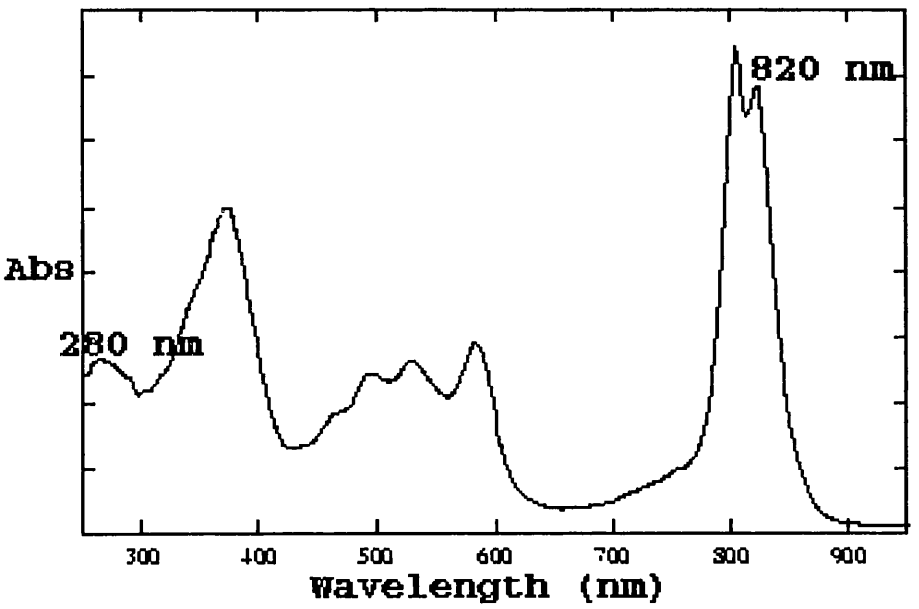

Figure 2.2: A typical absorption spectrum of the B800-820 LH complex from *Rps. acidophila* strain 7050

As a result of the nature of the complexes studied it was found necessary to introduce another spectrophotometric estimation of purity which is discussed in Section 3.2.3.

2.6.2 Gel filtration chromatography

On removal from the sucrose gradients the LH2 complexes were concentrated before being applied to the gel filtration column. A 2 ml aliquot was put into an Amicon 50K "Centricon" (Amicon, Inc., Beverly, USA) and centrifugation dialysis was used to concentrate the protein until an OD820/850 of 40 cm^{-1} was obtained.

Meanwhile, a 120ml Superdex 200 column (Pharmacia Biotech, Uppsala, Sweden), which was

connected to an Fast Protein Liquid Chromatography (FPLC) system, was equilibrated with two column volumes of 20 mM Tris-HCl, pH 8.0 which contained 0.1% LDAO. Once equilibration was complete, a 2 ml aliquot of the concentrated complex was filtered through a 22 μm filter and loaded onto the column. The sample was eluted with the equilibration buffer at a flow rate of 1 ml/min and an elution profile (protein absorption at 280 nm) obtained. The protein was collected from the column in 1 ml fractions.

2.6.3 Anion exchange chromatography

2.6.3.1 Watman DE52 column

Throughout the purification work three different anion-exchange columns were tested for their suitability, the first of which was a Watman DE52 column. A slurry of Watman DE52 diethylethyl-aminoethylcellulose (DEAE) anion exchange matrix was prepared in 20 mM Tris-HCl, pH 8.0, as per manufacturer's instructions. This was poured into a into a 5 cm diameter, gravity-fed glass chromatography column, to a height of $\sim$10 cm, and washed with 150 ml of 20 mM Tris-HCl, pH 8.0. The solubilised complex was taken straight from the sucrose gradients, ($OD_{820/850}$ of $\sim$ 10 cm^{-1}) and was slowly layered on top of the column using a pipette. Elution from the column was achieved by a stepwise gradient, in 50 mM steps, from 0 to 250 mM NaCl in 20 mM Tris-HCl, pH 8.0, 0.1% LDAO. Each step was allowed to flow until the eluent was colourless, suggesting that no further complex would elute at that particular salt concentration. All fractions were collected in $\sim$1 ml aliquots.

2.6.3.2 Q-Sepharose

A 12 ml by 1.5 ml Q-Sepharose column was connected to the FPLC system (Pharmacia Biotech, Uppsala, Sweden) and equilibrated with 50 ml of 20 mM Tris-HCl, pH 8.0, 0.1% LDAO. After equilibration, 5 ml of the solubilised complexes were taken directly from the sucrose gradients, filtered through a 22 μm membrane and loaded onto the column. The protein was then washed with 40 ml of the equilibration buffer before a salt gradient of 0 to 250 mM NaCl, in 20 mM Tris-HCl, pH 8.0, 0.1% LDAO was run at 1 ml/min. The gradient was set up to run in the following

way: 0 - 10% NaCl in 10 minutes, 10 to 100% NaCl in a further 50 minutes. The eluting protein was monitored by its absorption at 280 nm and collected in 1 ml fractions.

2.6.3.3 Resource Q

A 1 ml Resource Q column (Pharmacia Biotech, Uppsala, Sweden) was attached to the FPLC and equilibrated using five column volumes of 20 mM Tris-HCl, pH 8.0, 0.1% LDAO. Again, 5 ml of the solubilised complexes were extracted from the sucrose gradients and filtered through a through a 22 μm membrane. The filtrate was then loaded onto the column and washed with four column volumes of the equilibration buffer. Elution was achieved by running a salt gradient of 0 to 200 mM NaCl[ii] in 20 mM Tris-HCl, pH 8.0, 0.1% LDAO at 2 ml/min. Once again the elution profile was monitored and the protein collected in 1 ml fractions.

Fractions from all chromatographic procedures were assayed spectrophotometrically (Sections 2.6.1 and 3.2.3) for their suitability in crystallisation trials.

2.7 Crystallisation

2.7.1 Detergent exchange

Prior to crystallisation the complex was generally exchanged into 1% β-octyl-glucopyranoside (β-OG) which contained 0.35 M NaCl in Tris-HCl, pH 8.0. To achieve this, 2 ml of the purified complex was transferred into a 50 K Centricon and centrifuged at 12,000 g until a minimum volume was achieved (~300 μl). The concentrated complex was then diluted with detergent-free buffer and again centrifuged to minimum volume. This step was repeated in an attempt to remove as much of the original detergent as possible. After the final wash, the complex was diluted with buffer containing the new detergent (and any additional salt) and the solution again centrifuged until the solution reached the concentration (@$OD_{850/820}$) required for crystallisation.

[ii] The gradients were optimised individually depending on the complex being purified

2.7.1.1 Crystallisation conditions

Crystallisation conditions were screened around the protocol used to obtain diffraction quality crystals of the B800-850 LH complex from *Rps. acidophila* strain 10050[96]. Similar conditions had also been used to grow crystals of both LH2 complexes from *Rps. cryptolactis*[98] and the B800-820 LH complex from *Rps. acidophila* strain 7750[16]. These crystals did not show high resolution diffraction, their poor quality was attributed to the purification protocols employed for the complexes[96]. The conditions used to obtain crystals of the B800-850 LH complex from *Rps. acidophila* strain 10050 were as follows:

- Protein-detergent solution ("Starting OD_{850}") : OD_{850} = 100 cm^{-1}
- Detergent: 1% β-OG
- Additional Salt: 0.35 M NaCl
- Precipitant: 1.0 M K_2HPO_4 (KP_i)
- Small amphiphile: 2.5% benzamidine hydrochloride (BA) (w/v)
- Well solution: 2.2 M ammonium sulphate (AMS), pH 9.3

Using the above conditions the protein would be prepared for crystallisation in the following systematic manner. After detergent exchange the protein was adjusted to give an $OD_{820/850}$ of 100 cm^{-1}, using the detergent solution of 1% β-OG, 0.35 M NaCl in buffer. Enough BA to make the final solution contain 2.5% (w/v) was then weighed accurately, placed in an eppendorf and the protein solution was added. The mixture was then vortexed until the precipitate dissolved (~30 seconds). To this, 1.0 M Kp_i was slowly added from a 4M stock solution in distilled water, pH ~9.2, with a pipette and the solution vortexed until a homogeneous colour was obtained, The final solution[iii] was then centrifuged at 13,000 rpm in an Eppendorf mini-centrifuge for 5 minutes to pellet any solid material.

[iii] It should be noted that the final protein solution therefore had an $OD_{820/850}$ of 75 cm^{-1}, a detergent concentration of 0.75% β-OG and a NaCl concentration of 0.26 M.

Crystallisation trials were set up using the sitting drop method for vapour diffusion. Originally 'Cryschem' trays (Charles Supper Company, Natick, USA) were used but these were later replaced with 'Linbro' trays containing poly-propelene bridges. 15 μl of the prepared protein solution was equilibrated against a 1 ml well solution of AMS, at the necessary concentration and pH and trays were incubated at 18°C.

2.7.2 Artificial mother liquor

Artificial mother liquor (AML) was required to work with crystals of the B800-820 LH complex from *Rps. acidophila* strain 7050. Steeping the crystals in AML allows them to be handled more easily and has been known to improve the resolution of the diffraction shown by the crystals[99]. Moreover, AML was needed to introduce cryoprotectant into the system (See Section 2.7.3).

Fortunately, AML had been previously formulated for use with the B800-850 LH complex from *Rps. acidophila* strain 10050[96] and the only change made to the protocol was to equilibrate the AML against the well solution used to produce crystals of the B800-820 LH complex. The AML consisted of 0.5% β-OG (w/v), 0.35 M NaCl and 1.5 M KP_i in 20 mM Tris-HCl, pH 8.0. Three 300 μl drops containing this AML were equilibrated against 8 ml of 2.3 M AMS at pH 9.7 for between 36 and 48 hours. This was achieved using a 10 cm diameter vapour diffusion dish, containing a 3 drop bridge (pictured in Cogdell & Hawthornthwaite 1993[23]).

2.7.3 Cryoprotectant

To protect the crystals from radiation damage, X-ray diffraction data was generally collected from crystals flash-cooled to 100K. For this, a cryoprotectant was required to safeguard the crystal against the cold air. A cryoprotectant had been previously devised for use with the crystals of the B800-850 LH complex from *Rps. acidophila* strain 10050[100]. This was found to work well with crystals of the B800-820 LH complex and was composed of 50% saturated sucrose and 50% AML. This was prepared by making a solution which contained 0.7 M NaCl and 3.0 M KP_i to which an equivalent amount of saturated sucrose was added. After mixing, 0.5% β-OG (w/v) was added and stirred slowly until the detergent dissolved. To the final solution phosphoric acid was added to give a final pH equal to the equilibrated AML.

Cryoprotectant was introduced slowly into the crystals by dialysis. A crystal was taken from the crystallisation drop using a thin walled quartz glass capillary tube, attached to a syringe and placed in a 10 μl microdialysis button (Cambridge repetition engineers ltd., England) containing 5 μl AML. Dampened molecularporous membrane tubing (Spectrum, Alondra, USA) was used to cover the well and the button placed upside down in a sealed vessel, containing cryoprotectant. The buttons were then incubated at 18°C for around 16 hours. For X-ray diffraction studies the crystals were loop mounted straight from the dialysis button and placed in the cryo-stream.

2.8 Mass spectrometry

2.8.1 Isolation of the apoproteins

The molecular weights and populations of the apoproteins, which comprise the LH complexes, were investigated using mass spectrometry. To achieve this, the protein must firstly be isolated by extraction of the pigment molecules from the complex.

A 7 : 2 (v/v) acetone : methanol solution was used to extract both the Bchl *a* and the carotenoid molecules[101]. Extraction was achieved by adding 2 ml of this solution to 30μl of the purified protein complexes, which had been exchanged previously into detergent-free buffer (using the method described in Section 2.7.1). The solution was then centrifuged at 5000 rpm for 15 minutes, producing a pellet containing the apoprotein and leaving "free" pigments and detergent molecules in the supernatant. The supernatant was discarded and the apoproteins were re-dissolved to remove any remaining pigments and again the solution centrifuged. This process was repeated until the pellet appeared colourless, suggesting that the protein was free of all pigment moieties.

2.8.2 Preparation of the sample

Protein was prepared for mass spectrometry as described by Schindler[102]. After isolation, the apoprotein was re-dissolved in a 2 : 5 : 2 chloroform : methanol : water (v/v/v) mixture which contained sufficient glacial acetic acid (HOAc) to make the final solution 1% HOAc. Enough solvent was added to obtain a protein concentration of ~2 mg/ml. For electrospray analysis, 2 : 5 : 2 chloroform : methanol : water (v/v/v), 1% glacial HOAc was also as the carrier solvent.

3. PERIPHERAL LIGHT HARVESTING COMPLEXES FROM RHODOPSEUDOMONAS CRYPTOLACTIS

3.1 Introduction

The initial work in this project was carried out on a recently discovered species of photosynthetic bacteria called *Rhodopseudomonas cryptolactis*[95]. *Rps. cryptolactis* is a thermotolerant species of purple non-sulphur bacteria and was first isolated in 1990 from hot springs in North America. Like certain other species and strains of purple bacteria, *Rps. cryptolactis* can produce both a B800-850 and a B800-820 LH complex, depending on its growth conditions. In contrast to other species of purple bacteria, there is very little published material concerning the characterisation of the photosynthetic apparatus of *Rps. cryptolactis* and the primary sequence of the apoproteins from the light harvesting (LH) complexes have yet to be determined.

Crystals of the both the B800-820 and the B800-850 LH complexes from *Rps. cryptolactis* had been reported previously, but showed diffraction to only 5.5 Å and 10 Å, respectively[98]. These crystals had been prepared using a purification and crystallisation protocol similar to the one employed to produce the first reported crystals of the B800-850 LH complex from *Rhodopseudomonas acidophila* strain 10050[103], which also diffracted poorly. However, with the LH complex from *Rps. acidophila* several changes were made to the original purification protocol over a period of time which eventually resulted in the growth of X-ray quality crystals and subsequent structure determination of the complex[1]. The purification and crystallisation protocols employed during the structure determination were reported to have great bearing on the level and reproducibility of observed diffraction[96]. The *original* and the *optimised* protocols for this complex are shown in Table 3.1.

"Some conclusions" were made regarding the increased crystal quality with respect to the changes in the practical work and these are described in detail previously[96]. It was concluded that

ORIGINAL PROTOCOL	OPTIMISED PROTOCOL
Solubilisation conditions	**Solubilisation conditions**
Protein with OD_{850} = 50 cm^{-1}	Protein with OD_{850} = 25 cm^{-1}
1% LDAO (v/v)	2% LDAO (v/v)
Incubated for 5 minutes at rm. temp.	Incubated for 2 hours at 4°C
Isolation of LH2 from LH1/RC	**Isolation of LH2 from LH1/RC**
Whatman DE52 column	Sucrose density centrifugation
Purification	**Purification**
120 ml Sephacryl S-200 column	120 ml Superdex 200 FPLC column
Detergent exchange	**Detergent exchange**
Mini DE52 column	Centrifugation dialysis
Integrity ratio	**Integrity ratio**
$I_r \geq 2.8$	$I_r \geq 3.0$
Crystallisation conditions	**Crystallisation conditions**
Protein solution: OD_{850} = 150 - 200 cm^{-1}	Protein solution: OD_{850} = 100 cm^{-1}
Intial Detergent: 1.0% β-OG	Initial Detergent: 1.0% β-OG
Precipitant: 0.9 M Kp_i	Precipitant: 1.0M Kp_i
Additional salt: None	Additional salt: 0.35 M NaCl
Small amphiphile: 2.5% BA	Small amphiphile: 2.5% BA
Well solution: 2.3 M AMS pH 9.3	Well solution: 2.1 M AMS pH 9.0
Incubation Temperature: 20°C	Incubation Temperature: 18°C

Table 3.1: The original and optimised protocols used in producing crystals of the B800-850 LH complex from *Rps. acidophila* strain 10050.

the marked improvement in the reproducibility and resolution of diffraction of the crystals was acheived using methods of separation based on size rather than charge[1]. Therefore, the primary aim of this section was to use a purification protocol based on size, in an attempt to obtain X-ray quality crystals of the B800-820 LH complex from *Rps. cryptolactis*, which would allow structure determination and eventual comparison with the crystal structure of the B800-850 LH complex from *Rps. acidophila* strain 10050[1].

Work began on the B800-820 LH complex using the *optimised* purification protocol and various parameters were changed as required. Subsequent biochemical analyses and crystallisation trails were also carried out on the B800-850 LH complex from *Rps. cryptolactis* and this chapter describes the work on both complexes. This work ended prematurely with the production of X-ray quality crystals from the B800-820 LH complex from a different species of bacteria: *Rps. acidophila* strain 7050 (see Chapters 4, 5 and 6). However, it was the experience gained from working with *Rps. cryptolactis* that allowed a relatively easy route to these crystals. This chapter aims to summarise the work carried out on *Rps. cryptolactis*, in the hope that it may be beneficial to the next researchers in this field.

3.2 The B800-820 light harvesting complex from Rps. cryptolactis

3.2.1 Cell growth

Working with proteins found in the photosynthetic membrane meant the that problems often encountered expressing and refolding membrane proteins were not an aspect of the project. Since photosynthetic membrane proteins are isolated from a natural source they are available in copious amounts and are generally well characterised. However, although growing cells of *Rps. cryptolactis* which contained LH2 complexes was straightforward, producing the B800-820 LH complex as the sole form of LH2 proved to be non-trivial. Therefore, the initial aim of the project was to produce cells that contained a single type of LH2 complex: the B800-820 light harvesting complex.

Obtaining cells which contained the B800-820 LH complex as the sole form of LH2 was considered very important. It was thought that similarities between the B800-820 and the B800-850 LH complexes would make separating the two complexes extremely difficult[29], and that lack

of a pure single complex would be detrimental to obtaining X-ray quality crystals. However, producing cells which contained the B800-820 LH complex alone was assumed entirely feasible since other species (and strains) of purple bacteria had been reported to produce a single B800-820 LH complex when grown under the correct conditions[16, 104, 101]. Like other species and strains of bacteria, *Rps. cryptolactis* was reported to produce the B800-820 LH complex when subject to reduced light intensity[95], although the effect of temperature and other environmental growth conditions had never been investigated for this species of bacteria.

Work began with an attempt to identify the correct light intensity for optimal production of the B800-820 LH complex. When this proved unsuccessful the effects of various other parameters were examined both individually and simultaneously over a period of several months. A brief outline of the various conditions that attempted is given below:

Light intensity:

- 1 x 25 W to 3 x 100 W incandescent light bulbs.
- Bulbs placed 30 cm to 100 cm from the cells.
- Varied or kept constant during cell growth.
- Cells grown behind bacteria containing the B800-850 LH complex at various light intensities[i].

Temperature

- Tested between 34°C and 46°C.
- Varied or kept constant during cell growth.
- Changed with or independent of light intensity.

[i] The most novel attempt to produce the B800-820 LH complex was an idea devised by Dr. Stephen M. Prince to use cells containing the B800-850 LH complex as a filter. It was thought that by specifically narrowing the wavelength range of the light available, the cells could be forced to produce the B800-820 LH complex. Although a bottle was designed especially for this purpose, cells grown behind the "B800-850 filter" did not grow at all under low light intensities and continued to grow with the B800-850 LH complex when the light intensity was high.

Growth media

- Decreased amounts of pyruvate (carbon source).
- pH varied from 6.4 to 7.2.

The above parameters were optimised until an absorption spectrum taken of the whole cells indicated the presence of the B800-820 LH complex only (Figure 3.1). To achieve this, cells were grown from single colonies at 42°C in a thermostatically controlled water tank surrounded by 6 x 100 W illuminated light bulbs. When enough bacteria had grown to fill a 500 ml bottle they were moved to a tank at 39°C and placed 30 cm from a single illuminated 40 W bulb. Cells were inoculated with 3:1 parts fresh growth media to grown bacteria every 1-2 days and after 3-4 inoculations the cells were producing the B800-820 LH complex, as shown in Figure 3.1.

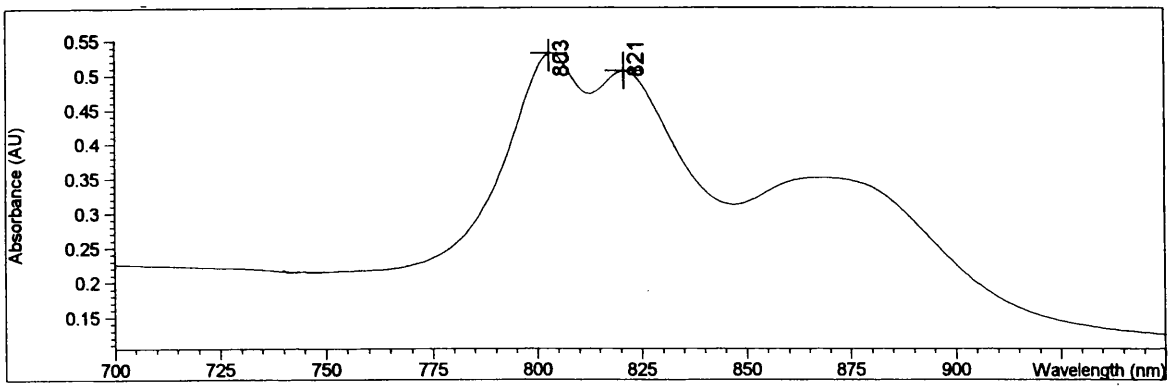

Figure 3.1: Whole cells of *Rps. cryptolactis* containing the B800-820 LH complex as the major form of LH2.

The major peak at ~875 nm is from the absorption of the Bchl a *molecules in LH1.*

Whilst working with the bacteria, several aspects of the growth of *Rps. cryptolactis* were noted which may be useful for those working with this species of bacteria. These can be found in Appendix A.

3.2.2 Purification

The aim of this section was to purify the B800-820 complex from *Rps. cryptolactis* using a purification protocol based on size, whilst using the integrity ratio (I_r) (see Section 2.6.1) to monitor both the purity and the integrity of the complex throughout the procedure. After the cell growth had been optimised to a level where only the B800-820 complex was assumed present, it was disappointing to realise that this was not the case. On removing the LH2 band from the sucrose gradients, the absorption spectrum showed that the sample still contained a certain amount of the B800-850 LH complex .

3.2.2.1 Initial detection of the B800-850 LH complex

The actual Bchl *a* absorption maxima of the B800-820 and the B800-850 LH complexes from *Rps. cryptolactis* are found at 800 nm and 819 nm and, at 804 nm and 858 nm, respectively. In a sample which predominantly contains the B800-820 LH complex, the presence of a small amount of the B800-850 LH complex can be detected easily by looking at the absorption spectrum. At 858 nm, the B850 absorption maximum in *Rps. cryptolactis* is spectroscopically distinct from the peak at 819 nm and gives rise to a individual absorption peak, denoted as the B850 shoulder (see Figure 3.2). This is not the case in bacteria where the B850 absorption peak lies nearer to the absorption due to the B820 molecules (see Section 4.3.3.3)

3.2.2.2 Gel filtration chromatography

B800-850 and B800-820 LH complexes from the same species of bacteria were reported to be of similar shape and size with the main difference residing in subtle changes in the apoprotein, which would in some way affect the Bchl *a* absorption maxima[5]. Also, native B800-820 LH and B800-850 LH complexes from *Rps. cryptolactis* were reported to run similarly on a SDS-PAGE system; with each having an apparent molecular weight of 85 Kd[98ii]. Consequently, it seemed that separating the two complexes based on size would be impractical. However, growing cells

[ii] It should be noted that the apparent weight of the complex on an electrophoretic gel can often be misleading as a result of bound detergent molecules[105]

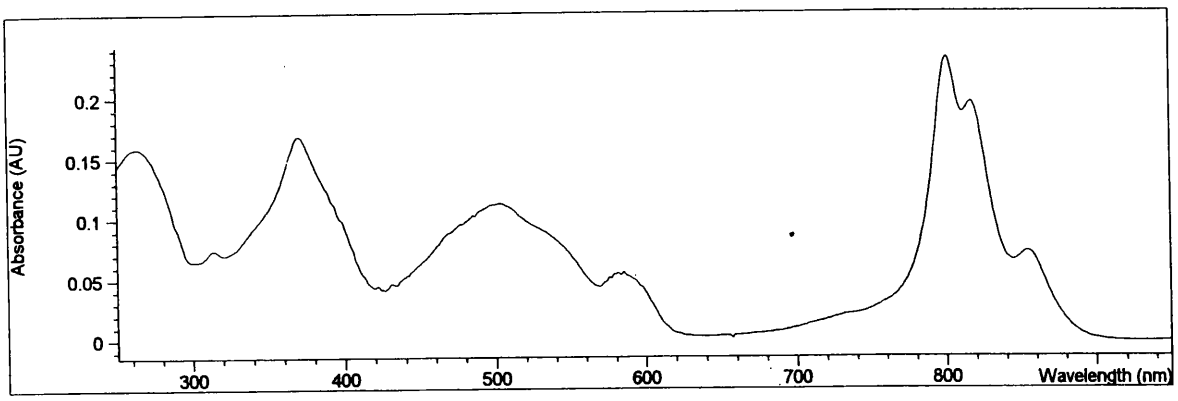

Figure 3.2: The absorption spectrum of the B800-820 LH complex which contains an amount of the B800-850 LH complex; shown by the peak at ~850 nm.

which produced the B800-820 complex as the only form of LH2 was more difficult than was first anticipated and it was decided to follow the intended protocol with the best sample available.

Running the complex down a molecular sieve column gave surprising results. As the protein eluted from the column, the protein concentration (OD_{280}) was detected using a UV-monitor. Plotted against time, a symmetrical elution profile was obtained, suggesting that no separation of the two complexes had been achieved. However, assaying each of the fractions individually gave a different result. Individual absorption spectra taken for each of the collected fractions showed that the amount of the B800-850 LH complex contaminating the sample decreased towards the latter end of the elution peak (Figure 3.3).

Unfortunately, the fractions which did not show an absorption peak at 850 nm were very dilute and generally had an integrity ratio (I_r) ≤ 2. Several attempts were made to optimise this procedure and although none of the modified parameters had a marked effect on the elution profile, it was noted that lower flow rates ($\leq$ 1 ml/min) did give a slightly better separation and that elution buffers containing detergent concentrations greater than 0.2% (v/v) lowered the I_r throughout the run. Overall, gel filtration chromatography gave very little of the B800-820 LH complex without a B850 shoulder and samples containing the most homogeneous form of the complex were very dilute and did not have values of $I_r > 3$. Nevertheless, crystallisation trials were set up using the

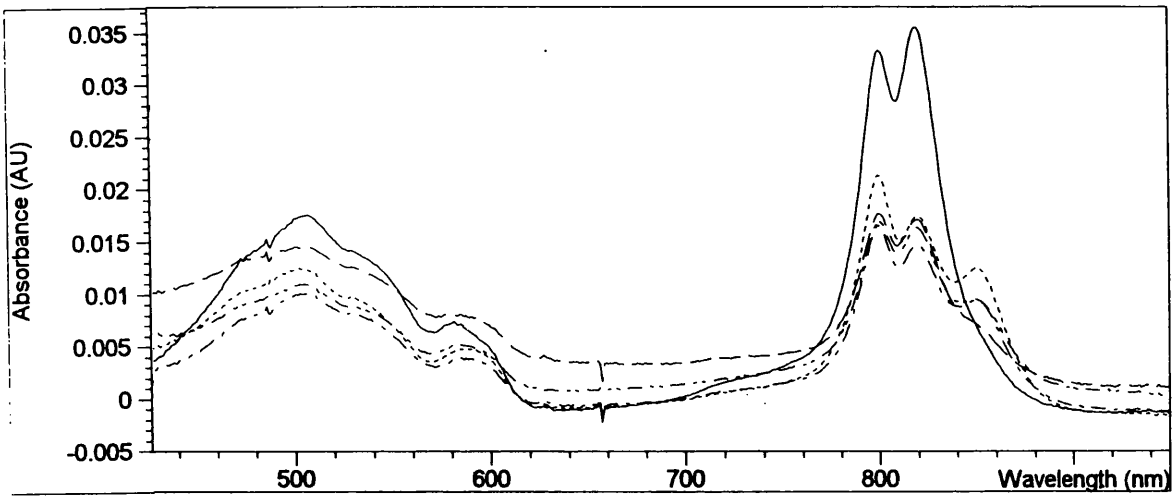

Figure 3.3: Fractions of the complex taken from the gel filtration column, showing that the B850 shoulder decreases towards the end of the run.

"best" protein available but these failed to yield any crystal forms.

In general large molecules will flow more rapidly through gel-filtration media than smaller molecules. The reason for this is that smaller molecules can diffuse more easily into the gel, whereas larger molecules are prevented by their size from doing so to the same extent. From this it would be easy assume that the B800-850 LH complex was larger than, or of a different shape to, the B800-820 LH complex. However, with membrane proteins the situation can often be more complicated. The inclusion of varying amounts of lipids in solubilised complexes can render the complexes buoyant as a result of density factors rather than aggregate size. Also, non-ideal interactions between the complexes and the chromatographic media can yield misleading results[59]. Therefore, it is not clear whether the modest separation was a result of a difference in the shape and/or size of the native complexes *in vivo* or because differences in the detergent solubilised protein and/or their interactions with the chromatographic media. However, what it did imply was that there was some scope for attempting to separate a mixture of LH2 complexes from *Rps. cryptolactis*.

3.2.2.3 *Sucrose gradients*

The gel filtration chromatography results suggested that a separation of the two complexes based on size or shape may have been possible. Since the initial isolation of LH2 from LH1 and the RC is achieved by the use of sucrose density gradients (Section 2.5), it was decided to modify this procedure in an attempt to separate the two forms of LH2 at this stage in the purification. Initially, samples were taken from the top, middle and bottom of the LH2 band in a standard gradient, and an absorption spectrum of each sample was measured. From these it could be clearly seen that the B850 shoulder in the complex increased towards the bottom of the band (Figure 3.4).

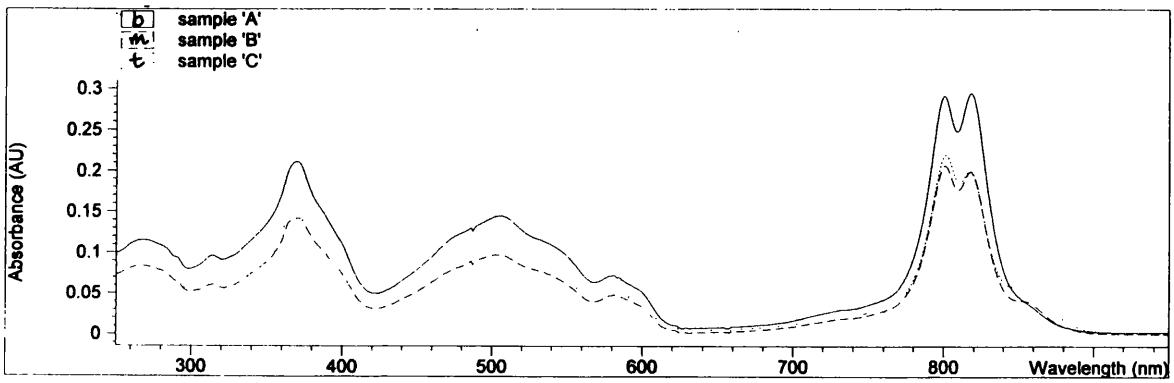

Figure 3.4: The absorption spectra of three samples taken from the top (t), middle (m) and bottom (b) of the LH2 band of a sucrose gradient.

The separation of a mixture using density centrifugation is generally achieved because of differences in the mass, density or shape of the components[106]: a 200kD protein will move twice as fast as a 100 kD protein as the sedimentation velocity if a particle is proportional to its mass; a dense particle will move more rapidly than a less dense one as the opposing buoyancy is smaller for a less dense particle, and the shape is important as dissimilarly shaped molecules will move through the solution at varying speeds because of differences in their viscous drags. On centrifugation, the B800-850 LH complex moved through the solution further than the B800-820 LH complex. This corroborates the results from the molecular sieve column in showing the two detergent-solubilised complexes to be different in shape or size, with the B800-850 LH complex

being the "larger" of the two.

The general method used for sucrose density centrifugation employs the use of discontinuous density gradients. Although this is a standard procedure, it is considered fairly elementary and continuous gradients are often used where a more effective separation of sample components is required. In an attempt to improve this procedure, continuous gradients of varying concentrations were poured: 0.0 M - 0.8 M sucrose; 0.0 M - 0.6 M sucrose; 0.2 M - 0.6 M sucrose in buffer, 0.1% LDAO, but no improvement in the separation of the two complexes was accomplished.

3.2.2.4 Initial anion exchange columns

Improving the purification protocol from which X-ray quality crystals of the B800-850 LH complex from *Rps. acidophila* strain 10050 were obtained, removed all of the steps which purified using charge. From these results it was assumed that anion-exchange chromatography would not provide the ideal purification procedure for LH2 complexes[96]. However, lack of homogeneity in the complex would also hinder the formation of X-ray quality crystals and since separation on size did not seem possible, anion-exchange chromatography was attempted. Experimental procedures were carried out as described in Section 2.6.3.

Initially, protein taken from the sucrose gradients was loaded onto a gravity-driven Whatman DE52 column and a small amount of the sample which did not bind was collected. An absorption spectrum showed the sample to contain the B800-850 LH complex, however it was denatured (I_r ~0.9) and cross-contaminated with the B800-820 complex. Adding 50 mM NaCl in buffer, 0.1% LDAO to the column caused several other fractions to elute. The absorption spectra of these samples showed the B800-850 LH complex to be present in varying amounts with respect to the B800-820 LH complex. The remaining protein eluted in the presence of 100 mM NaCl, with the B850 shoulder gradually decreasing (but not completely disappearing) towards the end of the run.

Fractions with the smallest peaks at 850 nm were collected and subsequently loaded onto the molecular sieve column. However, this did not produce any greater separation of the two complexes than had been achieved using gel filtration alone. Changes in the protocol, *e.g.*, stepwise gradients with smaller changes in the salt concentration, did not improve the results. Again, only a small amount of protein deemed suitable for crystallisation trials was collected but no

crystals were obtained.

Along with the gravity-driven column, DEAE Sephacel and Q-Sepharose anion exchange columns were used on a Fast Protein Liquid Chromatography (FPLC) (Pharmacia Biotech, Uppsala, Sweden) system. A range of continuous and step-wise gradients were tested but no improvement on the above was protocol was achieved for either column. In an attempt to obtain more of the B800-820 LH complex all of the samples which were discarded for crystallisation trials were pooled together, because they contained an amount of the B800-850 LH complex. These were dialysed overnight against Tris-HCl, pH 8.0 which contained 0.1% LDAO to remove the salt. The salt-free complexes were then reapplied to both columns but the absorption spectra of all the collected fractions showed peaks at 850 nm, implying that no further separation was possible using these methods. From these purification runs several crystallisation trials were set up but no crystal forms were obtained.

3.2.2.5 Anion exchange chromatography using a Resource Q column

In contrast to the above anion exchange columns, elution of the complexes from a Resource Q column (Pharmacia Biotech, Uppsala, Sweden) showed a marked improvement in separating the two LH complexes compared using a molecular sieve.

The protein was loaded onto the 1 ml column and a small amount which did not bind and was collected. Predominately, this sample contained the B800-850 LH complex, although it was rather denatured.

After washing the column with 5 mls of Tris-HCl, pH 8.0 containing 0.1% LDAO, several step-wise and continuous salt gradients were employed to elute the protein. The gradient which gave the best separation was 0 - 200 mM NaCl in 20 minutes and using this, the protein eluted as a series of peaks. Fractions containing the largest amounts of the B800-850 LH complex eluted first and those with the least B850 shoulder eluted towards the end of the run. A diagram of a typical elution profile and the corresponding absorption spectra from a range of samples is shown in Figures 3.6 and 3.7. Using this column the B850 shoulder disappeared much earlier in the elution profile than had been witnessed previously, leaving a sufficent amount of 'shoulder-free' protein that more extensive crystallisation screens could be attempted.

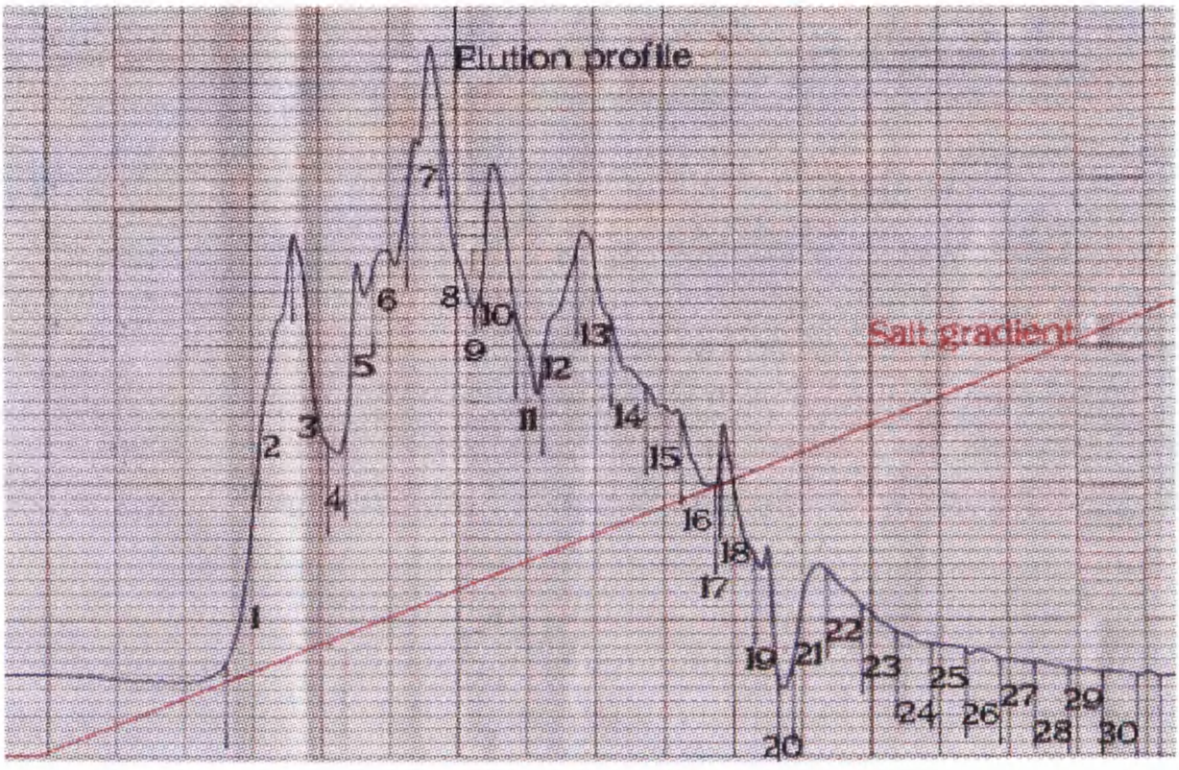

Figure 3.5: A general elution profile obtained for the B800-820 LH complex when purified using a Resource Q column.

The fractions collected are numbered 1 to 30

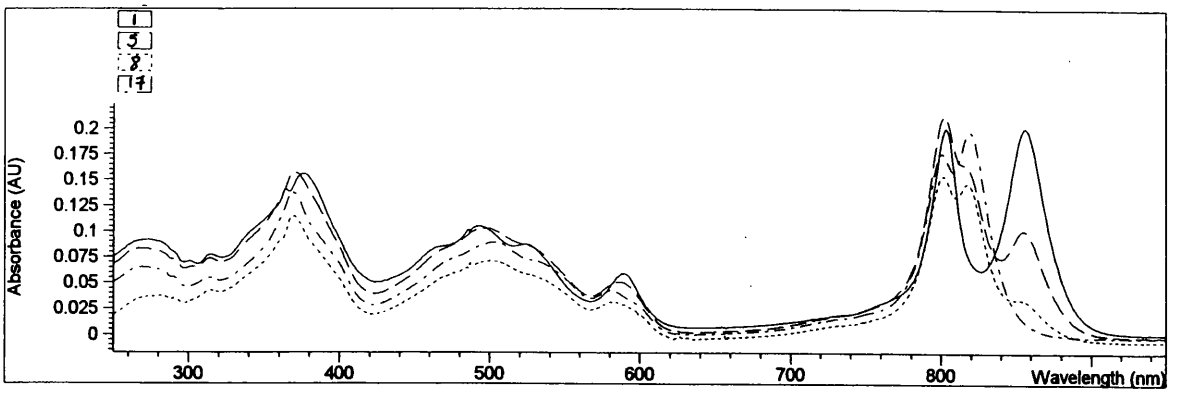

Figure 3.6: The absorption spectra obtained from fractions numbered 1, 5, 8 and 17 from the above purification run.

By around fraction number 14 there was no noticable B850 absorption peak.

Other advantages of this small column were that a single purification run took around 40 minutes with only a few minutes required between runs to re-equilibrate the column. This allowed the salt gradient to be optimised in a few hours and many purification runs to be carried out in the same day. Given a limited yield, this was important in order to be able to set up crystallisation trials soon after purification.

3.2.3 Measuring the homogeneity of the complex

When a sample of the B800-820 LH complex contained a significant amount of the B800-850 LH complex, the "impurity" could be seen easily in the absorption spectra by the presence of the B850 shoulder. However, once it was established that this impurity could be minimised or, in fact, removed, it became apparent that a method of monitoring the B800-850 LH complex at low concentrations would be required. This was particularly relevant as the protein did not elute from the Resource Q column as two distinct peaks but instead as a procession of small peaks.

To monitor the homogeneity of the complex, the ratio of the B820 to B800 absorption peaks was calculated. Both types of LH2 complex contain similarly absorbing B800 molecules and consequently the presence of the B800-850 LH complex enhances the 800 nm absorption peak relative to the 820 nm peak (see Figure 3.8). The ratio calculated from the peak heights has

been termed the "Peak ratio" and shall be denoted P_r. Since there were no published values for P_r, those calculated were set as standards to measure the effectiveness of subsequent purification procedures.

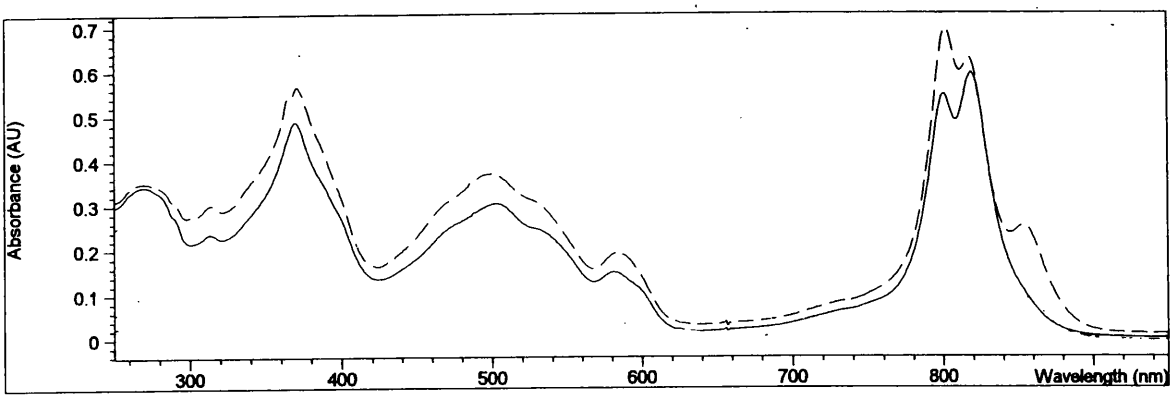

Figure 3.7: Absorption spectra highlighting the difference in the 800 and 820 nm peak heights when a B800-850 impurity is present in the sample.

It is also reasonable to calculate the difference in heights between the absorption from the B850 and the B820 molecules, but as the B850 shoulder decreases this value becomes less stable. From the Resource Q column, ratios at 819 nm : 800 nm and at 819 nm : 858 nm were calculated from each of the collected fractions. From these the correlation co-efficient between the two sets of ratios was calculated using CORREL in Xcel (Microsoft) and they were found to be 96% correlated.

In general, samples of the B800-820 LH complex from *Rps. cryptolactis* with $P_r \geq 1.1$ and $I_r \geq 3.0$ were chosen for crystallisation trials. After the protein was purified, several samples were taken for analysis using mass spectrometry. The results obtained showed at least four peaks present in the region 5 - 7kD implying that the complex contains multiple polypeptides. However, the results were inconclusive in predicting the molecular weight and abaundance of the polypeptides but have been included in Appendix B as a reference for any further purification work carried out on the complex.

3.2.4 *Solubilisation conditions*

One of the final experiments carried out on the B800-820 LH complex from *Rps. cryptolactis* was to test the effect of altering the concentration of detergent used to solubilise the complex from the cell membrane. Before solubilisation, the protein was divided into four separate aliquots, each having an OD_{820} of 40 cm^{-1}. These batches were made to contain 0.5%, 1.0%, 1.5% and 2.0% LDAO (v/v) and incubated for 1 hour. No other changes were made to the purification protocol and after the samples were removed from the sucrose gradients (all of which were in 0.1% LDAO), the absorption spectrum of each was measured. At this stage all of the samples had a P_r of ~0.9 and were then taken individually and applied to a Resource Q column. All of the samples gave similar elution profiles and which allowed 30 fractions (numbered 1 - 30) to be collected and assayed spectrophotometrically, (see Figure 3.6) for a typical elution profile. From these assays it was normal to collect fractions with $P_r \geq 1.1$ for use in crystallisation trials and the concentration of the protein generally decreased with fraction number *e.g.* fractions numbered 25 - 30 were dilute in comparison to the earlier fractions. Accordingly, it was that found solubilising with higher concentrations of detergent resulted in less protein being collected for crystallisation trials. Moreover, the P_r of the collected fractions of this protein were also lower than the P_r of the corresponding fractions from protein which had been solubilised with less detergent. This can be seen in Table 3.2.

CSB	Frac. Col.	P_r range
0.5%	13 - 25	1.12 - 1.23
1.0%	16 - 25	1.11 - 1.21
1.5%	17 - 25	1.08 - 1.17
2.0%	18 - 25	1.06 - 1.13

Table 3.2: Solubilisation conditions and the effect of the purification of the complex.

- CSB : Concentration of the solubilisation detergent
- Frac. Col. : The fractions collected for use in crystallisation trials.
- P_r range: The range of P_r corresponding to the first and last collected fractions.

From these results, it appears that using a high detergent concentration is not beneficial when

solubilising this complex, as lower concentrations gave an increase in both the amount of protein obtained and in the homogeneity of the complex. However, what is not known is the effect that such low concentrations would have on completely removing the membrane lipids from the complex and if this would effect the likelihood of crystal formation and/or the crystal quality. However, small crystals were obtained using 0.5% LDAO as the solubilising detergent and these are described in the next section, in a summary of all the crystals obtained of this complex.

3.2.5 Crystallisation

Crystallisation trials were set up after each purification run and a summary of the different ranges of conditions attempted is given in Table 3.3.

Parameter	Units	Values	In steps of
Protein absorption at 820 nm	cm^{-1}	40 - 120	10
Precipitant: Kp_i	M	0.8 & 0.2	N/A
Well solution: AMS	M	2.1 - 2.5	0.2
Well solution: AMS	pH	9.3 - 9.9	0.1
Added salt: NaCl	M	0.35	N/A
Small Amphiphile: BA	% (w/v)	2.5	N/A

Table 3.3: Crystallisation parameters screened.
All protein was crystallised in 0.75% β-OG.

Crystals of the B800-820 LH complex were not obtained unless the Resource Q column was employed to purify the protein. Several wells contained small crystals and some of them were tested for their suitability in X-ray analysis, no diffraction was observed. The time and detergent concentration used to achieve solubilisation of the complexes differed although the protein solution was always at a concentration which gave OD_{820} of 40 cm^{-1}. The successful solubilisation (Solb. Cond.) and crystallisation conditions are given in Table 3.4 where OD_{820} cm^{-1} was the "starting OD" of the protein (see Section 2.7).

Solb. Cond	OD_{820} cm^{-1}	Kp_i (M)	AMS (pH)	Results
2% LDAO, 1 hour	70	1.0	9.5	~50μl x 50μl; thin with poor-defined morphology
2% LDAO, 1 hour	70	0.8	9.3	~50μl x 50μl; tabular but not single
2% LDAO, 1 hour	110	1.0	9.5	micro-crystals
2% LDAO, 1 hour	80	1.0	9.3	~100μl x 100μl; poorly-defined morphology
0.5% LDAO, 1 hour	70	0.8	9.4	tiny, thin crystals, well-defined (cubic?) morphology
1% LDAO, 3 hours	90	0.8	9.5 & 9.7	50μm x 50μm x 0.5μm; well-defined morphology (cubic?) (see Figure 3.8

Table 3.4: Crystals obtained for the B800-820 LH complex from *Rps. cryptolactis.*

All protein was crystallised against 2.3M AMS and contained 2.5% (w/v) BA

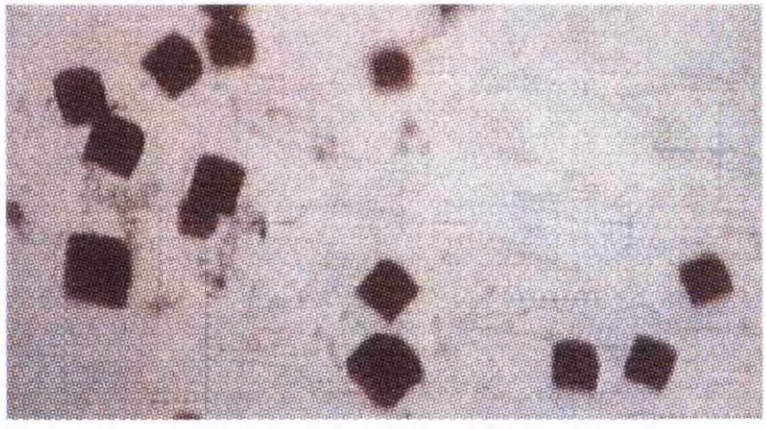

Figure 3.8: Crystals of the B800-820 LH complex from *Rps. cryptolactis*

3.3 *The B800-850 LH complex from* Rps. cryptolactis

Although the original aim of the work carried out in this thesis was structure elucidation of a B800-820 light harvesting complex (more specifically from *Rps. cryptolactis*), problems with the initial growth of the bacterium meant that there was time to work on other complexes. The first complex chosen for this purpose was the B800-850 LH complex from the same species of bacteria. This high-light grown complex was chosen primarily for its apparent ease of growth, *i.e.*, cells of *Rps. cryptolactis* were thought to produce the B800-850 complex as a single LH2 complex without much difficulty. Also, because of the differences in the structures of the B800-850 LH complexes from *Rps. acidophila* strain 10050[1] and *Rhodospirillum* (*Rs.*) *molischianum*[30] there are many questions that only further structural analysis of additional LH complexes will answer.

3.3.0.1 *Cell growth*

Cells were grown as outlined in Chapter 2, Section 2.2. More specifically, the cells were grown in a thermostatically-controlled water bath at 42°C which was surrounded by 6 x 100 W incandescent light bulbs. Cells were inoculated using 3:1 fresh growth media to grown bacteria. General observations on the growth of *Rps. cryptolactis* are also given in Appendix A.

3.3.0.2 *Crystallisation*

Like the B800-820 LH complex, the initial protocol used to purify this complex closely followed the method employed to produce X-ray quality crystals of the B800-850 LH complex from *Rps. acidophila* strain 10050. Several purification runs were carried out using this procedure with only the crystallisation conditions being changed. A large number of sitting drop trays were set up using a variety of conditions and the parameters were changed both individually and simultaneously, using protein with the maximum value of I_r available (generally around 2.6). These parameters are not outlined in detail as a lack of results prevented any real rationale from being applied to the system. However, the ranges of conditions are summarised in Table 3.5.

Every trial, with the exception of one, produced amorphous precipitation and denatured pro-

Parameter	Units	Values	In steps of
Protein absorption at 850 nm	cm^{-1}	20 - 140	10
Precipitant: Kp_i	M	0.5 - 1.5	0.1
Well solution: AMS	M	1.5 - 3.0	0.1
Well solution: AMS	pH	9.0 - 10.0	0.1
Added salt: NaCl	M	0.0 - 0.35	0.02
Small Amphiphile: BA	% (w/v)	0.0 - 4.0	0.5

Table 3.5: Initial crystallisation parameters screened

tein[iii]. The only micro-crystalline precipitate observed throughout this work was from protein which had been solubilised in 2% LDAO for 3 hours, had an I_r of 2.0 and an P_r of 1.15, a starting OD_{850} of 70 cm^{-1} and was crystallised in the presence of 0.8% KP_i and 2.5% BA (w/v) and against a well solution of 2.4 M AMS at pH 9.3. Obtaining this "crystal form" was, however, found to be irreproducible.

During the time spent on crystallisation, the speed of purification was also considered, and although the entire procedure (from extracting the complex to setting up crystallisation trials) was accelerated from 5 days to 2.5 days, no noticeable effect on crystallisation was observed. At this stage the failure in the crystallisation trials was ascribed to some aspect of the purification procedure and it was decided to begin to improve on this by re-analysing the solubilisation conditions.

3.3.1 Solubilisation

Improvements made to the purification protocol for the B800-850 LH complex from *Rps. acidophila* strain 10050, which led to growth of X-ray quality crystals, included changes in the parameters used to solubilise the complex[96]. The time, protein concentration and detergent concentration used in solubilising the complex were all different from those used in the *original* protocol (see Section 3.1).

[iii] As the complex denatures the solution changes from the colour attributed to the carotenoid (e.g. purple or orange) to green resulting from the "free" Bchl *a* in solution.

3.3.1.1 *Detergent concentration and protein concentration*

The protein and the detergent concentration were the first parameters to be varied when solubilising the complex from the cell membrane. Two batches of protein were prepared in buffer for solubilisation: one with a starting OD_{850} of 25 cm^{-1} (Batch A) and another with an OD_{850} of 50 cm^{-1} (Batch B). Each batch was divided into 5 separate aliquots with enough detergent added to make them 0.5%, 1.0%, 2.0%, 3.0% and 4.0% LDAO (v/v) ($A/B_{0.5}$, A/B_1, A/B_2, A/B_3 and A/B_4, respectively) and the samples incubated for 1 hour, at 4°C.

In addition to monitoring the effect that the different solubilisation conditions had on obtaining crystals of the complex, the fraction of complex released from the cell membrane was also measured. To observe this the absorption was measured at 858 nm after detergent was added to the cells (OD_{pre}) and then again from the supernatant (containing the solubilised complexes) once the unsolubilised material had been removed (OD_{aft}) (see Section 1.14 for solubilisation details). From the results $\frac{OD_{aft}}{OD_{pre}}$ was calculated for all samples and the results shown in Table 3.6.

Protein	$\frac{OD_{aft}}{OD_{pre}}$	Protein	$\frac{OD_{aft}}{OD_{pre}}$
$A_{0.5}$	0.77	$B_{0.5}$	0.77
$A_{1.0}$	0.83	$B_{1.0}$	0.80
$A_{2.0}$	0.84	$B_{2.0}$	0.83
$A_{3.0}$	0.82	$B_{3.0}$	0.81
$A_{4.0}$	0.80	$B_{4.0}$	0.79

Table 3.6: Differing protein concentrations (A and B) showing the effect of detergent on the amount of complex released from the cell membrane.

From these results it can be seen that there are no dramatic effects on the quantity of protein retrieved from the cells. However, the maximum amount of protein in solution was attained when a detergent concentration of between 1% and 2% LDAO was used. The slight drop in the ratio after 2% is assumed to be a result of the complex denaturing and hence it would appear that solubilising with 3% detergent or above could be detrimental to the complex. From Table 3.6 it can also be observed that with a higher protein concentration slightly more detergent is required to affect the solubilisation.

All of the individual protein solutions were purified using gel filtration chromatography and corresponding crystallisation trials set up; no crystals were obtained.

3.3.1.2 Solubilisation against time

In a experiment similar to the above, the detergent concentration was kept constant and the time used to achieve solubilisation was varied. Again, the protein was divided into two batches, A (OD_{850} of 25 cm^{-1}) and B (OD_{850} 50 cm^{-1}). Each of these were divided into 6 individual samples denoted A"*time*" and B"*time*" and solubilised for 15, 30, 60, 90, 120 and 150 minutes. The absorption at 858 nm was again measured before solubilisation (OD_{pre}) and also from the supernatant after solubilisation had been effected (OD_{aft}). The results reported in Table 3.7.

Protein	$\frac{OD_{aft}}{OD_{pre}}$	Protein	$\frac{OD_{aft}}{OD_{pre}}$
A_{15}	0.87	B_{15}	0.76
A_{30}	0.81	B_{30}	0.78
A_{60}	0.83	B_{60}	0.76
A_{90}	0.81	B_{90}	0.72
A_{120}	0.83	B_{120}	0.72
A_{150}	0.75	B_{150}	0.74

Table 3.7: Differing protein concentrations (A and B) showing the effect of time on the amount of complex released from the cell membrane.

Again no dramatic effect was observed on the amount of the complex released from the cell membrane. However, it did suggest that a longer time period was not beneficial in releasing the complex from the membrane and that it may actually have been slightly detrimental. This is contrary to what was reported for solubilising the B800-850 LH complex from *Rps. acidophila* strain 10050, where incubating the protein for a longer period of time was though to be beneficial in obtaining X-ray quality crystals[96]. From this set of results, it appeared that solubilisation was effected more successfully when the protein concentration was lower and this agreed with similar changes made to the solubilisation conditions for the B800-850 LH complex from *Rps. acidophila* strain 10050[96]. All of the separate batches of protein were used individually in crystallisation trials but no improvement in obtaining crystals was observed.

These experiments, which looked at the solubilisation parameters, gave no evidence to suggest that an increase in time and detergent concentration were beneficial when solubilising the complex, even though both of these were increased from the *original* to the *optimised* purification protocol for the B800-850 LH complex from *Rps. acidophila* strain 10050. From these two protocols the concentration of protein used was halved and these experiments confirmed that working with a lower concentration of protein allowed a slightly more effective solubilisation. However, since no crystals forms were observed it is difficult to say whether or not these parameters played (or would play) a part in obtaining X-ray quality crystals of the complex.

3.3.2 Purification

Since crystallising the complex was continually unsuccessful it was decided to change the purification methods. At this stage, the separation of the B800-850 LH complex from the B800-820 LH complex had already been achieved using the Resource Q anion exchange column and all previous B800-850 LH complexes had been purified using gel-filtration chromatography because it was assumed that only the B800-850 LH complex was present. However, the presence of a B800-820 LH complex is not easily observed by examination of the absorption spectra because the 819 nm peak lies in the valley between the 800 nm and the 858 nm peaks and so does not give a peak that is distinct from the absorption peaks from the B800-850 LH complex (see Figure 3.10). Therefore, anion exchange chromatography was employed in an attempt to identify any amount of the B800-820 LH complex which may have been present and perhaps impeding the formation of crystals.

3.3.2.1 Anion exchange chromatography

Protein taken from the sucrose gradients was loaded onto a Resource Q column and a salt gradient of 0 - 200 mM NaCl was set up to run over 20 minutes. However, the protein began to elute in the presence of $\sim$25 mM NaCl, at which stage the salt gradient was kept constant. The initial fractions collected were assayed spectrophotometrically and appeared to contain the B800-850 LH complex alone. Once the protein ceased eluting the salt gradient was allowed to continue and at higher salt concentrations the presence of the B800-820 LH complex was observed, although these fractions

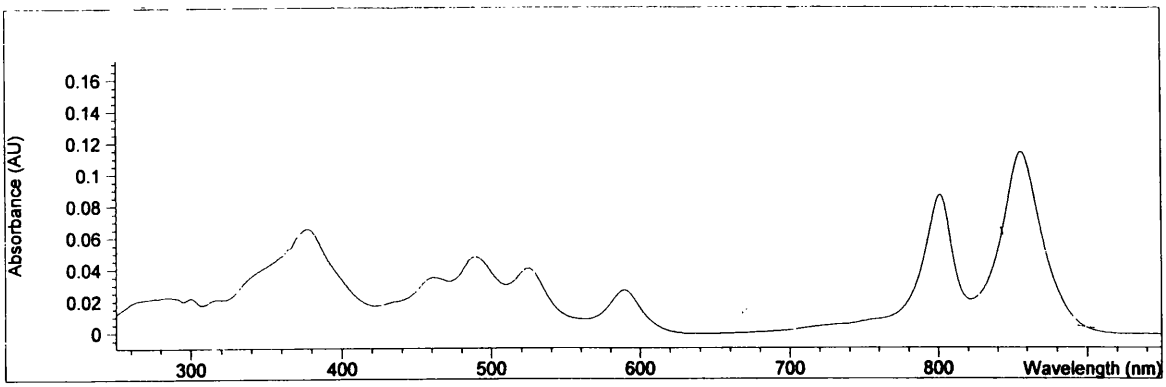

Figure 3.9: The absorption spectrum of the B800-850 LH complex which is cross contaminated with the B800-820 LH complex.

were dilute and the sample denatured. For all of the collected fractions, the value of P_r (800 nm: 850 nm) was calculated and was found to decrease towards the end of the run. Two different salt gradients were attempted and protein which had a $P_r \geq 1.1$ and an $I_r \geq 3.0$ was collected for use in crystallisation trials but again no crystals were obtained.

To show the improvement in the removal of the B800-820 LH complex using the Resource Q column and the use of P_r, a comparison of the values of P_r plotted against the fraction number for the Resource Q column and the molecular sieve column for the B800-850 LH complex from *Rps. cryptolactis* are shown in Figure 3.11.

At this stage the project was taken over by a final year honours student, Iain Mitchell. He optimised the salt gradient but found that the value of P_r did not differ much from those given above. Iain also observed that similar values of P_r were obtained regardless of the amount of B800-820 LH complex present in the sample at the beginning of the preparation.

3.3.3 Detergent exchange

After the introduction of the anion-exchange column the crystallisation detergent was changed from 1% β-OG, 350mM NaCl in Tris-HCl, pH 8.0 to 0.2% LDAO which contained 2% glycerol in the same buffer. Crystallisations set up using a standard crystallisation screen (see Table 3.3 for

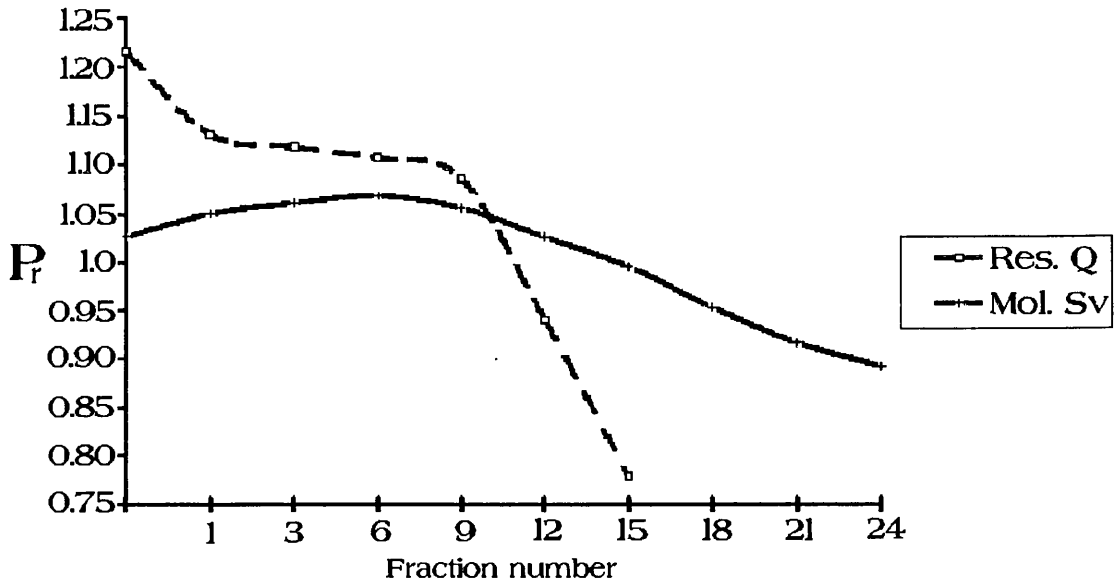

Figure 3.10: P_r plotted against equivalent fraction numbers: The lower the value of P_r, the more the B800-820 "impurity" is present.

From the graph it can be seen that the values for P_r change dramtically when the Resource Q column was employed showing that a greater separation of the two complexes was achieved.

general crystallisation conditions) produced micro-crystalline precipitate (Figure 3.11).

Figure 3.11: Micro-crystalline precipitate of the B800-850 LH complex from *Rps. cryptolactis*

The most encouraging aspect of this precipitate was that it retained the colour of the intact complexes. It seems that although the complex was previously reported to crystallise in 1% β-OG[98] it may be worthwhile testing other crystallisation detergents.

It should also be noted that mass spectrometry (MS) results for the complex showed the presence of at least 3 peaks in the region of 5 - 5.6 kD which suggests that the complex may have more than a single α and β polypeptide. The primary sequence of the apoproteins from this species of bacteria are not known and the MS results obtained were inconclusive but have been included in Appendix B as a reference for any further purification work carried out on the complex.

4. B800-820 LIGHT HARVESTING COMPLEXES FROM RHODOPSEUDOMONAS ACIDOPHILA STRAINS 7750 AND 7050

4.1 Introduction

This section of work was carried out on B800-820 LH complexes from the purple bacterium *Rhodopseudomonas* (*Rps.*) *acidophila* strains 7750 and 7050. *Rps. acidophila* was first isolated in 1969[94] and takes its name from the fact that the optimal pH for its growth is 5.2. To date, the light harvesting (LH) complexes from strains 10050, 7750 and 7050 of *Rps. acidophila* have been well characterised. Strain 10050 produces a single type of peripheral light harvesting (LH2) complex: the B800-850 LH complex. Strains 7750 and 7050 can both produce a B800-820 LH complex, in addition to the B800-850 LH complex, depending on the cell growth conditions. Like many other species of bacteria, strain 7050 synthesises the B800-820 LH complex in response to reduced light intensity. However, strain 7750 is more unusual in that it produces a B800-820 LH complex in response to a reduction in temperature[29].

The B800-850 LH complexes from all three strains and the B800-820 LH complex from strain 7050 are composed of a single α and β apoprotein. The B800-820 LH complex from strain 7750 is reported to be composed of two α (α_1, α_2) and two β (β_1, β_2) apoproteins[16]. The primary sequence of the apoproteins from the all of the peripheral light harvesting complexes from all strains of *Rps. acidophila* have been determined[107], with the exception of α_2.

The first reported crystals of a LH2 complex from *Rps. acidophila* were those of the B800-850 LH complex from strain 10050[103]. This was also the first LH2 complex to have its 3D structure determined by X-ray crystallography[1]. Crystals of the B800-820 LH complex from *Rps. acidophila* strain 7750[16] have also been obtained although crystallisation has not been reported for any other LH2 complex from this species.

The objective of this section was to produce X-ray quality crystals of a B800-820 LH complex,

from either *Rps. acidophila* strain 7750 or 7050. Again, the aim was to improve on any purification protocols attempted previously and to begin by closely following the successful methods used to obtain X-ray quality crystals of the B800-850 LH complex from *Rps. acidophila* strain 10050 (see Section 3.1). By comparison with the light harvesting complexes from *Rps. cryptolactis*, only a modest amount of time was spent on developing purification protocols for these complexes and the experience gained from working with *Rps. cryptolactis* was found invaluable, particularly for latter work on strain 7050.

4.2 The B800-820 LH complex from Rps. acidophila strain 7750

4.2.1 Introduction

The crystals of the B800-820 LH complex from *Rps. acidophila* strain 7750 had not shown diffraction beyond 6Åresolution[16] and like the poorly diffracting crystals from strain 10050, the complex had been purified using a mixture of techniques based on both size and charge. Therefore, the initial aim was similar to that for working with the LH2 complexes from *Rps. cryptolactis*, *i.e.* to modify the original purification protocol used on strain 10050, adopting the methods employed to crystallise the B800-850 LH complex from *Rps. acidophila* strain 10050. In the latter stages of this work, experience gained from working with *Rps. cryptolactis* was also considered.

4.2.2 Cell growth

Unlike *Rps. cryptolactis*, the growth conditions for *Rps. acidophila* had been well documented[101, 104]. As stated previously, *Rps. acidophila* strain 7750 synthesises the B800-820 LH complex in response to a lowering of the growth temperature. The cells were initially grown at room temperature in front of three 100 W incandescent light bulbs (high light (HL) conditions). Once grown, the cells were used to inoculated fresh growth media, using 8 parts media to 1 part grown bacteria. When sufficient cells had grown to inoculate a 500 ml bottle, they were transferred to a temperature-controlled water tank at 22°C and the available light now came from two 40 W illu-

minated light bulbs placed 30 cm from the bottles[i]. Fresh cells were inoculated every 2-3 days and after 3-4 inoculations the absorption spectra from the cells showed the presence of a B800-820 LH complex (see Figure 4.1).

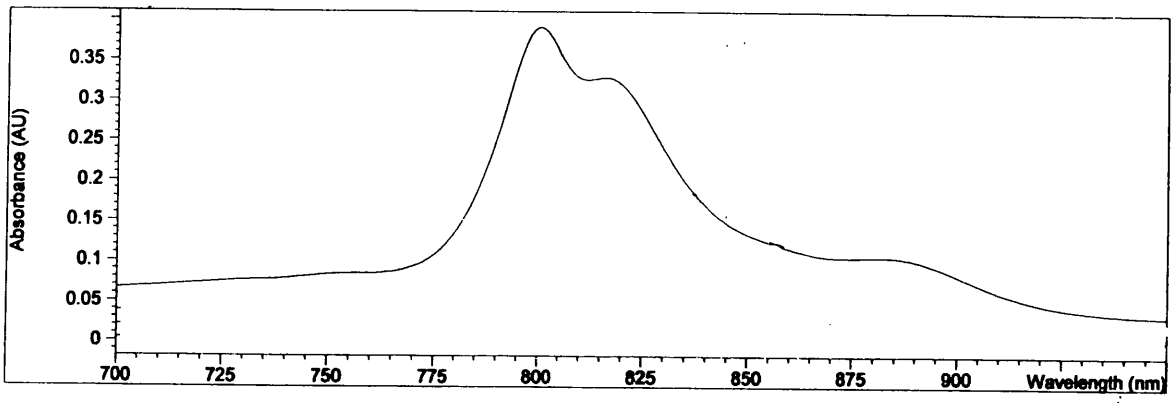

Figure 4.1: Whole cells of *Rps. acidophila* strain 7750 containing the B800-820 LH complex.

4.2.3 Solubilisation

The conditions used to solubilise the B800-820 LH complex from *Rps. acidophila* strain 7750 were not altered throughout the various purification procedures employed. The membranes were adjusted to give an OD_{820} of 25 cm^{-1}, to which 2% LDAO (v/v) was added and the solution incubated for 2 hours, at 4°C. On removal from the sucrose gradients the LH2 band gave an absorption spectrum which suggested that only the B800-820 LH complex was present, *i.e.*, there was no obvious absorption peak at 850 nm (see Figure 4.2).

4.2.4 Purification

4.2.4.1 Gel filtration chromatography

The complex was initially purified using a molecular sieve column and a symmetrical elution profile was obtained for the run. All 1 ml fractions were assayed spectrophotometrically and

[i] For this study, the complex was grown under reduced light conditions although it is not known if this had any effect on the type of complex present.

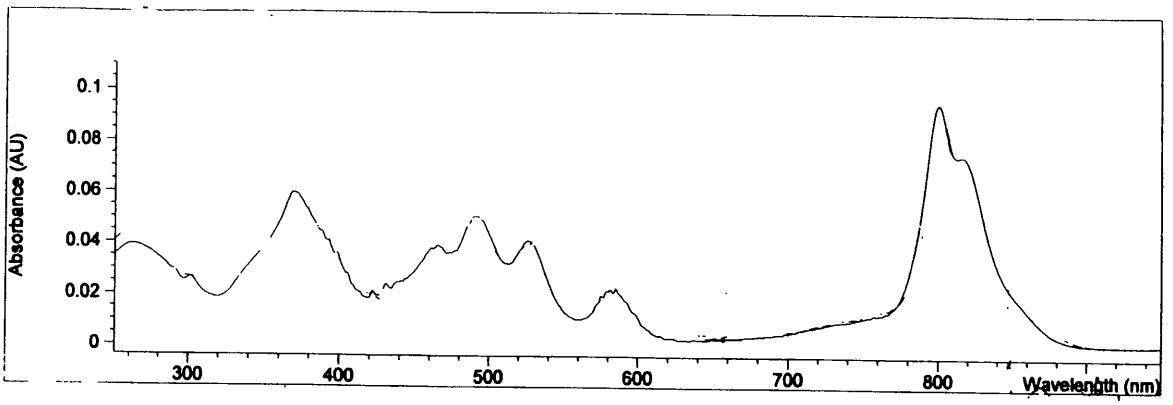

Figure 4.2: The absorption spectrum of the isolated LH2 band taken from the sucrose gradients.

from the absorption spectra there was little evidence to suggest that a B800-850 LH complex was present in the sample, *i.e.*, none of the fractions showed a B850 absorption peak. However, on re-examination of the absorption spectra some time later it was noticed that the values of the purity ratio (P_r) changed gradually over the elution peak, showing values ranging from $\sim$0.7 to $\sim$0.8. For crystallisation trials column fractions with $I_r \geq 3$ were collected but no crystals were obtained.

4.2.4.2 Anion exchange chromatography

Anion-exchange chromatography was later employed in an attempt to further purify the complex and to investigate the possibility of cross-contamination with the B800-850 LH complex. Initially, the protein was loaded straight from the sucrose gradients onto a DEAE Sephacel anion exchange column but the complex did not bind. Subsequently, purification using a Resource Q column was attempted and again a quantity of the protein did not bind to the column. This was collected and the absorption spectrum showed the presence of a slight B850 shoulder (see Figure 4.3).

Elution of the complex was achieved using the salt gradient previously optimised for the purification of the B800-820 LH complex from *Rps. cryptolactis*. However, most of the protein had left the column by the time the 40 mM NaCl was added. Absorption spectra were taken from all of the collected 1 ml fractions and the value of P_r was calculated for each one. From these a slight difference was observed in the values of P_r from $\sim$0.7 to $\sim$0.8 with increasing NaCl concentra-

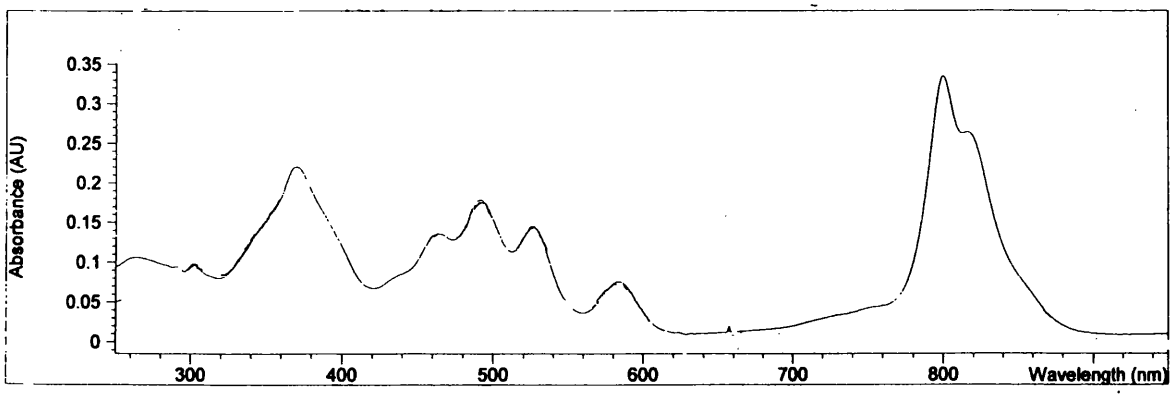

Figure 4.3: The absorption spectrum of the initial fraction collected from the Resource Q column.

tion. Several unsuccessful attempts were made to optimise the salt gradient, however, the greatest value of P_r obtained for this complex remained around 0.8.

From these results, there was no evidence to suggest that any real separation of the two forms of LH2 had been achieved. This may have been because of the purification procedure or simply because there was not a great deal of the B800-850 LH complex present in the sample. Fractions which contained $I_r \geq 3$ and $P_r \geq 0.8$ were collected for use in crystallisation trials.

4.2.5 Crystallisation

Crystallisation of the B800-820 LH complex from *Rps. acidophila* strain 7750 was attempted using the range of conditions tried is shown in Table 4.1.

Parameter	Units	Values	In steps of
Starting OD_{820}[ii]	cm^{-1}	80 - 140	10
Precipitant: Kp_i	M	0.8 - 1.2	0.1
Well solution: AMS	M	2.1 - 2.5	0.1
Well solution: AMS	pH	9.0 - 9.5	0.1
Small Amphiphile: BA	%, (w/v)	2.5	N/A

Table 4.1: Ranges of crystallisation conditions attempted.

The initial protein solution was in 1% β-OG and 0.35 M NaCl prior to the addition of any crystallising agents.

The only promising results observed for this complex were unfortunately micro-crystalline. This protein was purified using the Resource Q column and crystallised succesfully under the following conditions:

- Protein solution: Starting $OD_{820} = 90\ cm^{-1}$
- Initial detergent solution: 1% β-OG, 0.35 M NaCl
- Precipitant: 0.8 M Kp_i, pH ~9.2
- Small amphiphile: 2.5% BA
- Well solution: 2.3 M AMS pH 9.0

4.2.6 Mass spectrometry

Mass spectrometry can be extremely useful when working with LH complexes for which the molecular weights of their apoproteins have been previously determined. This technique allows the presence of extraneous protein contaminants to be identified and in particular those present because of cross contamination of a second form of LH2. Therefore, the aim was to calculate the molecular weights of the apoproteins for the B800-850 and the B800-820 LH complexes from their published sequences[107] and to compare these results to those obtained from the mass spectrometer for the B800-820 LH complex.

The molecular weights of the apoproteins from *Rps. acidophila* strain 7750 were calculated from their primary sequences, with the exception of α_2 for which the primary sequence is not known. The results are shown in Table 4.2

Complex	Type	MW	Type	MW
B800-850	α	5653.7	β	4554.2
B800-820	α_1	5566.6	β_1	4721.4
B800-820	α_2	ud	β_2	4506.1

Table 4.2: Molecular weights of apoproteins from the LH2 complexes.

MW = molecular weight in Daltons (D) & ud = undetermined.

Prior to investigation of the apoproteins by electrospray mass spectrometry, the B800-820 LH complex from *Rps. acidophila* strain 7750 was purified by anion-exchange chromatography and the pigments extracted as described in Section 2.8.1. The major and minor peaks obtained from the mass spectrometer are shown in Table 4.3 along with the particular apoprotein that the peak might represent.

Abundance	MW	Apoprotein
Major	4721.5	β_1
Major	4583.5	?
Minor	4553.5	β
Minor	4744.4	?
Minor	5599.0	?

Table 4.3: Mass spectrometry results for the B800-820 LH complex from *Rps. acidophila* strain 7750.

It was difficult to account for all but the largest peak at 4721.5 D (β_1). However, the presence of a small peak at 4553.5 D suggests that the β-apoprotein from the B800-850 LH complex was present in the sample. From these results, it would also appear that α_1 was not soluble in the chosen solvent.

4.2.7 Discussion

From the purification and mass spectroscopy work, it was not obvious how much B800-850 LH complex was present, in the sample. However, assuming that a small amount was present then a different purification protocol would have to be employed for future work on this complex. However, since the B800-820 LH complex is comprised of multiple polypeptides, of which β_1 and β_2 contain a different number of amino-acids, only a few attempts were made to purify it. Although the mass spectrometry results did not confirm the presence of all the documented apoproteins, any form of multiple polypeptide would introduce a degree of heterogeneity into the preparation which would be almost impossible to remove. For this reason, it was decided that work would continue on the B800-820 LH complex from *Rps. acidophila* strain 7050, which was reported to consist of a single α- and β-apoprotein.

4.3 The B800-820 LH complex from Rps. acidophila strain 7050

The crystallisation of the B800-820 LH complex from *Rps. acidophila* had not been reported previously, although several attempts had been made to crystallise it[104]. Work began on this complex after a large amount of work on *Rps. cryptolactis* had been completed. Therefore, the aim was to apply the knowledge gained from working with *Rps. cryptolactis* to purify this complex.

4.3.1 Cell growth

Rps. acidophila strain 7050 produces a B800-820 LH complex in response to a reduction in light intensity. The principles applied to the growth of this strain of bacteria were the same as those used for growing *Rps. acidophila* strain 7750 (see Sections 2.2 and 4.2.2) and only changed when conditions specific to producing the B800-820 LH complex were required.

After 500 ml of cells were grown at high light conditions, the bacteria were moved to a temperature controlled water tank at 30°C. The light now available to the bacteria was reduced to one 25 W incandescent light bulb, which was placed 100 cm from the cells. This produced cells which absorbed at ~800 and ~820 nm, suggesting that only the B800-820 LH complex was present (see Figure 4.4).

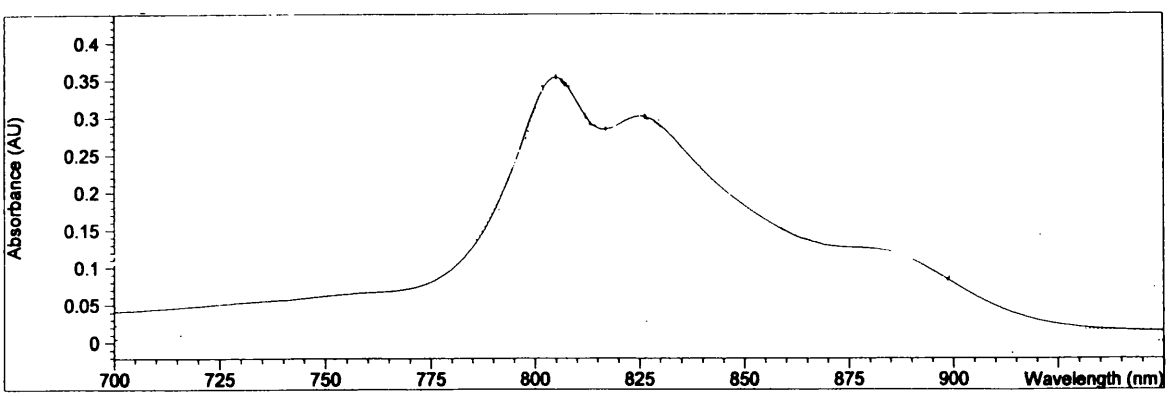

Figure 4.4: The absorption spectrum of the whole cells of *Rps. acidophila* strain 7050.

4.3.2 *Solubilisation*

The initial condition used to solubilise the B800-820 LH complex from *Rps. acidophila* strain 7050 were the same as those used for strain 7750. However, it was later decided to solubilise at a higher protein concentration where OD_{820} was 40 cm^{-1} and this remained constant throughout all subsequent purification procedures. Hence, after two passages through the French pressure cell, the membranes were diluted with buffer to give an OD_{820} of 40 cm^{-1}. To this, 2% LDAO (v/v) was added and the resulting solution incubated at 4°C for 3 hours. Like strain 7750, when the LH2 band was removed from the sucrose gradients, the absorption spectrum of the sample suggested that only the B800-820 complex was present in the cells (see Figure 4.5).

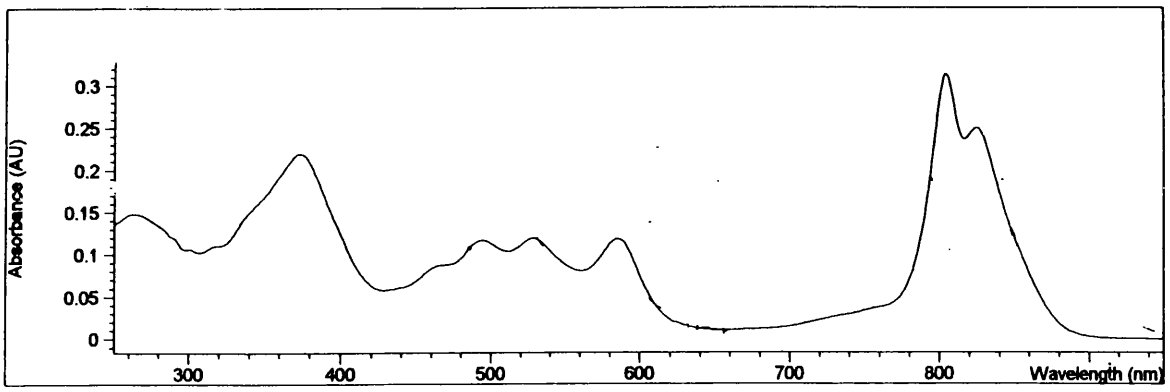

Figure 4.5: The absorption spectrum of the isolated LH2 band taken from the sucrose gradients.

4.3.3 *Purification*

4.3.3.1 *Anion-exchange chromatography*

The first purification method selected for the B800-820 LH complex from *Rps. acidophila* strain 7050 was anion-exchange chromatography using a Resource Q column. When the protein was loaded onto the column a small amount of the sample did not bind and was collected. This sample had absorption peaks at ~800 and ~850 nm but was denatured. Elution of the bound complex was subsequently achieved with an optimised salt gradient of 0 - 200 mM NaCl in 16 minutes. Initial

fractions contained the B800-850 LH complex with subsequent fractions containing a mixture of the B800-850 and the B800-820 LH complexes in varying amounts and at higher salt concentrations a pure B800-820 LH complex was obtained. Figures 4.6, 4.7 and 4.8 show a typical elution profile, a variety of the corresponding absorption spectra and comparative absorption spectra from the second and nineteenth fractions, respectively. For crystallisation trials, fractions with $P_r \geq 0.93$ and $I_r \geq 3.0$ were collected and these were typically obtained from fractions 18 - 21 of Figure 4.6; and X-ray quality crystals were obtained (see Section 4.3.4).

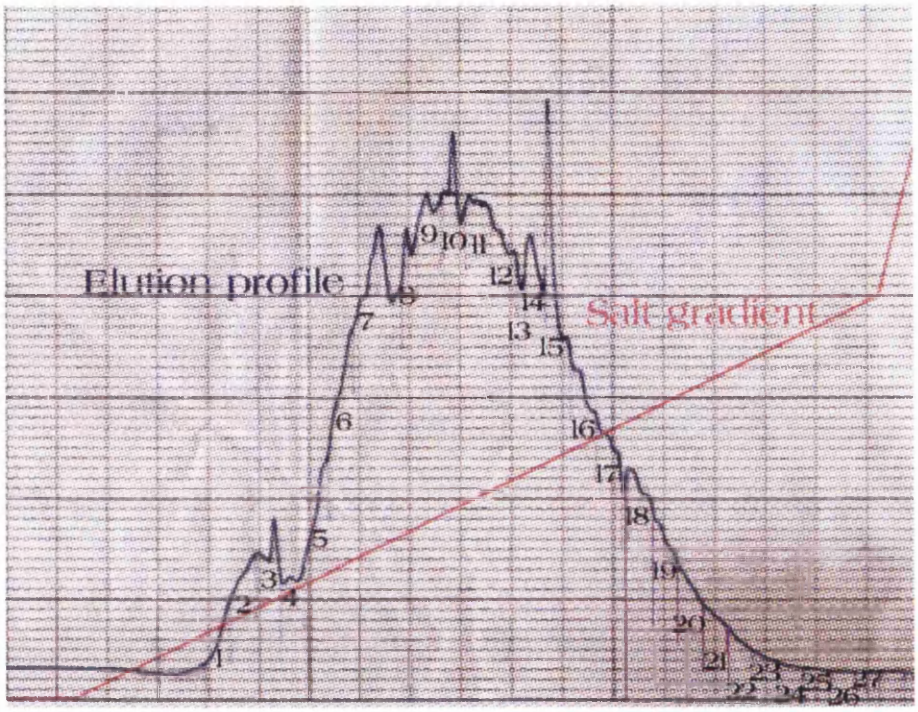

Figure 4.6: A typical elution profile obtained from the Resource Q column.
Fractions numbered 18 - 21 were generally collected from use in crystallisation trials

4.3.3.2 Gel filtration chromatography

The behaviour of the complex on a gel filtration column was investigated and compared to the results obtained from working with *Rps. cryptolactis*.

Applying the isolated complex to the molecular sieve did not result in any separation of the

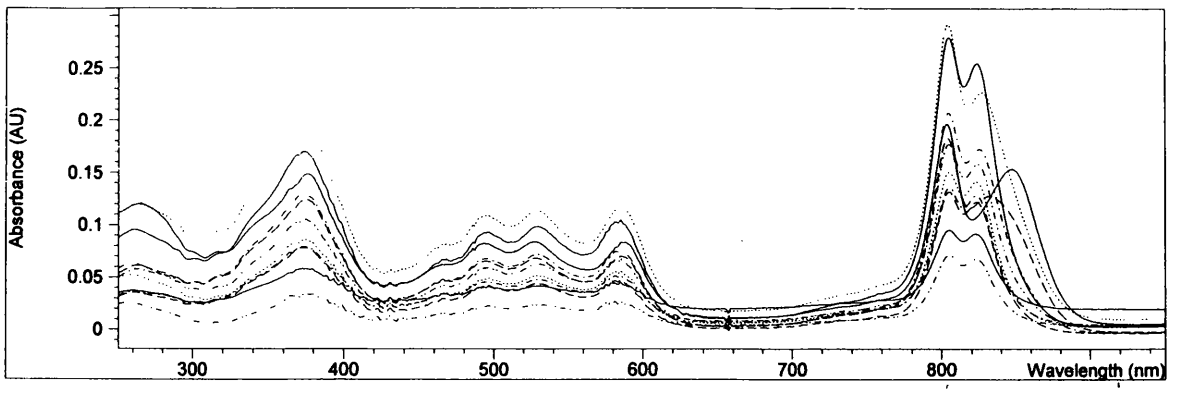

Figure 4.7: The absorption spectrum from a variety of collected fractions across the peak.

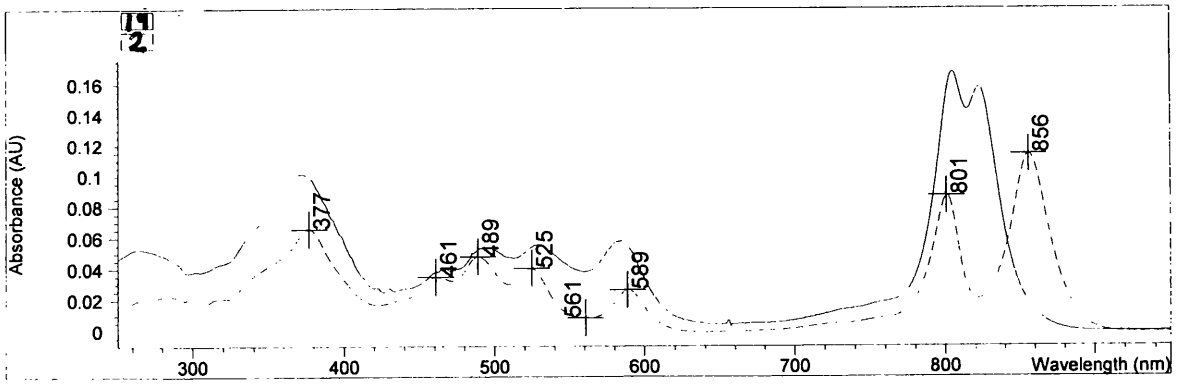

Figure 4.8: The absorption spectra from fractions numbered 2 and 19, showing the B800-850 the 800-820 LH complexes from *Rps. acidophila* strain 7050.

B800-850 LH complex from the B800-820 LH complex. The elution profile was a symmetrical peak and fractions assayed over the peak gave a consistent P_r of ~0.79; suggesting that no separation of the two forms of LH2 had been achieved. The I_r of the sample did increase from around 0.8 to 3.0 (underneath the peak), although this is a common feature when purifying LH2 complexes by gel filtration chromatography[96] and this increase in I_r was also observed when the protein was purified using the anion-exchange column. Additionally, using the molecular sieve before or after the anion exchange column did not result in an increase in either P_r or I_r, or in any noticeable improvement in the crystallisation of the complex. In fact, the crystallisation of the protein was less successful, in terms of both crystal size and quality, when this purification step was added to the protocol.

This suggested that, unlike the peripheral light harvesting complexes from *Rps. cryptolactis*, these protein-detergent complexes behaved similarly when applied to a gel filtration column and were of comparable shape and size.

4.3.3.3 Homogeneity

Using anion exchange chromatography revealed that although the isolated complex appeared to consist of a single form of LH2, this was not actually true. Previous reports of work carried out on the B800-820 LH complex from *Rps. acidophila* strain 7050, also appeared to assumed that samples contained only one type of LH complex as no reference was made which suggested otherwise[101, 16].

The reason for this was perhaps that, unlike analogous complexes from *Rps. cryptolactis*, in a sample which predominately contains the B800-820 LH complex, the presence of a small amount of the B800-850 LH complex cannot easily be detected by looking at the absorption spectrum. The Bchl *a* absorption maxima of the B800-820 and the B800-850 LH complexes from *Rps. acidophila* strain 7050 are found at 805 nm and 824 nm, and at 804 nm and 850 nm, respectively. The B820 absorption maximum is slightly red-shifted towards the maximum resulting from the B850 molecules and this results in the peak at 850 nm being less distinct than the corresponding B850 shoulder in an absorption spectrum from *Rps. cryptolactis* (see Section 3.2.2.1). This is shown in Figure 4.9 which compares an absorption spectrum of the B800-820 LH complex from

Rps. acidophila strain 7050 with a corresponding one from *Rps. cryptolactis* when both samples contain a B800-850 LH complex "impurity".

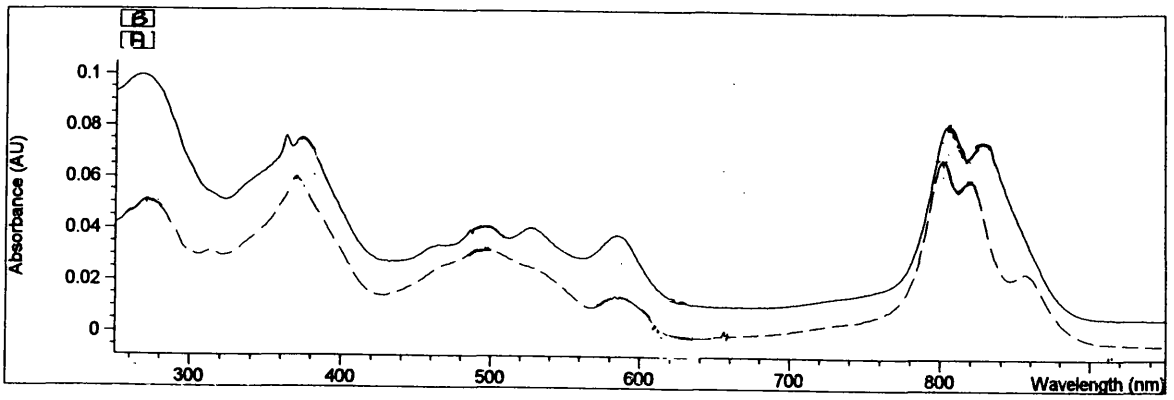

Figure 4.9: The absorption spectrum of the isolated LH2 band from sucrose gradient, from both *Rps. cryptolactis* (A) and *Rps. acidophila* strain 7050 (B).

4.3.4 Crystallisation

A variety of crystallisation trials were set up using the purified form of the B800-820 LH complex from *Rps. acidophila* strain 7050 which had been previously exchanged into 1% β-octylglucopyranoside (β-OG) in Tris buffer. A list of the ranges of attempted crystallisation conditions are shown in Table 4.4. Again, many of the parameter changes were investigated both individually and simultaneously.

Several of the above conditions produced crystals suitable for X-ray diffraction studies and these conditions are listed in Table 4.5.

The largest crystals were obtained under the following conditions:

- After purification the protein solution was exchanged into **1% β-OG** which contained **0.35 M NaCl** in buffer.
- The protein solution had a starting $\mathbf{OD_{820}}$ of $\mathbf{90\ cm^{-1}}$.
- Enough **BA** was added to make the final solution (including the KP_i) contain **2.5% (w/v)** BA.

Parameter	Units	Values	In steps of
Protein absorption at 820 nm	cm^{-1}	60 - 110	10
Precipitant: Kp_i	M	0.8 & 1.0	N/A
Well solution: AMS	M	2.1 - 2.7	0.2
Well solution: AMS	pH	9.1 - 9.9	0.2
Added salt: NaCl	M	0.35 & 0.17	N/A
Small Amphiphile: BA	%, (w/v)	2.5	N/A

Table 4.4: Range of crystallisation conditions attempted

Well solution	Protein $OD_{820}cm^{-1}$	KP_I (M)
2.3 M AMS pH 9.7	80 & 90	0.8 & 1.0
2.3 M AMS pH 9.5	90	1.0
2.3 M AMS pH 9.5	80 & 90	1.0
2.1 M AMS pH 9.5	80	0.8 & 1.0
2.1 M AMS pH 9.7	80 & 90	1.0
2.1 M AMS pH 9.9	90	1.0

Table 4.5: Successful crystallisation conditions.

All protein was prepared in 1% β-OG, 0.35 M NaCl; crystallised in the presence of 2.5 % (w/v) BA and incubated at 18°C.

- This solution was made **1.0 M KP_i**, from a 4 M stock solution in distilled H_2O.
- **15**μl drops were equilibrated against **2.3 M AMS** at **pH 9.7**.

Using these conditions, tabular crystals were obtained generally after 3 - 4 weeks and grew to a maximum size of 0.6 x 0.6 x 0.2 mm^3 (see Figure 4.3.4).

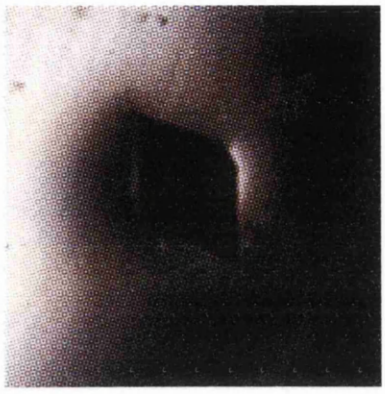

Figure 4.10: A crystal of the B800-820 LH complex from *Rps. acidophila* strain 7050.

Absorption spectra recorded from the dissolved crystals were identical to those from the purified complex, indicating that both contain the same complex assembly.

4.3.4.1 Crystallisation effects

Unlike all the other LH complexes investigated, the availability of X-ray quality crystals of *Rps. acidophila* strain 7050 meant that the effect of altering certain crystallisation parameters could be observed. Firstly, using an AMS solution with a pH $\leq$ 9.3 produced crystals with extremely poorly-defined morphology *i.e.* the crystals edges were not well defined .

Also, all of the crystallisation wells in which crystals grew, under went phase separation within four weeks of the crystals forming. This meant that it was important to synchronise crystal formation with X-ray beam time, as the crystals often drifted in to the detergent-rich phase, which was found to damage them. Crystals of the B800-850 LH complex from *Rps. acidophila* strain 10050 are optimally grown against a well solution of 2.3 M AMS at pH 9.3 and the problem of phase separation is seldom observed[82]. Apart from the pH of the well solution, the conditions used to crystallise the B800-820 LH complex from *Rps. acidophila* strain 7050 are very similar to those

used to crystallise the B800-850 LH complex from *Rps. acidophila* strain 10050 (see Sections 3.1 and 4.3.4, respectively). Consequently, it appears that crystallising the complex against a higher pH has effected the phase transition state of the system.

It was also noticed that phase separation was induced more quickly when attempting to crystallise the complex at temperatures lower that 18°C. This effect was also observed when the temperature was changed during the incubation period and hence it was found necessary to leave the trays undisturbed throughout the crystal growth period.

4.3.5 Mass spectrometry

The molecular weights of the apoproteins (as calculated from the primary sequences) for the B800-820 and the B800-850 LH complexes for this strain of bacteria are shown in Table 4.6.

Complex	Type	MW	Type	MW
B800-820	α	5545.6	β	4725.4
B800-850	α	5655.7	β	5278.0

Table 4.6: Molecular weights of apoproteins from the LH2 complexes.
MW = molecular weight in Daltons (D)

The molecular weights and populations of the apoproteins from the purified B800-820 LH complex from *Rps. acidophila* strain 7050 were analysed by mass spectrometry, essentially to monitor any cross contamination of the B800-850 LH complex. Two different samples were prepared for analysis and before the apoproteins were isolated, an absorption spectrum of both intact complexes was taken and the calculated P_r was 0.98 for sample A and 0.94 for sample B (see below). Mass spectrometry was carried out using a MALDI mass spectrophotometer at the Proteome facility, University of Aberdeen and the results are shown in Table 4.7.

Neither samples gave peaks which corresponded to the α-apoprotein from the B800-820 LH complex. This was also observed for the B800-820 LH complex from *Rps. acidophila* strain 7750 and is thought to be a result of these proteins being insoluble in the chosen solvent. However, these results showed that sample B contained a certain amount of the B800-850 LH complex; shown by the peak at 5277.3 D (although this peak was minor in comparison to the other observed

Sample	MW	Apoprotein
A	4725.4	β (B800-820)
B	4725.4	β (B800-820)
B	5277.3	β (B800-850)

Table 4.7: Mass spectrometry results for the B800-820 LH complex from *Rps. acidophila* strain 7050.

peak). Sample B also had a lower value of P_r than sample A and this suggests that along with the purity ratio, routine use of mass spectrometry would be an effective means of monitoring the purity of crystallisation samples. Mass spectrometry also revealed that unlike the other complexes used throughout the project, the B800-820 LH complex from *Rps. acidophila* strain 7050 did not contain various apoprotein contaminants.

4.3.6 Discussion

Crystallisation of the B800-820 LH complex from *Rps. acidophila* strain 7050 has shown the importance of an adequate purification protocol when attempting to crystallise membrane proteins. The major problem encountered when working with this species of bacteria was not how to remove the impurity but recognising that the impurity existed. Once this was achieved the experience gained from working with *Rps. cryptolactis* made the purification process somewhat straightforward.

5. STRUCTURE DETERMINATION

5.1 Introduction

This chapter describes the structure solution process for the B800-820 light-harvesting complex from *Rps. acidophila* strain 7050. As a result of the limited availability and reproducibility of crystals, all X-ray diffraction data were collected on beamline 9.6 at the Daresbury Laboratory Synchrotron Radiation Source using a MAR Research imaging-plate system. The majority of the programs used during structure determination were from the CCP4 suite[108], although certain others are mentioned and are referenced individually.

5.2 Crystal handling

Initial attempts at data collection used a crystal mounted in a thin-walled quartz glass capillary tube, at room temperature. A crystal taken from the crystallisation drop without further treatment showed diffraction to no better than 7 Å resolution. However, removing the crystal from the drop and steeping in artificial mother liquor (AML) for approximately one minute before mounting resulted in diffraction to around 3.5 Å. After collecting two or three frames, the resolution limit of the data decreased, implying that the crystals were susceptible to radiation damage. Cryoprotectant was slowly introduced into a crystal, which had been previously steeped in AML, by a serial dilution of 1μl every 5 minutes for 30 minutes. This crystal was loop mounted and flash-cooled to 100K using an Oxford Cryosystems Cryostream and showed diffraction to around 3.3 Å resolution, allowing a native data set to be collected.

Subsequently, a 2.8 Å data set was collected at 100K from a crystals which had been exposed to cryoprotectant by dialysis. Diffraction was also observed to around 2.4 Å but the data was not collected as the crystal was not single. The 2.4 Å diffraction data appeared to have a lower mosaic spread and diffuse scatter than the previously collected data. This reduction in the mosaic spread

was assumed to be a result of the decreased time taken to remove the crystal from the cryoprotectant and placing it in the cold air stream *i.e.* by freezing the crystal quicker. A comparison of the 3.3 and the 2.4 Å diffraction patterns are shown in Figures 5.1 and 5.2.

5.3 Data Collection and processing

2.8Å and 3.3Å native data sets were collected from two different crystals as described previously. All data were collected with a X- rays with a wavelength of 0.87 Å, processed using DENZO[109, 110] and scaled with SCALEPACK[109]. Data were indexed with DENZO, and showed that the crystals belonged to space group R32 with hexagonal cell dimensions $a = 117.20$ Å, $c = 295.14$ Å. Identical space group and very similar unit cell were observed for crystals of the B800-850 LH complex from *Rps. acidophila* strain 10050[1].

For the 2.8 Å diffraction data, both a high and a low resolution data set (4.4 Å) were collected from a single crystal. This was necessary as the radiation dosage required to collect the high resolution data resulted in the low resolution spots being saturated on the image plate. These data sets were later merged and every measurement from each dataset was used as input to scaling. Statistics for the various data sets are given in Table 5.1.

The 3.3 Å data were used until a structure solution was obtained, by which time the merged 2.8 Å data set had been collected. This data was then used in subsequent refinement procedures. The 2.8 Å data are somewhat anisotropic which results in the high R-factor in the highest resolution shell.

Scaled data were reduced using a series of programs from the CCP4 software suite in order:

- ROTAPREP: Used to convert SCALEPACK output to MTZ format, suitable for input into the CCP4 suite.
- SORTMTZ: Sorts the MTZ file so that all equivalent indices are adjacent.
- TRUNCATE[111]: Converts the intensities to amplitudes, calculates a Wilson plot[112] and puts the data on an absolute scale.
- UNIQUE: Generates a list of unique reflections, regardless of whether data has been mea-

Figure 5.1: A representative example of a 3.3 Å diffraction pattern

Figure 5.2: A representative example of a 2.4 Å diffraction pattern.

Here the pattern has a lower mosaic spread and lower diffuse scatter.

Data set	3.3 Å	2.8 Å	4.4 Å	Merged (2.8 Å and 4.4 Å)
Detector	Mar 30 cm	Mar 30 cm	Mar 30 cm	N/A
Resolution (Å)	12.5 - 3.3	23.0 - 2.8	50.0 - 4.4	50.0 - 2.8
High Res. (Å)	3.36 - 3.30	2.85 - 2.8	4.48 - 4.4	2.85 - 2.8
Osc. Rng. (°)	1.0	0.5	2.0	N/A
Comp.	87.0%	99.0%	99.3%	99.5%
Comp. HR	75.6%	97.8%	98.4%	99.2%
Mult.	3.3	3.2	3.4	3.7
Ref.	12070	19561	5194	19611
R_{merge}	6.8%	7.9%	5.1%	6.5%
R_{merge} HR	14.0%	51.7%	6.5%	57.0%
$\frac{<I>}{\sigma<I>} > 3$	91.0%	64.5%	73.6%	67.6%
$\frac{<I>}{\sigma<I>}$ HR[i]	5.7	-	-	1.3

Table 5.1: Statistics for collected and merged data sets.

All data were collected using X-rays with a wavelength of 0.87 Å.

High Res = Highest resolution data shell.

Osc. Rng. = Oscillation range of image in degrees.

Comp. = Overall completeness of data.

Comp. HR = Completeness of data in the highest resolution shell.

Mult. = Overall multiplicity of data.

N. Ref. = Total number of unique reflections measured.

R_{merge}: Defined as $R_{merge} = \Sigma_h \Sigma_j \frac{|\bar{I}(h) - I(h)_j|}{\Sigma_h \bar{I}(h)}$, where $\bar{I}(h)$ is the mean intensity

R_{merge} HR = R_{merge} in the highest resolution shell.

$\frac{<I>}{\sigma<I>} > 3$ = Overall data with $\frac{<I>}{\sigma<I>}$ greater than 3.

$\frac{<I>}{\sigma<I>}$ HR > 3 = $\frac{<I>}{\sigma<I>}$ in the highest resolution shell.

[i]These values were obtained by Dr. Stephen Prince using the program MOSFLM.

sured for them.

- FREERFLAG: Tags a randomly chosen percentage of reflections for cross validation purposes.

If it is assumed that all atoms scatter equally and that there is a random distribution of atoms throughout the unit cell, a Wison plot can be calculated and from this plot the temperature factor (B) of the atoms can be estimated, where B is related to the mean-square amplitude ($\bar{u^2}$) of atomic vibration by:

$$B = 8\pi^2\bar{u^2} \tag{5.1}$$

The Wilson plots generated by TRUNCATE gave B estimates (slope = -2B) of 88 Å^2 and 61 Å^2 for the original (3.3 Å) and the new (2.8 Å) data set, respectively (see Figure 5.3 for an example). The high B factors are attributed to disorder in the crystal, which is also observed in crystals of the B800-850 LH complex from *Rps. acidophila* strain 10050[100] and is thought to be a consequence of the high solvent content (~72%[1]) and the bound detergent molecules.

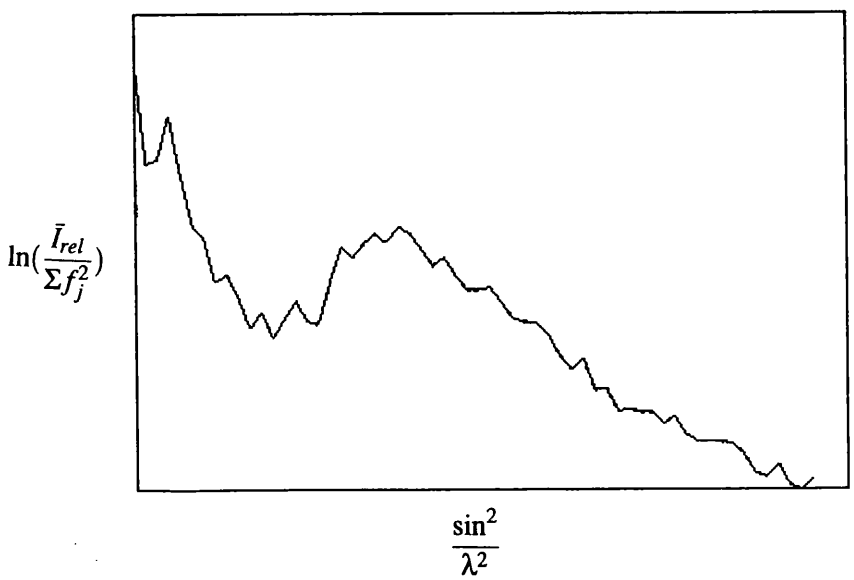

Figure 5.3: The Wilson plot obtained for the merged data set.

Data used in the resolution range 4.0 - 3.3 Å.

5.4 *Patterson solution*

A native Patterson map was calculated from the 3.3 Å diffraction data and was compared to a similar map calculated using corresponding data from the B800-850 complex from *Rps. acidophila* strain 10050[96], using the program OVERLAPMAP. Both maps were calculated from data in the resolution range of 12.5 to 3.3Å and the $w = 0$ Harker section of each map is shown in Figures 5.4 and 5.5. The comparison gave an overall correlation coefficient of 77% rising to 95% at the Harker section $w = 0$, indicating that the two complexes are very nearly isostructural.

5.5 *Molecular Replacement*

The structure was solved by the Molecular Replacement (MR) method using the program AMoRe[113]. The search model consisted of the apoproteins of the asymmetric unit of the B800-850 LH complex from *Rps. acidophila* strain 10050[1]; with the pigment moieties removed. The α- and β-apoproteins of the two complexes are 68 and 71% identical (Figures 5.6 and 5.7), and in the search model the residues which differed had their Cβ positions removed.

Using data over the whole resolution range, from 12.5 Å to 3.3 Å, failed to provide a solution. However, reducing the resolution range to include only data from 10 Å to 4 Å provided clear solutions. The calculated rotation function showed two equivalent solutions, with correlation coefficients only marginally greater than the next highest rotation function peaks (Figure 5.8). However, a translation search and subsequent rigid body refinement provided two equivalent solutions that were significantly better than any others both in terms of correlation coefficient and R-factor[114] (Figures 5.9, 5.10, 5.11 and 5.12).

After rigid body refinement, the model solution had favourable crystal contacts; a correlation coefficient of 50.4% and a R-factor of 43.4%, at 4 Å resolution. The search model was transformed by the output orientation matrix given by AMoRe using the program LSQKAB[115]. The position in the cell of the model with respect to the search model corresponded to zero rotation and a translation (d_x, d_y d_z) of -0.31Å -0.05Å -0.38Å, with respect to the orthonormal cell axes. This solution was used to phase the initial electron density maps. This density was compared with the B800-850 LH complex from *Rps. acidophila* strain 10050. From these initial maps the most

Native Patterson maps: Harker section $w = 0$

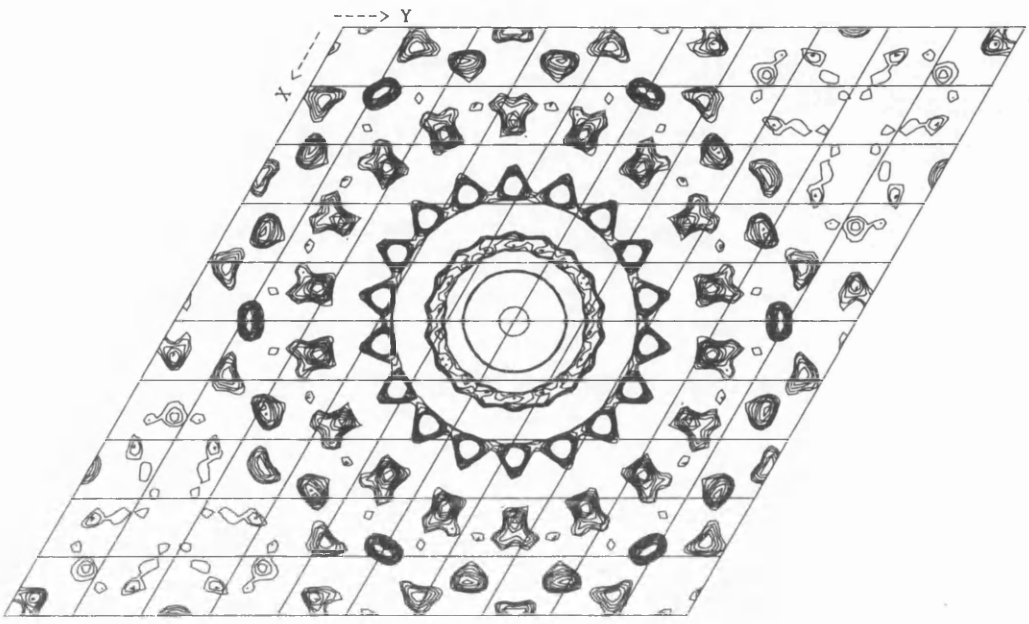

Figure 5.4: B800-820 LH complex from *Rps. acidophila* strain 7050

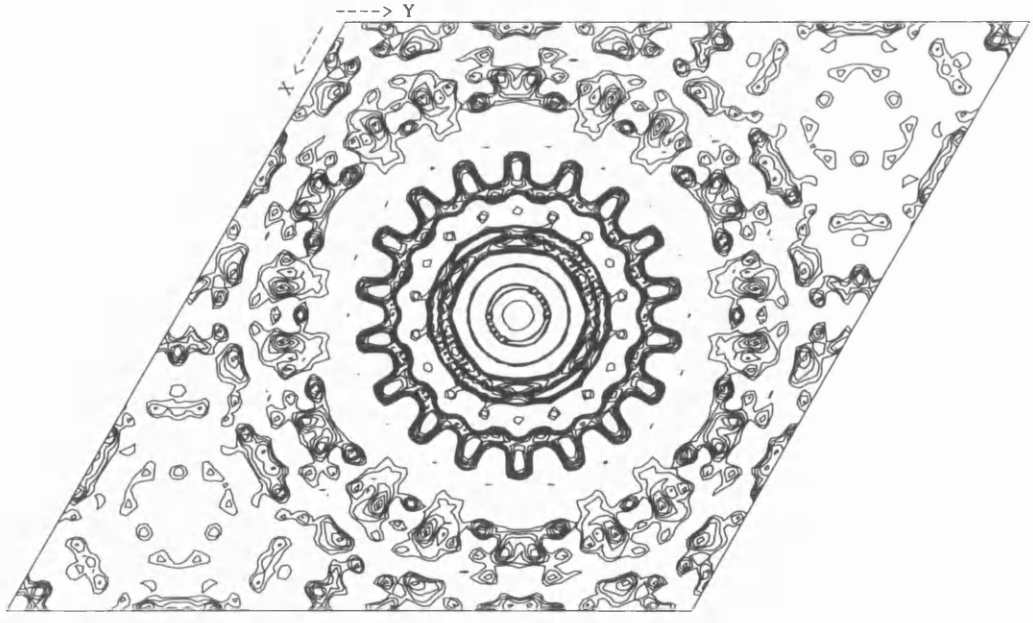

Figure 5.5: B800-850 LH complex from *Rps. acidophila* strain 10050

Figure 5.6: A comparison of the α-apoproteins from the two complexes

Differing residues are highlighted in white

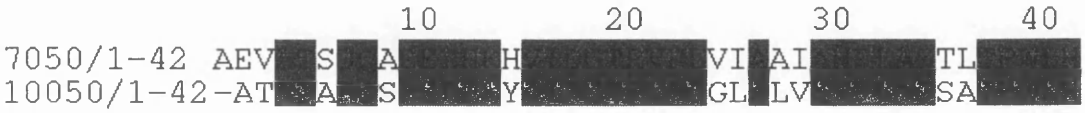

Figure 5.7: A comparison of the β-apoproteins from the two complexes

Differing residues are highlighted in white

pronounced difference between the structures was a positional shift of the αB820 phytyl chain with respect to the αB850 phytyl chain (See Figure 5.13).

5.6 Phase improvement

Before phase improvement, initial rigid body refinement was implemented using the program RESTRAIN[116] with the α- and β-apoproteins and the pigments chosen as rigid bodies. The overall structure has three-fold non-crystallographic symmetry (NCS), with a 360/9° rotation axix which is co-axial with the crystallographic three-fold and after the initial refinement the NCS matrices were calculated with LSQKAB. To remove some of the model bias and improve the map, the phase set was improved using solvent flattening, histogram matching[117, 118] and NCS averaging. All phase improvement procedures were undertaken with the program DM[119]. The mask was derived with the program NCSMASK, using a sphere radius of 3.0Å around all the atoms from an α, β pair of apoproteins with the associated Bacteriochlorophyll *a* (Bchl *a*) molecules (B800, αB820 & βB820). This mask gave an estimated solvent content of 55%. Phase improvement resulted in an improved map with an R_{free} of 26%, NCS correlation between the three equivalent density regions of 0.95, and a mean figure of merit of 0.84 for the phase set. Representative examples of

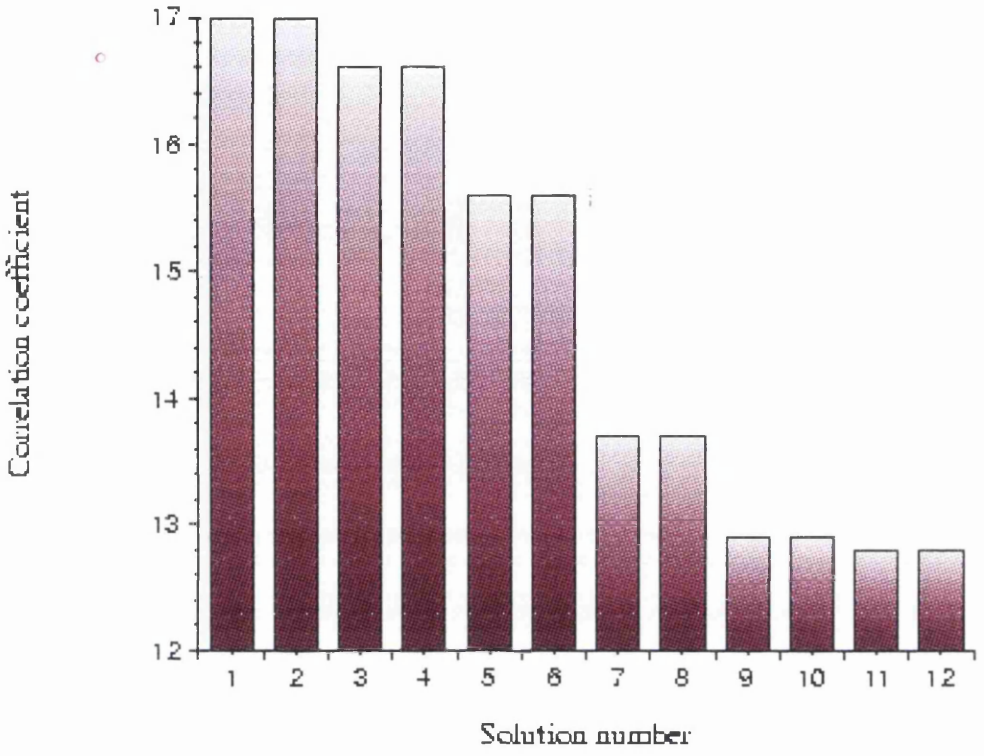

Figure 5.8: Rotation function solutions

Solutions 1 and 2 have correlation coefficients which are only marginally greater than the next best solutions.

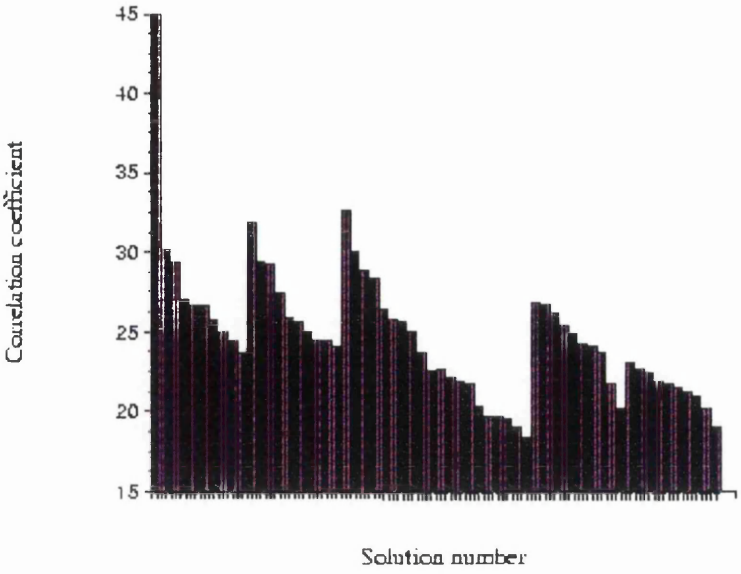

Figure 5.9: Translation function solutions

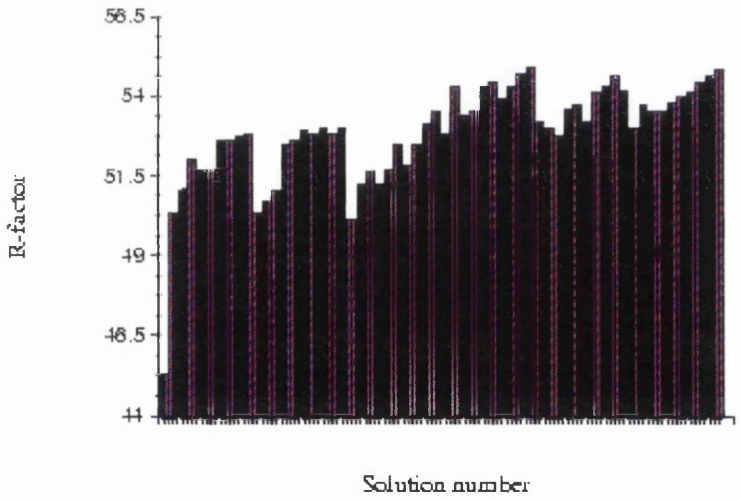

Figure 5.10: Translation function solutions

Solutions 1 and 2 now have greater correlation coefficients and smaller R-factors than the other solutions.

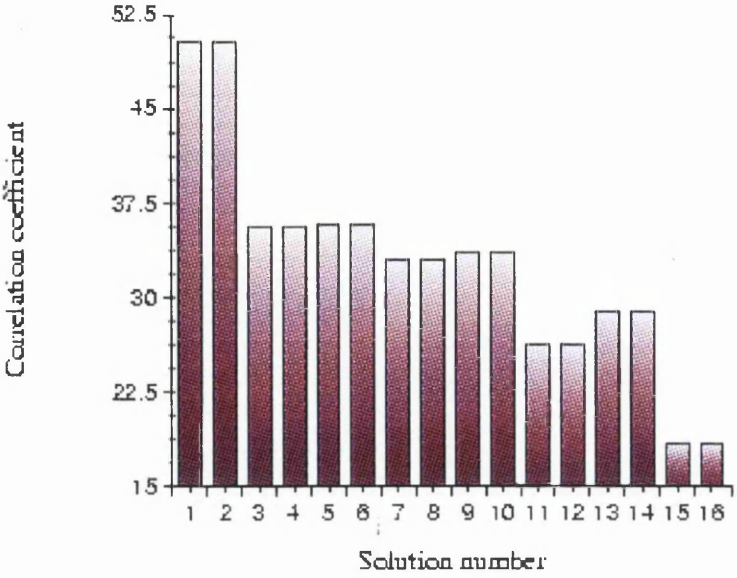

Figure 5.11: Rigid-body fitted solutions

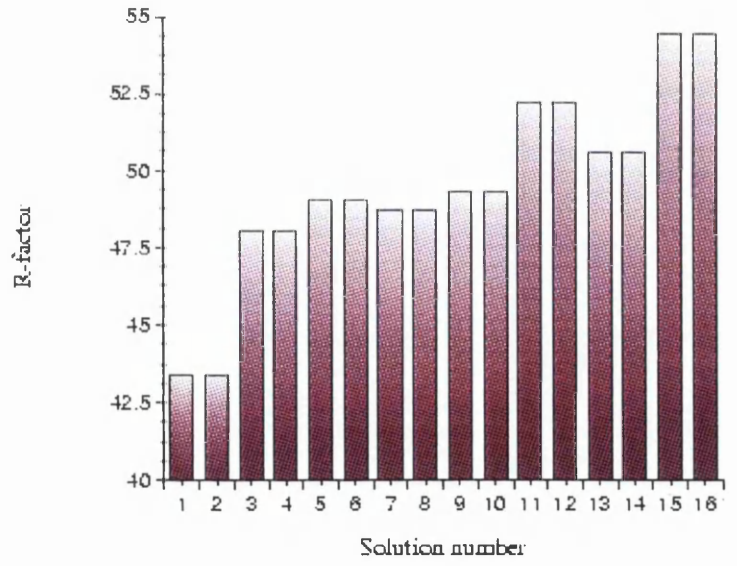

Figure 5.12: Rigid-body fitted solutions

Again, it can be seen that solutions 1 and 2 are significantly better than the other solutions.

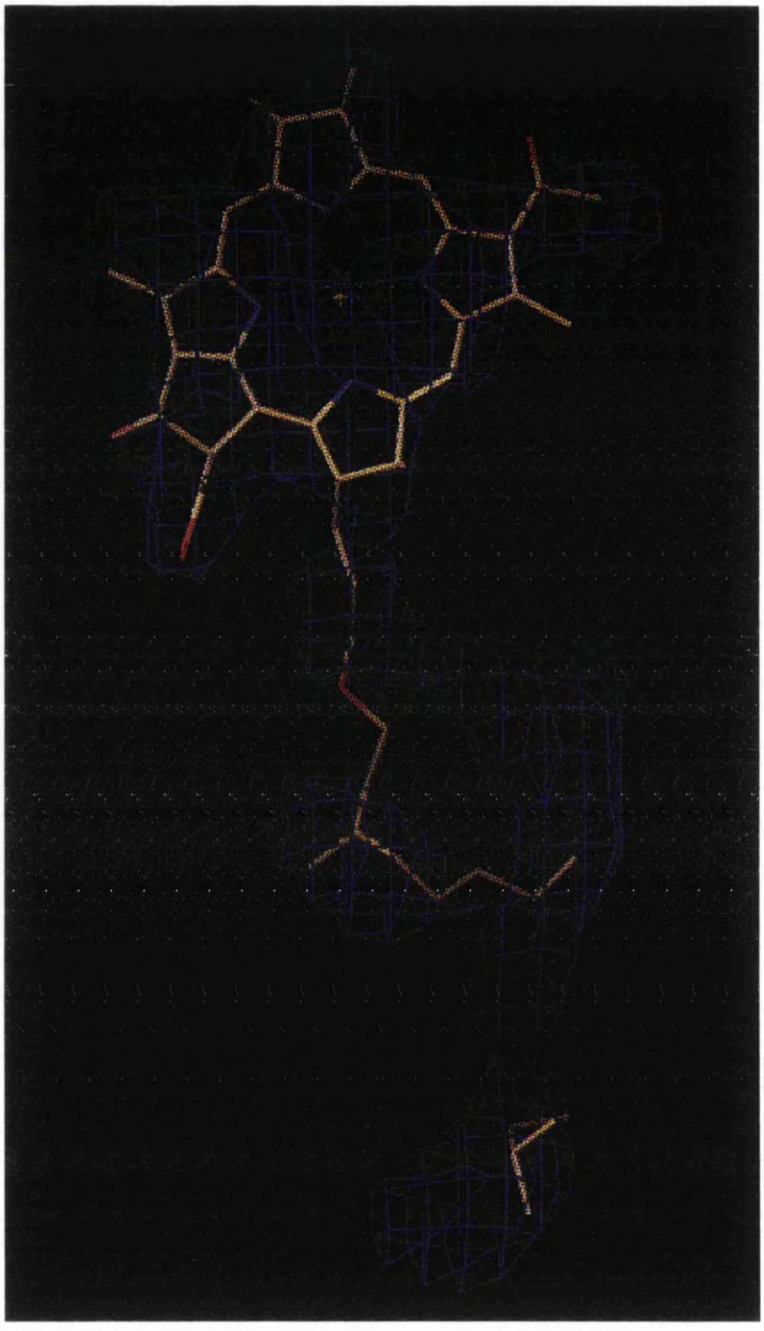

Figure 5.13: A section of the original 2fo-fc MR map, showing a shift in the αB820 phytyl chain.

the phase-improved maps are shown in Figures 5.14 and 5.15.

5.6.1 PROTIN *dictionaries*

After initial rigid body refinement with RESTRAIN, refinement was continued with the program REFMAC[120], where geometric restraints are defined using PROTIN. The use of REFMAC required PROTIN dictionaries to be created for the pigment molecules Bchl *a* and the carotenoid rhodopinal glucoside. The molecules were built by selecting, from the Cambridge Structural Database[121] (CSD), high resolution (> 1Å) structures and parts of structures that corresponded to sections of the pigment molecules. The major structural fragment used in the model of bacteriochlorophyll *a* was a derivative of a molecule called methyl bacteriopheophorbide *a*[122], with the main part of the phytyl chain being taken from the crystal structure of a phytyl-hydraquinone[123]. The backbone of the carotenoid was constructed from the crystal structure of β-carotene[124] and the glucoside head group was taken from the structure of a molecule of β-octyl glucopyranoside[125]. The remaining part of the structures were taken from molecules in the database which contained the required fragments.

Fractional co-ordinates were obtained from the CSD and COORDCONV was used convert these to orthogonal co-ordinates in PDB (Protein Data Bank) format. LSQKAB was used to map structural fragments onto the model and the stereochemistry was manually refined using O[126]. After the assembly of the complete, molecules the PROTIN dictionary was created using MAKEDICT. For this 5 planar groups were defined for the Bchl *a*: 4 for the porphyrin head group and another at the top of the phytyl chain. For the highly conjugated carotenoid molecule, a total of 12 overlapping planar groups were defined. These dictionary entries were added to the standard PROTIN dictionaries for use in refinement.

5.7 Refinement

The data now described are the 2.8Å merged data set. From the data a Free-R set[127, 128] of reflections was excluded to validate the significance of individual steps throughout the refinement process. For this and all subsequent refinement procedures 5 % of of the reflections were omitted from the working set. The rigid body refinement resulted in a total R.M.S. shift of 0.19 Åfor the

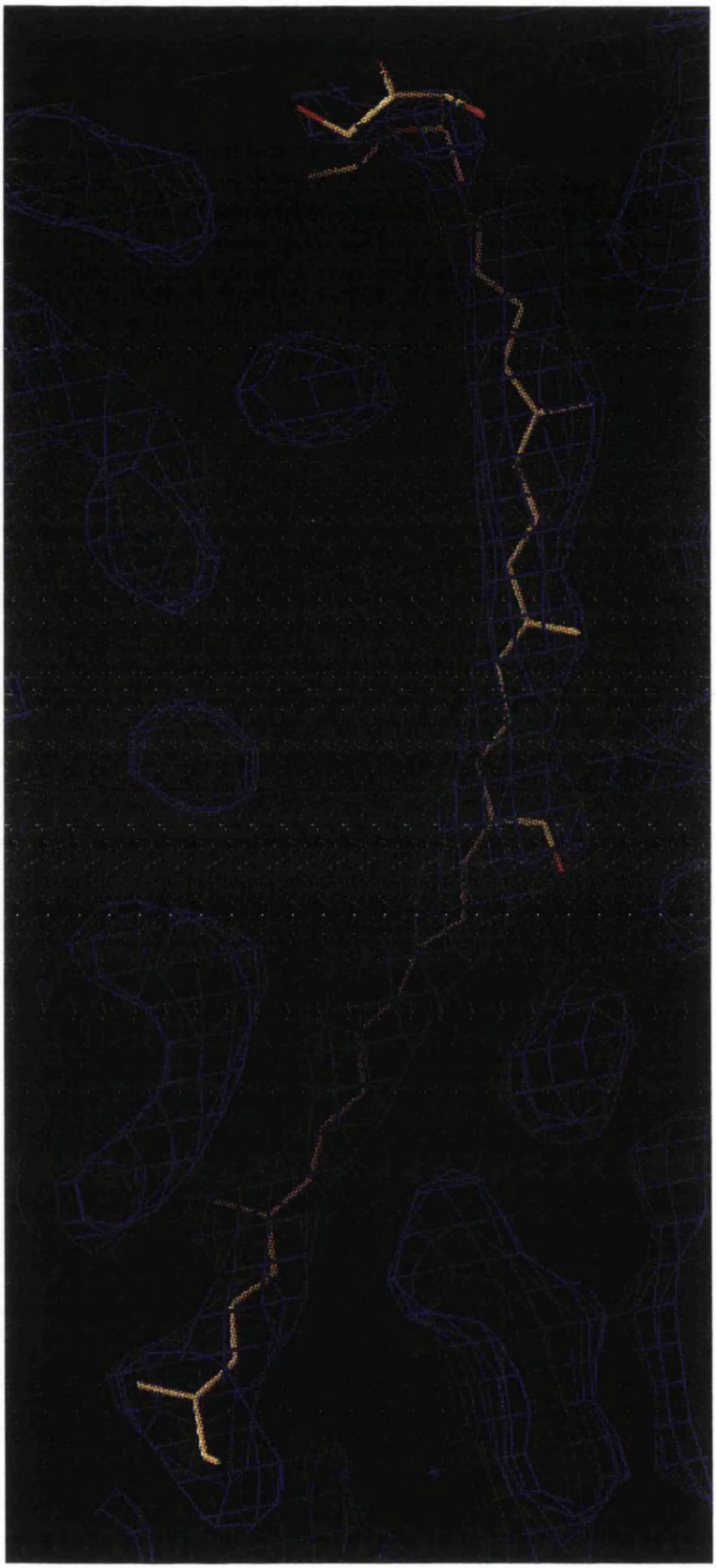

Figure 5.14: A section of the phase improved MR map showing the electron density around the carotenoid, rhodopinal glucoside.

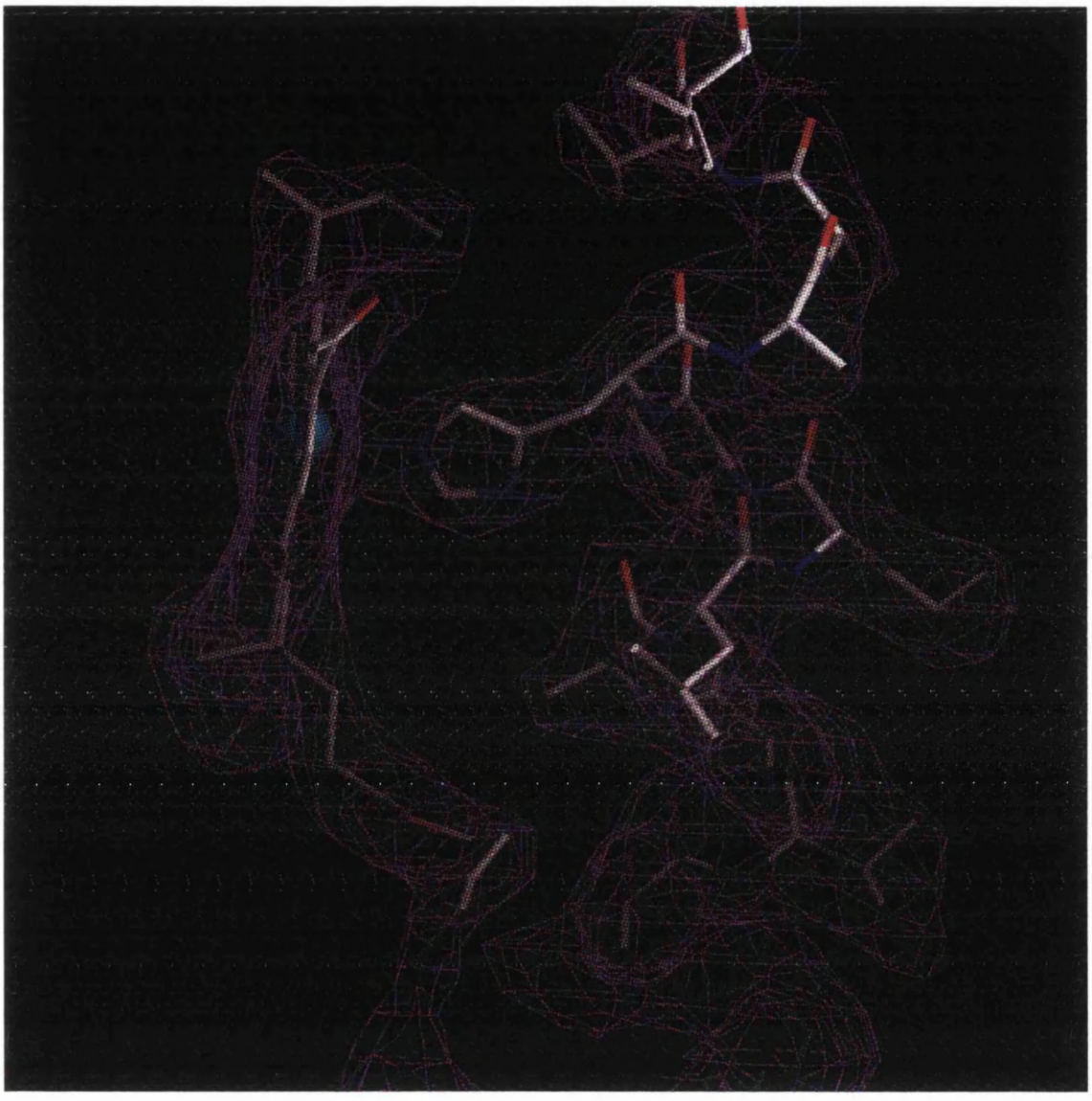

Figure 5.15: The phase improved MR map showing the electron density around a section of the α-apoprotein coordinating to αB820 through a histidine residue.

input co-ordinates and a R_f and R_{free}, of 42.85 % and 43.22 %, respectively where,

R_f or reliability index is defined as

$$R_f = \frac{\Sigma_{h \notin X} ||F_o(h)| - |F_c(h)||}{\Sigma_{h \notin X} |F_o(h)|} \tag{5.2}$$

and the Free R-factor (R_{free}) is defined as

$$R_{free} = \frac{\Sigma_{h \in X} ||F_o(h)| - |F_c(h)||}{\Sigma_{h \in X} |F_o(h)|} \tag{5.3}$$

where $F_o(h)$ and $F_c(h)$ are observed and calculated structure factors, respectively. X represents the "Free R set" excluded from refinement calculations.

Refinement used all available data; this is questionable by conventional methodology as the R_{merge} (Equation 5.1) in the highest resolution shell was 57%. However, REFMAC assigns weights to individual reflections based on their standard deviations which allows the weaker reflections to be included in the refinement procedure. Minimisation was by the sparse matrix method using the "-loglikelihood" residual. Individual isotropic B factor refinement was implemented for all atoms and F_o and F_c scaled anisotropically. Tight NCS restraints were applied throughout refinement to the main and side chains of the NCS related α- and β-apoproteins and to the related pigments. Relaxing these restaints resulted in an increase in R_{free} and so strict NCS constraints were maintained. The current R_f and R_{free} are 25.3 and 29.0% respectively. In the latter stages of refinement, the resolution was cut back to 3.0Å, where the R_{merge} is 38 % and this resulted in R_f and R_{free} of 24.8 and 28.6%, respectively.

At the end of each refinement cycle, electron density maps were calculated from the coefficients output by REFMAC using FFT. Individual refinement stages were interspersed with manual rebuilding using the program O[126].

The crystal asymmetric unit contains three protomers, each of which consists of an α- and a β-apoprotein, two B820 and a B800 molecule and a carotenoid. The electron density map allows a tracing of residues 1-47 of the α-apoprotein, most of the β-apoprotein and all of the pigment molecules. Exceptions to this are residues 41 and 42 of the β-apoprotein, where the side chains have been removed as there is no density present for them. Electron density for the carotenoid

head group is also missing and these atoms have been excluded from refinement. In the crystal structure of the B800-850 LH complex, an area of density is attributed to the presence of the detergent molecule β-octylglucoside[1] or a partial carotenoid[48]. Density is not present at a similar position in the electron density maps of the B800-820 LH complex although there are areas of density for which density has still to be assigned. Thirty-two water molecules were positioned using the X-SOLVATE feature in QUANTA.

The accuracy of the structure was checked using the validation program PROCHECK[129]. The RMS deviations of the model from the target geometries are 0.02Å for the bond lengths and 3.83° for the bond angles. A Ramachandran[130] plot for the structure is shown in Figure 5.16, showing that the majority of the protein is helical and that 93.0% of residues lie in the most favourable regions.

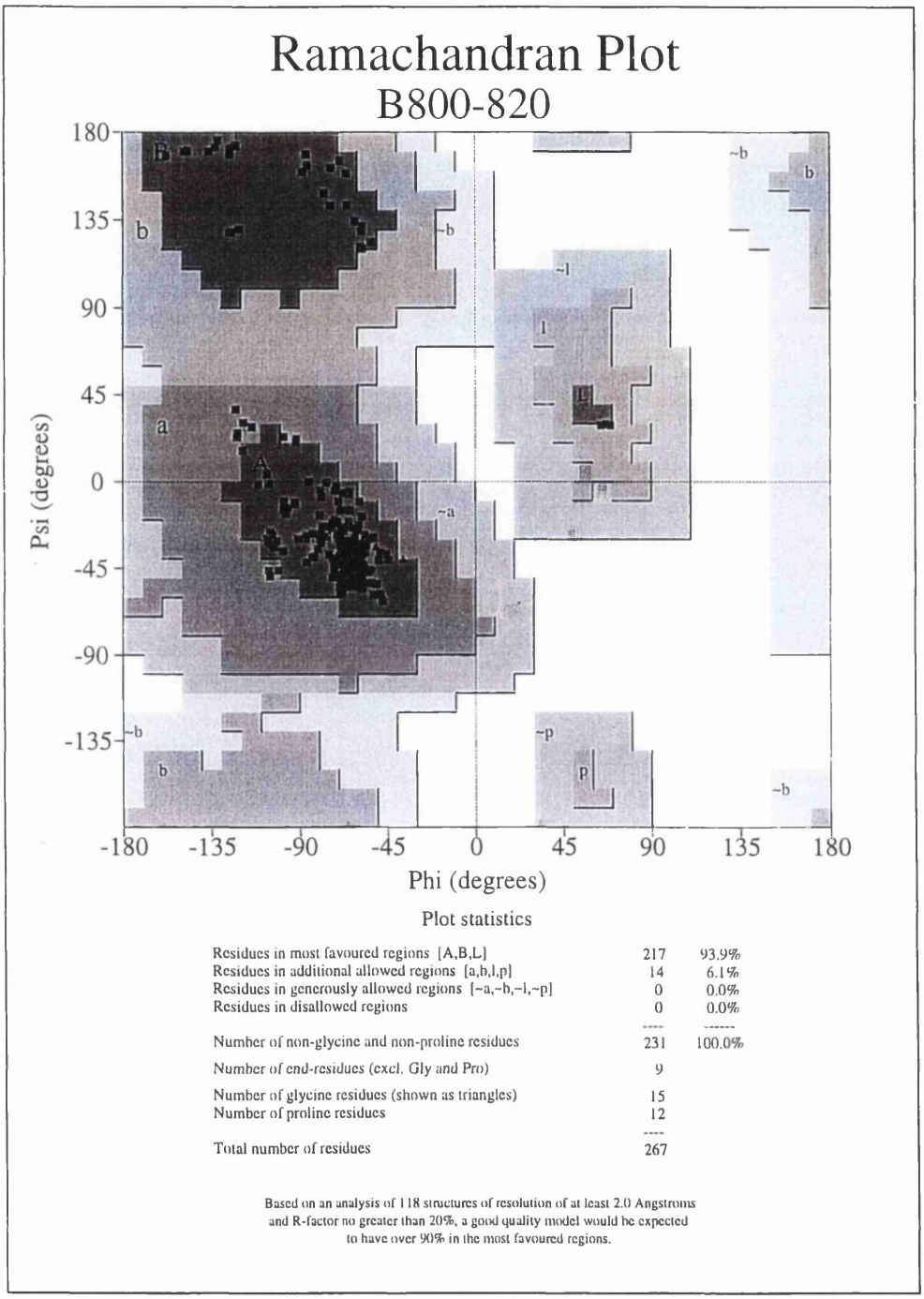

Plot statistics

Residues in most favoured regions [A,B,L]	217	93.9%
Residues in additional allowed regions [a,b,l,p]	14	6.1%
Residues in generously allowed regions [~a,~b,~l,~p]	0	0.0%
Residues in disallowed regions	0	0.0%
Number of non-glycine and non-proline residues	231	100.0%
Number of end-residues (excl. Gly and Pro)	9	
Number of glycine residues (shown as triangles)	15	
Number of proline residues	12	
Total number of residues	267	

Based on an analysis of 118 structures of resolution of at least 2.0 Angstroms and R-factor no greater than 20%, a good quality model would be expected to have over 90% in the most favoured regions.

Figure 5.16: Ramachandran plot

6. DISCUSSION

6.1 Introduction

This chapter describes the structure of the B800-820 LH complex from *Rps. acidophila* strain 7050 and compares it to the B800-850 LH complex from *Rps. acidophila* strain 10050[1]. An overall comparison of the two structures is given and possible structural reasons for the spectroscopic differences between the two complexes are also discussed. A comparison of the α- and the β-apoproteins from the two complexes and their proposed membrane spanning regions[17] is shown in Figures 6.1 and 6.2. In order to keep the numbering consistent for the chains in both complexes the residues in the β chain of the B800-820 LH complex are numbered 0,1,2,3... etc.

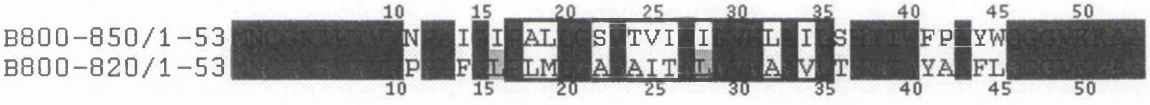

Figure 6.1: A comparison of the primary sequence of the α-apoproteins.
The conserved residues are shaded and the membrane spanning region is outlined.

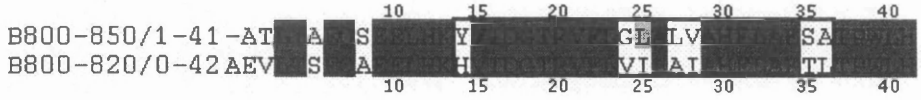

Figure 6.2: A comparison of the primary sequence of the β-apoproteins.

The numbering scheme used to describe the pigments is shown in Figure 6.3 and throughout this chapter the two complexes will be simply referred to as the "B800-850 LH complex" and the "B800-820 LH complex".

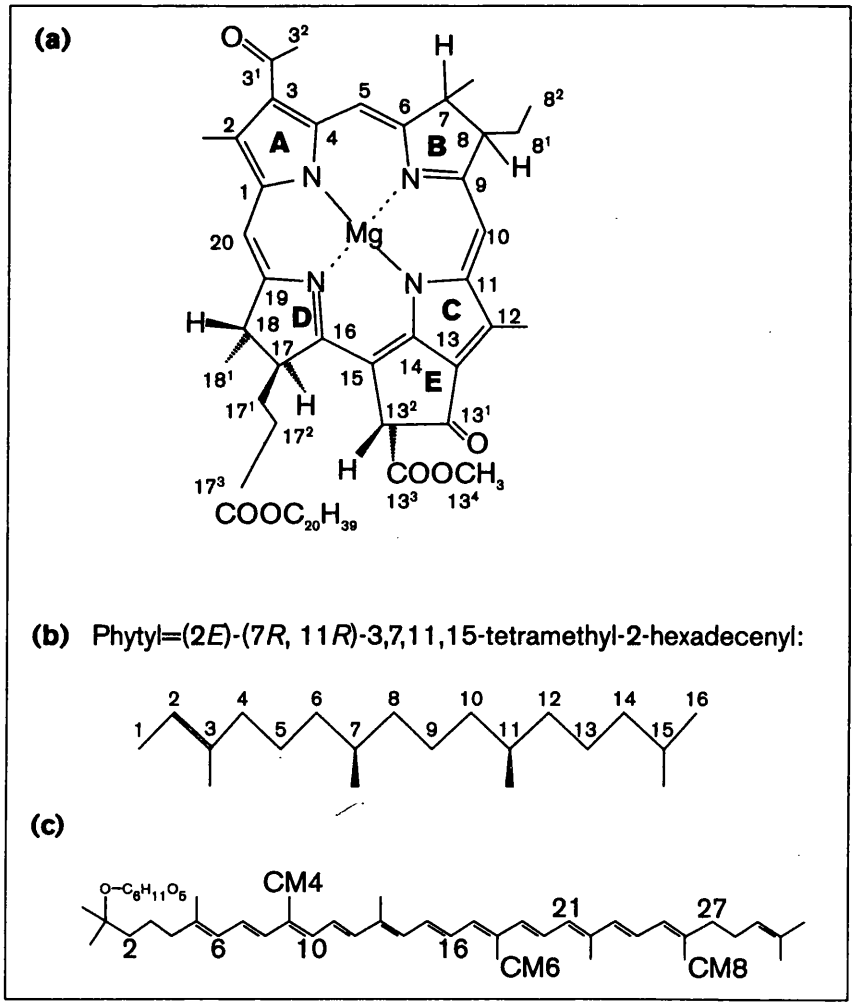

Figure 6.3: Structure of (a) Bchl *a*, (b) the phytyl chain and (c) the carotenoid from the B800-850 LH complex, rhodopin glucoside.

The carbon numbering and ring labelling for Bchl *a* is that approved by IUPAC-IUB.[131]

The carotenoid of the B800-820 LH complex has and additional acetyl group at position CM5, labelled OA1.

6.2 *The overall assembly*

Like the B800-850 LH complex, the minimal unit of the B800-820 LH complex consists of two apoproteins (α and β), three bacteriochlorophyll *a* (Bchl *a*) molecules (αB820, βB820 and B800) and a carotenoid (rhodopinal glucoside (RpalG)). The topology of both complexes is identical and the relative positions of the pigment moieties, with respect to the apoproteins are very similar.

The apoproteins in the asymmetric unit of the B800-820 LH complex were overlaid with those in the B800-850 LH complex using LSQKAB[108]. A second transformation, which mapped the pigments of the overlaid B800-820 LH complex onto the pigments in the B800-850 LH complex was also determined. This allowed the rms shifts of the centres of mass of analogous pigment molecules to be calculated *e.g.* αB820 with αB850, and the results are shown in Table 6.1.

Pigment	αB820	βB820	B800	RpalG
rms dev. (Å)	0.43	0.72	0.24	0.44

Table 6.1: Rms deviation of the pigment positions in the B800-820 LH complex when compared to those in the B800-850 LH complex.

rms. dev = rms (root mean square) deviation

Equivalent structural elements in the two complexes were also compared by calculating the rms deviation of their coordinate positions using LSQKAB. The rms deviations of the coordinates of the pigments and, of the Cα positions of the apoproteins are shown in Table 6.2.

Section	α	β	αB820	βB820	B800	RpalG
rms dev. (Å)	0.39	0.48	1.74	1.43	1.00	0.66

Table 6.2: Rms deviation of the coordinates of individual structural elements in the B800-820 LH complex when compared to those in the B800-850 LH complex.

These results demonstrate that the positions of the B800 and the carotenoid molecules in the two LH complexes are more similar than those of the B850 molecules.

6.2.1 *The nonameric arrangement*

The nonameric arrangement of the B800-820 LH complex is almost identical to that seen in the B800-850 LH complex[1] and shall only be described briefly. Like the B800-850 LH complex, the α and β apoproteins in the B800-820 LH complex each form transmembrane helices which are arranged with almost exact nine-fold symmetry in two concentric circles. The nine α-apoproteins form an inner ring with an outer ring formed by the β-apoproteins. Eighteen B820 molecules, nine B800 molecules and nine carotenoid molecules are located within these two protein cylinders.

The B820 molecules form a overlapping ring which is sandwiched between the apoproteins approximately 10 Å from the presumed periplasmic membrane surface[1], with their bacteriochlorin plane lying perpendicular to the membrane surface. The B800 molecules are located further into the membrane and are situated between adjacent β-apoproteins with the bacteriochlorin plane lying parallel to the plane of the membrane. The carotenoid molecules span the depth of the entire complex. Figures 6.4 and 6.5 illustrate the entire assembly of the B800-820 LH complex which is almost identical (from this view) to the B800-850 LH complex from *Rps. acidophila* strain 10050 (see Section 1.5).

6.2.2 *Protein-protein contacts*

Hydrogen bonds (H-bonds) between the apoproteins in the B800-850 LH complex were (unexpectedly) only found within extramembranous regions. Within the membrane spanning region, protein-pigment and pigment-pigment interactions were found to be dominant. The protein-protein H-bonds are thought govern the oligomeric state and hence (play a part in) the overall formation of the complex[48]. These H-bonds are summarised in Table 6.3 and a comparison of the H-bonding between apoproteins in the B800-820 LH complex is shown in Table 6.4. Amino-acid types and symbols are given in Appendix C.

From these tables, the differences found between the H1 bonds are a result of a singe complimentary change in the amino sequences of the β-apoprotein. In the B800-850 LH complex Ser β8 becomes an Ala residue, and it is this change which prevents the B800-820 LH complex forming a H-bond described analogous to that for the B800-850 LH complex. However, a complimentary change is observed at position 5 on the same apoprotein: a residue which exists as Ala in the

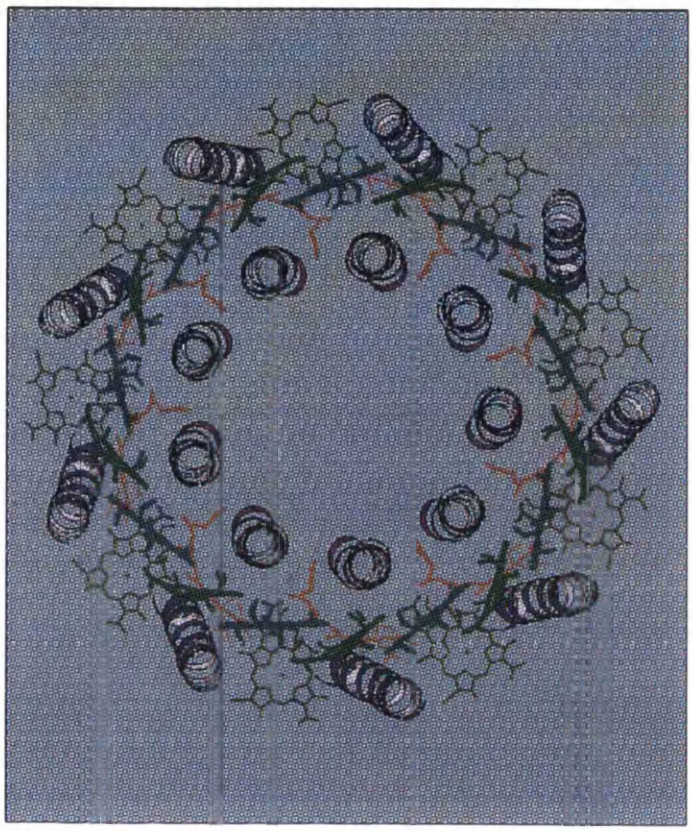

Figure 6.4: The B800-820 LH complex viewed from above the membrane surface.

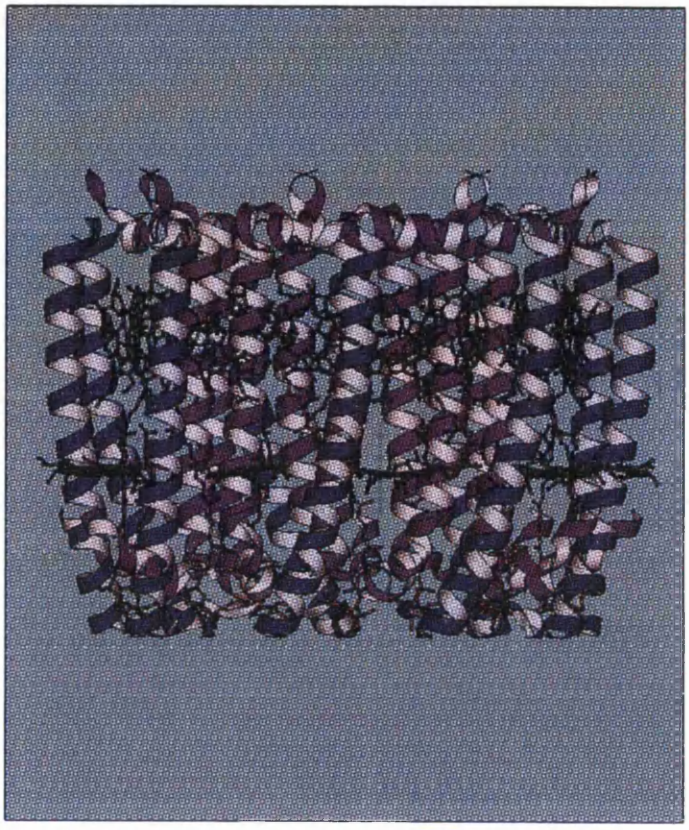

Figure 6.5: The B800-820 LH complex viewed perpendicular to the membrane surface.

Bond no.	Residue	Atom	Residue	Atom	Distance (Å)
H1	Gly α4	O	Ser β8	OG	2.58
H2	Trp α7	O	Leu β3	N	2.99
H3	Thr α39	N	Gln (+)α46	OE1	2.65
H4	Trp α40	NE1	Trp (+)α45	O	2.81
H5	Tyr α44	OH	Trp (+)β39	NE1	3.22

Table 6.3: Hydrogen bonding between the apoproteins of the B800-850 LH complex.

(+) and (-) indicate proceeding/preceding protein chain anticlockwise around the membrane normal.

Data taken from Prince et al. 97.[48]

Bond no.	Residue	Atom	Residue	Atom	Distance (Å)
H1	Lys α5	NZ	Ser β5	OG	2.81
H2	Trp α7	O	Leu β3	N	2.88
H3	Thr α39	N	Gln (+) α46	OE1	2.93
H4	Trp α40	NE1	Leu (+) α45	O	3.02
H5	fMet α1	OT	His β12	ND1	2.92

Table 6.4: Hydrogen bonding between the apoproteins of the B800-820 LH complex.

(+) indicates the proceeding protein chain anticlockwise around the membrane normal.

B800-850 LH complex is present as Ser in the B800-820 LH complex (see Figure 6.6).

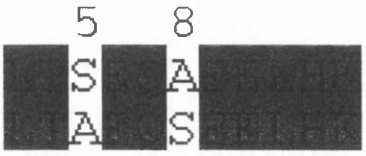

Figure 6.6: The N-termini of the β-apoproteins highlighting a complimentary change in residues at positions 5 and 8.

It is this residue which forms a H-bond H1 with Lys α5 resulting in H1 of the B800-820 LH complex. The reason for the difference in the H-bonding pattern at the N-terminal end of the complexes is unclear. However, Ala β5 of the B800-850 LH complex is reported to insert into the hydrophobic section of the membrane, along with the alternate residues Leu β3 and Ala β1[1]. This is not the case for the B800-820 LH complex, where the corresponding residues Ser, Glu and Leu, respectively. The β-chain of the B800-820 LH complex is one residue longer than the analogous chain in the B800-850 LH complex and in this complex the hydrophobic residues Ala β0, Val β2 and Leu β3 are instead inserted into the membrane. It appears that β5 in the B800-820 LH complex is not required to insert into the membrane because of the extra residue and is therefore used to form a H-bond with an adjacent apoprotein.

Bonds H2 and H3 are found between identical residues in both complexes and for the formation of H4 the residues at position 45 on the α-apoprotein are different. However, the H4 bonds themselves are very similar because they are formed between NE1 of Trp α40 to the main chain oxygen on α45.

H-bond H5 in the B800-850 LH complex is absent in the B800-820 LH complex and no analogous bond was found in this region of the structure. This bond is broken because Tyr α44 is replaced by Phe α44, removing the OH group which was involved in bonding. However, an extra H-bond was found at through the C-terminal oxygen of the α-apoprotein of the B800-820 LH complex and although this bond was not reported for the B800-850 LH complex, the residue which contribute to this bond are identical and their positions very similar. Consequently, this bond would also be expected in the B800-850 LH complex.

In the B800-850 LH complex residues Tyr α44 and Trp α45 (involved in H-bonds no. 4

and 5) are also involved in B850 coordination and are thought to be important in regulating the spectroscopic properties of the complexes (see Section 6.4.2). Therefore, the change in residue type at the N-terminal end of the complex appears to be functional rather than structural, whereas the changes observed at the C-termini of the complexes are slightly more difficult to account for.

6.3 The individual protomer

The crystallographic asymmetric unit comprises one third of the entire complex and contains three individual protomer units. Each protomer unit can be described as the unique portion of the molecule upon which the application of three-fold non-crystallographic symmetry (NCS) generates the asymmetric unit. Application of the crystallographic three-fold to the asymmetric unit then generates entire nonamer. Figure 6.7 shows the nonameric assembly with the asymmetric unit highlighted.

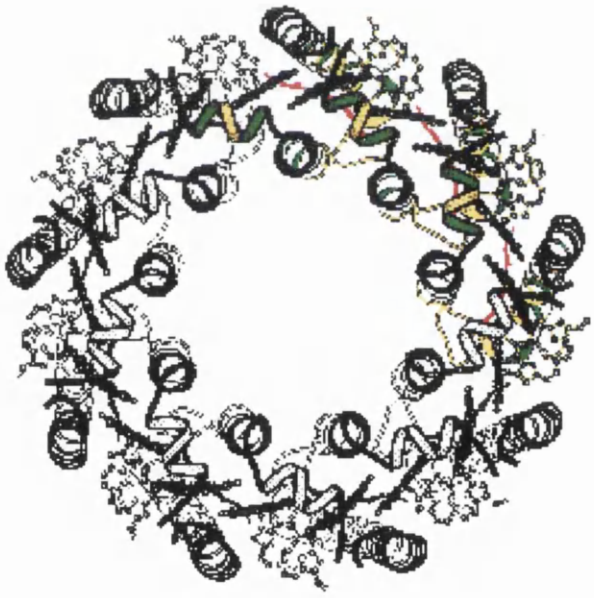

Figure 6.7: The highlighted asymmetric unit of the entire nonomer.
Diagram courtesy of Dr. Stephen Prince

Each protomer unit consists of an α- and a β-apoprotein, two B820 molecules, one B800 molecule and the carotenoid rhodopinal glucoside. The choice of protomer is arbitrary and is not

in any way correlated to the photosynthetic function of the molecule. Overlaying the apoproteins from the B800-820 complex with those from the B800-850 LH complex gives an idea of the structural similarity between the two protomers (see Figure 6.8).

The most obvious difference between the two protomers is the shift in the αB820 phytyl chain and this is discussed in Section 6.3.3.

6.3.1 The protomer apoproteins

As described previously, the principal structure in both the α- and β-apoproteins is a long α-helical domain, which is assumed to span the cell membrane[17]. The helical components of both apoproteins from the B800-820 LH complex are summarised in Table 6.5 and a comparative table showing the helices from the B800-850 LH complex is shown in Table 6.6.

Helix no.	Residues	Helix Type	Length (Å)	Sequence
1	α6 - α9	α	6.70	**IWTV**
2	α12 - α36	α	37.28	**PAFGLPLMLGAVAIT ALLVHAAVLT**
3	α40 - α46	α	10.54	**WYAAFLQ**
4	β6 - β37	α	46.80	**SEQAEELHKHVIDGTRVFL**VIAAIAHFLAFTL

Table 6.5: Helical components of the α and β (Helix 4) apoproteins from the B800-820 LH complex. The residues conserved in both complexes are **highlighted**

Secondary structural elements generated by PROMOTIF.[132]

Helix no.	Residues	Helix Type	Length (Å)	Sequence
1	α4 - α8	3_{10}	10.04	**GKIWT**
2	α12 - α36	α	37.21	**PAIGIPALLGSVTVIAILVHLAILS**
3	α40 - α46	α	10.38	**WFPAYWQ**
4	β6 - β37	α	47.02	**AEQSEELHKYVIDGTRVFL**GLALVAHFLAFSA

Table 6.6: Helical components of the α- and β- (Helix 4) apoproteins from the B800-850 LH complex. *Data taken from McDermott 97.*[96]

The α- and β-apoproteins from the B800-820 LH complex adopt an almost identical conformation to the apoproteins from the B800-850 LH complex (see Figure 6.8) and the structural

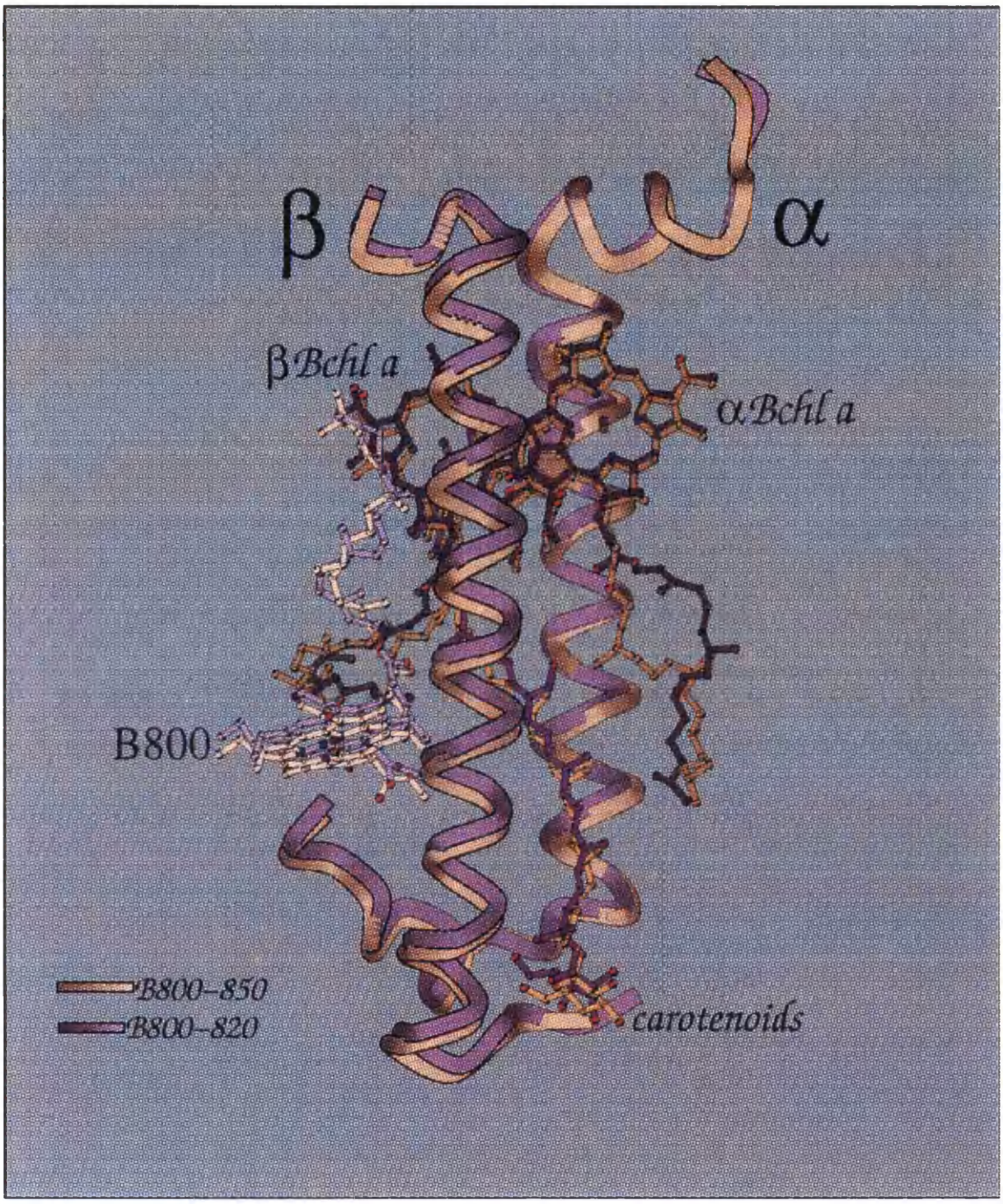

Figure 6.8: Comparison of the protomer of the B800-820 LH complex with that of the B800-850 LH complex.

similarity can be attributed to similarity in the primary sequences of analogous apoproteins. On the β-subunit of both complexes, the N-terminal end of the helical domain is stabilised by an interaction between βThr4 and βGlu7 and this helix ends when it is disrupted at the C-terminus by the sole proline (in both sequences): βPro38.

The secondary structure elements of the α-apoproteins are slightly more difficult to define. The first ten residues at the N-terminal end of the α-apoproteins are identical in both complexes. Nevertheless, differences were predicted for the secondary structure and position of the short N-terminal helix. However, very little difference in the conformation or H-bonding pattern of the two helices can be seen.

The H-bonding pattern between residues α3 and α10 is characteristic of a 3_{10} helix, in both complexes (see Table 6.7).

B800-850			B800-820		
Gln3 O	→	Ile6 N	Gln3 O	→	Ile6 N
Gly4 O	→	Thr7 N	Gly4 O	→	-
Lys5 O	→	Thr8 N	Lys5 O	→	Thr8 N
Ile6 O	→	Val9 N & Val10 N	Ile6 O	→	Val9 N & Val10 N

Table 6.7: Hydrogen bonding within the first 10 residues of the α-apoproteins.

The only difference found between the internal H-bonding patterns was the absence of a H-bond from Gly4 O to Thr7 N in the B800-850 LH complex. The reason for this change was that Gly4 moves away from Thr7 N (by ~1.3 Å) to form a H-bond with the Ser residue found at β8 in the B800-820 LH complex (see Section 6.2.2). However, these residues do remain in an orientation suitable for H-bond formation, although the distance between them increases to ~4.3 Å. The φ and ψ angles for each individual residue were also measured and the results are shown in Table 6.8.

From these angles, the only significant differences occur in the ψ angles of Gly4 and the φ angles of Lys5. The pitch of these helices was calculated to be 6.6 in the B800-850 LH complex[96] and 5.8 in the B800-820 LH complex. All three programs, PROMOTIF[132], PROCHECK[129] and WHATIF, predicted the same differences in secondary structure for the α-subunits although and

LH complex	B800-850		B800-820	
Residue	ϕ	ψ	ϕ	ψ
Gly3	-109.4	20.4	-122	23.2
Gly4	-51.8	-20.9	-44.8	-40.8
Lys5	-90.9	11.7	-59.9	-10.2
Ile6	-64.0	-33.1	-48.5	-36.8
Trp7	-73.5	6.6	-76.1	-0.5
Thr8	-91.5	-22.4	-96.2	-13.7
Val9	-106.5	-31.6	-101.9	-30.8
Val10	-108.9	124.1	-120.8	130.2

Table 6.8: The ϕ and ψ angles of the fist ten residues of the α-apoproteins.

all three use the DSSP alogorithm[133]. It is difficult to define exactly why the helices appear to be similar and yet are predicted differently. However, the change in the H-bonding and consequently in the ϕ and ψ angles of residues 3 and 4, respectively, appears to give the helix in the B800-820 a less tightly packed arrangement, which may account for it being defined as an α- over a 3_{10} helix even though the H-bonding is characteristic of the latter.

6.3.2 The carotenoid

The carotenoid composition for *Rps. acidophila* strain 7050 grown at high and low light intensities has been determined previously[101] (Table 6.9).

Light intensity	RalG	RolG	RpG	Ral	R	SP	AHRV	LY
High light	-	-	34.3	-	37.1	2.4	3.9	22.0
Low light	61.2	6.7	1.2	4.7	10.1	1.7	1.7	9.2

Table 6.9: Percentage carotenoid composition for *Rps. acidophila* strain 7050

Figures taken from Gardiner 1992[101]

The major carotenoid found in the B800-820 LH complex from *Rps. acidophila* strain 7050 is therefore rhodopinal glucoside (RpalG) which is an oxidised form of rhodopin glucoside (RpG), the carotenoid in the B800-850 LH complex.

Energy transfer from RpalG to the B820 molecules occurs in around 3 pico seconds[134][i] (ps), whereas the equivalent transfer in the B800-850 LH complex takes approximately 6 ps [19]. The energy transfer mechanism involving carotenoids is one of the least understood energy processes within photosynthetic systems although an increasing number of articles which relate to this topic are now being produced[2, 135]. The absorption spectrum of RpalG is red-shifted with respect to the absorption spectrum of RpG[2] and this, along with closer contact between carotenoid and B820 molecules (as opposed to B850 molecules), was thought to be responsible for the increased speed of transfer between the two sets of pigments.

Despite the slight structural difference in RpalG and RpG, both chromophores adopt an almost identical conformation within the LH complexes (see Figure 6.9).

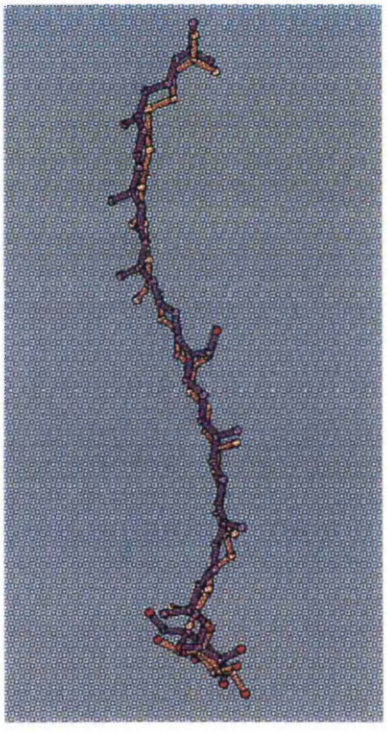

Figure 6.9: The carotenoid from the B800-820 (purple) and the B800-850 LH complexes.

In both structures, the glucoside head group is disordered, despite making a number of contacts within H-bonding distance of charged residues on adjacent helices, which are the only strong

[i] one pico second = 10^{-12} seconds

(< 2.6 Å) H-bonds to the carotenoid molecule in either structure. There was also slight ambiguity in the positioning of the keto group of RpalG which is documented to be on position C13 of the molecule[136]. However, density in the region of C18 suggests that this is also a potential position for this group. There are no possible H-bond contacts (from adjacent apoproteins), at either position which would a imply preference. Unlike the B800-850 LH complex there was no density found for the presence of a detergent molecule or a partial carotenoid.

The only difference observed between the two carotenoids was in the positioning of the residues from C13 to C26, where RpalG deviates from the route taken by RpG by ~1 Å. Comparing the two LH complexes, this shift repositions the carotenoid in the B800-820 LH complex ~0.5 Å closer to the bacteriochlorin ring of βB820 from positions C20 to C26 (see Figure 6.10).

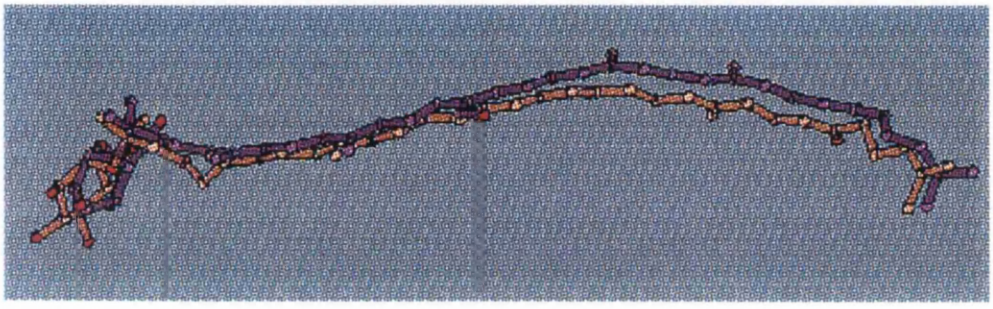

Figure 6.10: The 0.5 Å shift in the positions of the carotenoids, from position C20.
RpalG : Purple; RpG : Yellow

This shift also appears to move the carotenoid slightly closer to the bacteriochlorin head group of the αB850 molecule on the proceeding protomer, although this shift is smaller and consequently more difficult to quantify. The movement in the carotenoid position appears to be correlated to a larger shift observed in the phytyl chain of the proceeding αB850 molecule (see Figure 6.11) (the difference in the phytyl chains can also be seen in Figure 6.8).

Here the carbon at position 8 (C8) on αB820 has moved ~8 Å towards the carotenoid molecules, when compared to the corresponding phytyl chain of αB850. If RpalG had remained in the same position as RpG, the CM6 methyl group would only have been around 1.8 Å away from the methyl group at position C11 on the αB820 molecule. Therefore, the carotenoid has presumably moved to avoid an adverse steric interaction. This would also have been observed for the methyl groups

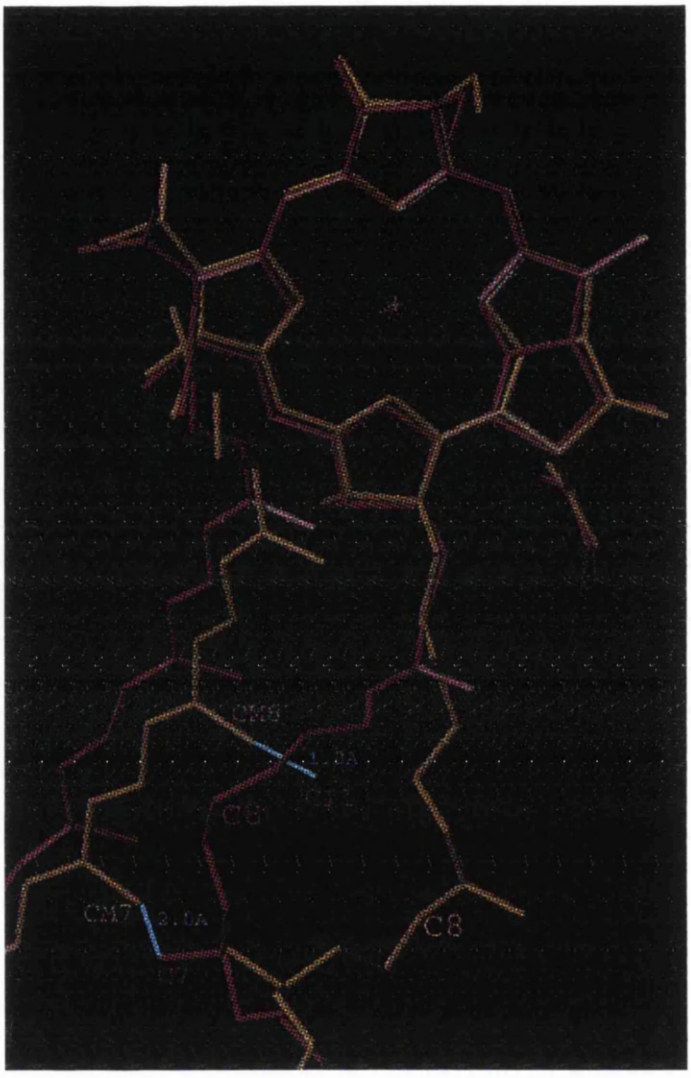

Figure 6.11: Position C8 of the αB820 has moved ~8 Å closer to the carotenoid molecules than αB850.

αB820 : Purple; αB850 : Yellow

at positions CM7 of RpalG and C7 of αB820, where the resulting distance would have been 2.0 Å. For the new position of RpalG the distances between these two sets of methyl groups are 3.6 and 3.3 Å, respectively.

The increased speed of energy transfer between the carotenoid and Bchl *a* molecules was attributed to closer contacts between the two sets of pigments, although it is not obvious from the structure (at current resolution) if closer contacts to the bacteriochlorin rings play a part in this.

6.3.3 The phytyl chains

In the B800-850 LH complex the phytyl chains of the Bchl *a* molecules were found to act as an "unexpected alignment tool" with respect to correctly orientating their transition dipoles for energy transfer[131]. This section briefly describes the differences observed in the positions and conformations of the phytyl chains from each of the three populations of Bchl *a* molecules: B800, αB820 and βB820 of the B800-820 LH complex, with the corresponding chains in the B800-850 LH complex.

In the B800-820 complex the phytyl chain of the B800 molecule follows a very similar route through the membrane as the phytyl chain of the analogous molecule in the B800-850 LH complex. Slight differences are observed as the methyl groups at the base of the chain (position C5) face in opposite directions, and in the B800-820 LH complex the chain extends around 2.5 Åbeyond the terminal position in the analogous molecule. The end of this chain in the B800-820 LH complex rests ~3.5 Åabove the acetyl group on ring A of a βB820 molecule, whereas in the B800-850 LH complex this distance is closer to 5 Å. The reason for these differences is currently unclear, as the hydrophobic chain in both LH complexes does not make any close contacts with any of the other pigments or the side chains on adjacent apoproteins.

The βB820 phytyl chain wraps once around the phytyl chain from an ascending B800 molecule, in the same way that the phytyl chain from the βB850 does in the B800-850 LH complex. In the B800-850 LH complex the tail of the phytyl chain (after phytyl atom C6) passes across the face of the B800 molecule making several contacts. In the B800-820 LH complex this chain again passes across the face of the B800 molecule but the terminal dimethyls do not rest beneath the bacteriochlorin and instead extend beyond this into a position which would have previously been

occupied by the αB850 phytyl chain (see Figure 6.12).

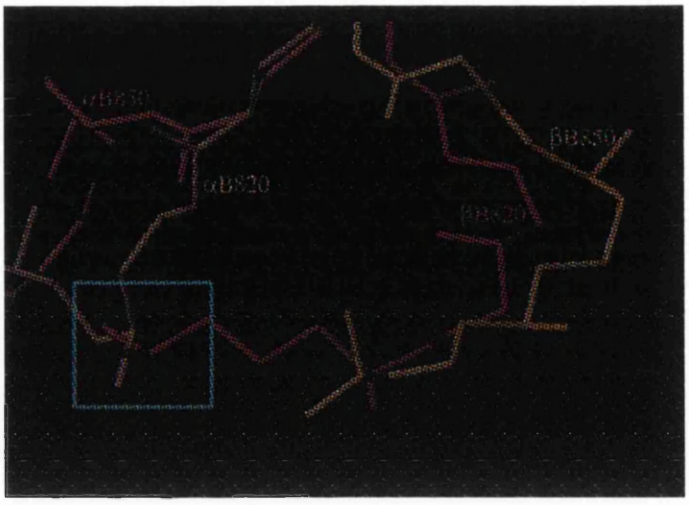

Figure 6.12: The phytyl chains from the B800 and the B820/850 molecules

The B800 chain of the B800-820 LH complex runs into the position that the αB850 chain would occupy

Purple : B800-820 LH complex; Yellow: B800-850 LH complex Yellow

The phytyl chains from the αB850/820 molecules are the most extended of the all the Bchl *a* molecules. As described previously, the movement observed in the phytyl chain of the αB820 molecule was the most prominent change initially observed between the two LH complexes. This chain in the B800-820 LH complex terminates at almost the same position as the equivalent chain in the B800-850 LH complex; making close contacts (< 4 Å) with the ether group on ring E of the B800 molecule. However, it changes the direction that it takes through the membrane as the torsion angles around the bonds between the atoms $C17^2$ and $C17^3$ differ by 100° in the two complexes.

The reason for such a large shift is quite difficult to decipher and there does not appear to be any change in the primary sequences of the apoproteins which is obviously responsible. The only change in the primary sequences which might be involved occurs at positions 26 on the α-apoprotein. Residue Ile α26 in the B800-850 LH complex is present as Thr in the B800-820 LH complex. Replacing the α-subunit with of the B800-850 LH complex with the α-subunit of the B800-820 LH complex reveals steric interactions (~2.3 Å) between atom C4 on the phytyl chain and the methyl group (CG2) of Ile α26 of the B800-820 LH complex. This implies that within

the B800-850 LH complex it would be less energetically favourable for the αB850 phytyl chain to take the position occupied by the αB820 phytyl chain.

Examining the interactions solely between the pigments it would be easy to assume that the shift in the αB820 phytyl could also be attributed to the re-positioning of the βB820 phytyl chain (described above). This chain runs directly into the space previously occupied by the αB850 molecule and consequently the αB820 chain appears to deflect away from this chain (see Figure 6.12) avoiding a collision with the extended βB820 chain. However, the converse could also be true. If the αB820 chain moved prior to the βB820 chain, it could also be possible that this chain extended into the "free" space left by the shift. From the structure there does not appear to be any obvious reason why the βB820 chain extends further than the chain from βB850. It may be advantageous to calculate the energy difference between the conformations of the two phytyl chains from the β- coordinated molecules. Assuming that the βB820 chain was of lower energy it is reasonable to say that it moved into the space vacated by the shift of the αB820 phytyl chain.

6.3.4 Packing of the chromophores

Within the B800-850 LH complex the phytyl chains and the carotenoid molecule intertwined elegantly and the mutual interactions between the molecules suggested that both would contribute to the stability of the overall assembly of the complex[131]. The tightly packed arrangement of the chromophores is best visualised using βB850, B800 and the carotenoid from one protomer, and αB850 from the proceeding protomer anticlockwise around the membrane normal (see Figure 6.13).

From this angle, an analogous set of pigments chosen from the B800-820 LH complex appear to have a similar packing arrangement, although a few small differences can be observed (see Figure 6.14).

Here the small shift in the B800 phytyl chain, where it extends lightly further around the βB820 head group can be observed. The βB820 phytyl chain also extends further than that from the βB850 molecule. Consequently, this chain "hugs" the pigment assembly more tightly by extending beyond the position where the carotenoid sits. This view also shows the large deviation between the phytyl chains of α850 and α820 and the extended conformation of the βB820 phytyl

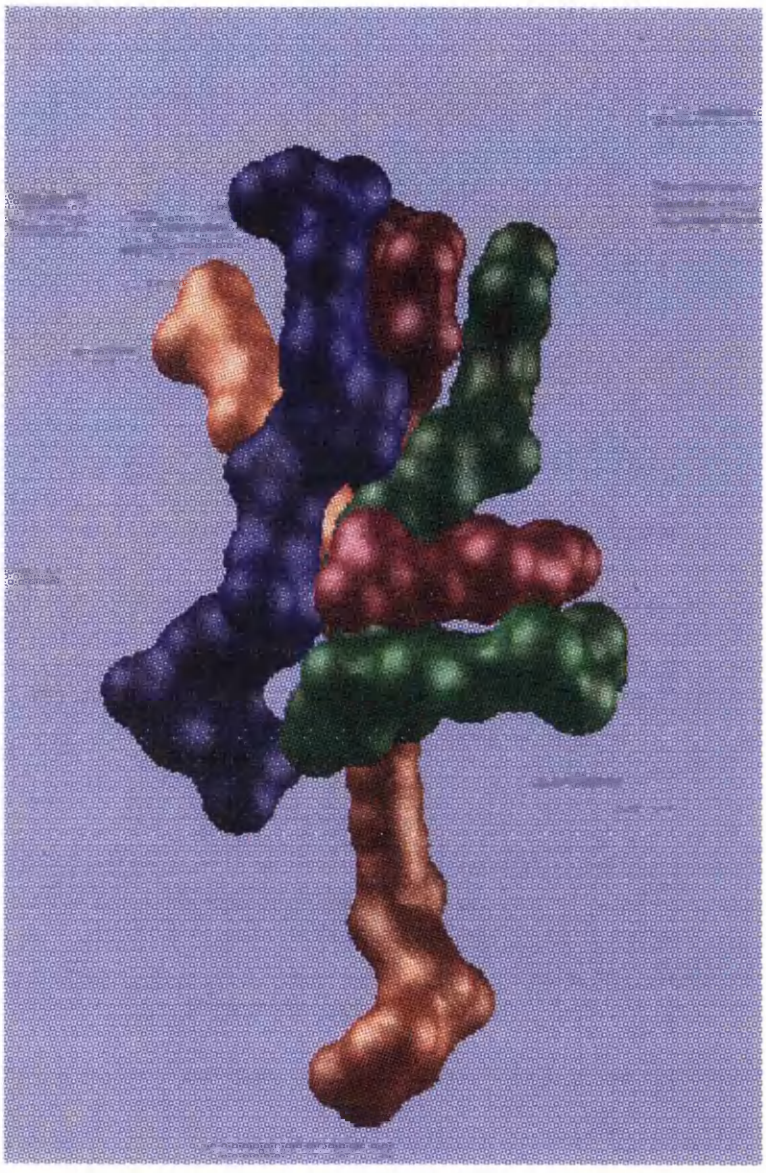

Figure 6.13: The chromophores of the B800-850 LH complex, represented as molecular surfaces BLUE: αB850; RED: βB850; GREEN: B800 and RED: RpG

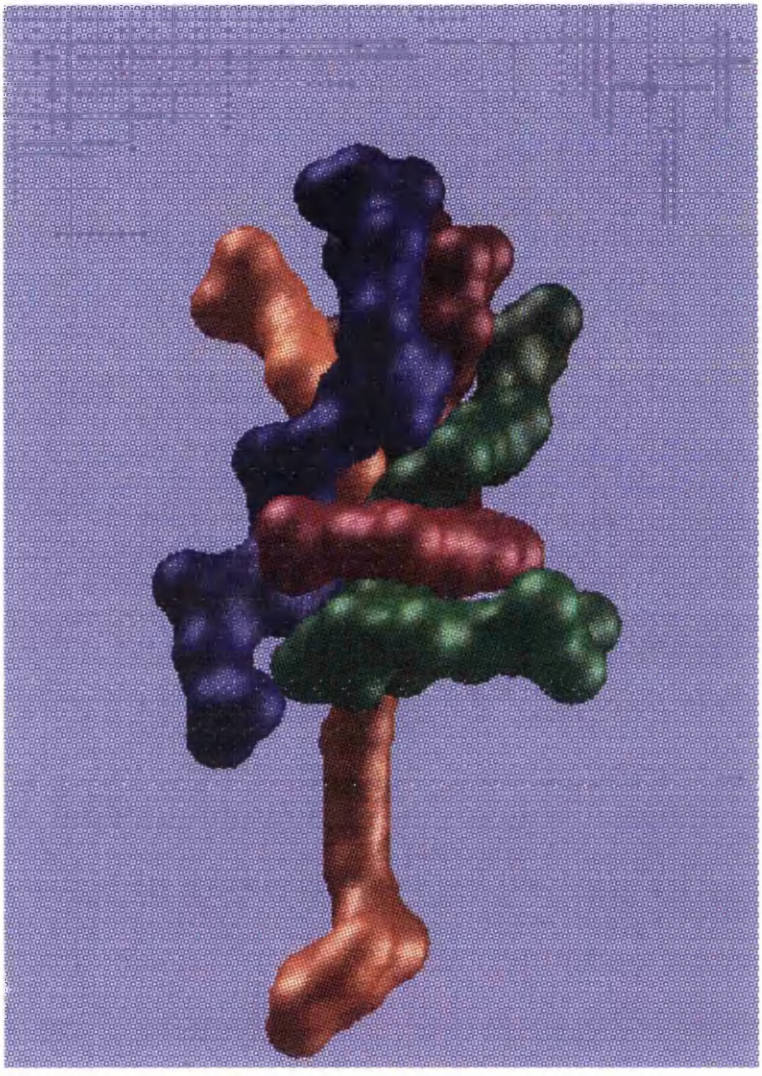

Figure 6.14: The chromophores of the B800-820 LH complex, represented as molecular surfaces.
BLUE: αB820; RED: βB820; GREEN: B800 and RED: RpG

chain into the vacant space.

Flipping the arrangement round by 180°, in order to have the carotenoid molecule at the front of the image, the packing of the Bchl *a* and the carotenoid molecules now be seen (see Figures 6.16 and 6.15).

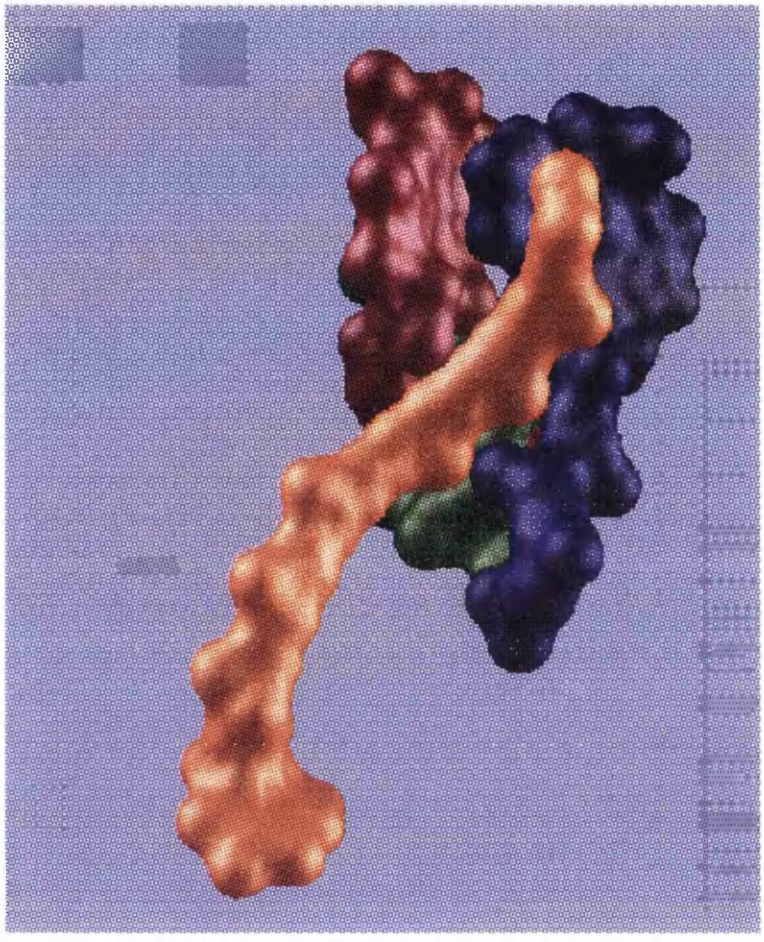

Figure 6.15: The chromophores of the B800-850 LH complex, showing the packing of the Bchl *a* molecules around the carotenoid.

BLUE: αB820; RED: βB820; GREEN: B800 and RED: RpG

From these diagrams, both the βB820 bacteriochlorin ring and the αB820 phytyl chain bind more tightly around the carotenoid than the corresponding chromophores in the B800-850 LH complex. The closer packing of RpalG and the βB820 head group is a consequence only of the

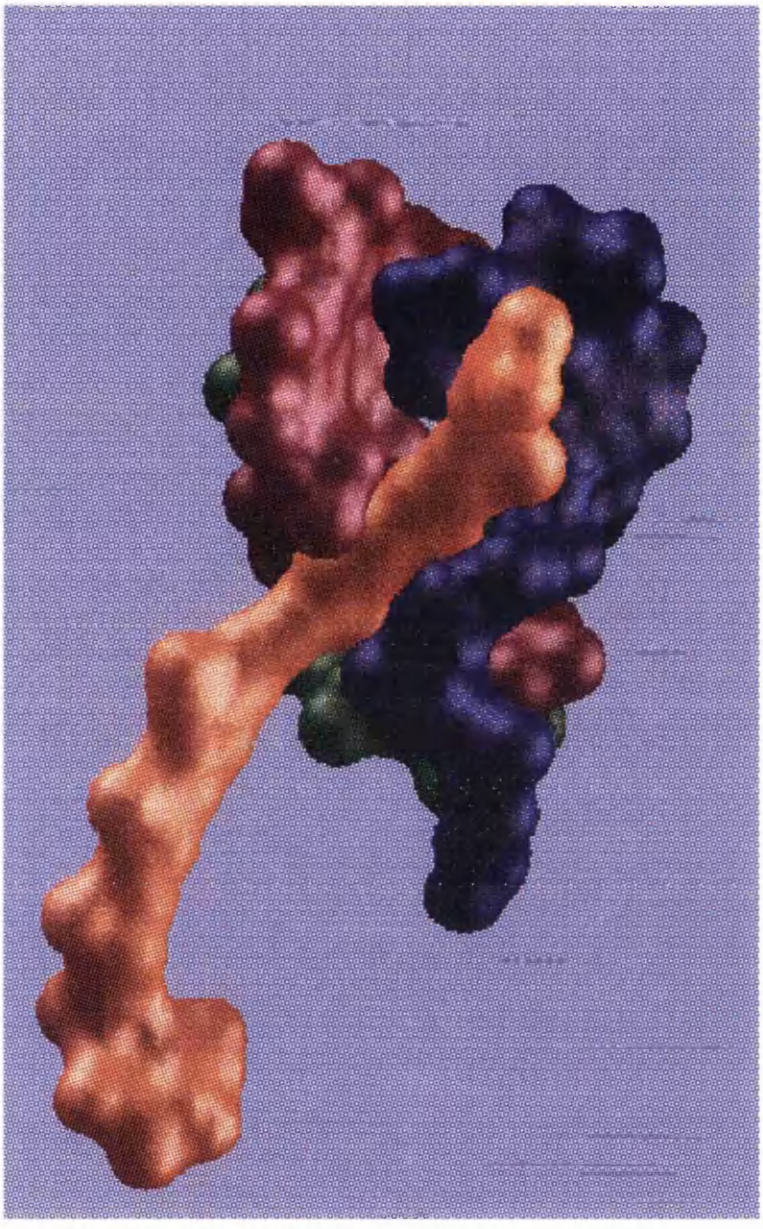

Figure 6.16: The chromophores of the B800-820 LH complex, showing the packing of the Bchl *a* molecules around the carotenoid.

BLUE: αB820; RED: βB820; GREEN: B800 and RED: RpG

$\sim$1 Åshift in the carotenoid itself (as described above), as the position of the bacteriochlorin ring does not change between the two complexes. However, the decrease in the distance between RpalG and the phytyl chain is a consequence of the large shift displayed by the chain itself.

When two or more of the pigment protomers of the B800-850 LH complex are represented by molecular surfaces and placed side by side, there is an obvious hole in the arrangement[131] . This contains Phe β22 which is cradled in a bed of oxygen atoms, from the Bchl *a* molecules and their phytyl chains[131] and can be thought of as acting as a ball in a ball-and-socket joint. In this complex these oxygens are all ether oxygens, either from the ring E ether or the ether oxygen on the phytyl chain itself. This residue is highly conserved throughout all species of purple bacteria[5]. In the B800-820 complex the arrangement is almost identical with the only difference being from αB820. Here, the rotation in the phytyl chain moves the ether group on $C17_3$ away from the Phe, however in its new position the acetyl group takes up an almost identical position at around 3.4 Å.

6.4 Bacteriochlorophyll a molecules

As described previously, the B800-820 LH complex produces a sharper and more efficient light harvesting funnel towards the reaction centre than the B800-850 LH complex. It achieves this by modulating the absorption properties of its chromophores and in particular those of the 850 nm absorbing Bchl *a* molecules; to absorb at 820 nm. In the B800-850 LH complex the local environment of these molecules was shown to be influenced by only a few protein contacts[48]. The reason for the blue shift in the absorption spectrum of these molecules was suggested to be a result of the loss of two H-bonds from Tyr α44 and Tyr α45 to an acetyl group ($O3^1$) of the B850 molecules, along with the strengthening of another to $O13^1$[47] (see Section 1.7.2).

This section describes the local environment of the Bchl *a* molecules of the B800-820 and the B800-850 LH complex; the effects that certain environmental parameters have on the absorption spectra of Bchl *a* molecules; and possible reasons for the spectral blue shift in the B800-820 LH complex.

6.4.1 *The B800 molecules*

The B800 molecules from both LH complexes are coordinated through their central Mg ions to the extended N-terminus of the α apoprotein, assumed to be a formylated methionine residue at α1. The only other H-bond to the molecule is from NE of βArg20 to the acetyl group ($O3^1$) on ring A of the bacteriochlorin and, which is also present in both LH complexes. In the B800-850 LH complex, nine apoprotein contacts (< 4.2 Å) to B800 were found[48] and all of these interacting residues are conserved in the B800-820 LH complex. Hence, the local environment of the B800 molecules was found to be the same in both LH complexes, with the only observed changes residing within the phytyl chains of the molecules.

6.4.2 *The B820 molecules*

The primary interaction between the B850/820 molecules and the apoprotein is the coordination of the central Mg^{2+} through a conserved histidine residue[41]. Additionally, the B850 bacteriochlorin rings also make several other contacts (< 4.2 Å) with the apoproteins. There are a total of 12 protein contacts to αB850 and a further 16 to βB850[48]. The contacting residues of the apoproteins in the B800-850 LH complex were compared to those at equivalent positions on the analogous subunits of the B800-820 LH complex. Five of the residues which formed contacts to αB850 and four which formed contacts to βB820 were found to differ in the B800-820 LH complex. Three of these unconserved residues, Trp α45, Tyr α44 and Ile α34, contact both B850 molecules and in the B800-820 LH complex the residues at the equivalent positions are Leu, Phe and Val, respectively. Additionally, contacts made to αB850 from Phe α41 and Leu β25 are found as Tyr α41 and Ile β25 in the B800-820 LH complex; and Ile α26 which contacts βB850 is Thr in the B800-820 LH complex. Tables 6.10 and 6.11 give details of the variance found in the apoprotein-bacteriochlorin contacts between the two complexes and consequently the differences in their local environments. There are no additional contacts to either αB820 or βB820.

Along with the ligation of the Mg^{2+} to the histidine residues, the only other interactions reported to influence the environment of the B850 molecules were the residues Trp α45 and Tyr α44. Tables 6.10 and 6.11 show that these residues form H-bonds to the C3 acetyl group on ring A ($O3^1$) of the α- and β-coordinated Bchl *a*, respectively. Comparing these interactions with those

Mol.	Atom	Residue	Atom	Dist. (Å)	Mol.	Atom	Residue	Atom	Dist (Å)
αB850	$O3^1$	**Trp α45**	NE1	2.97	αB820	$O3^1$	**Leu α45**	CD2	4.12
αB850	C5	Phe α41	CZ	3.70	αB820	$O3^1$	Tyr α41	OH	2.47
αB850	$C8^1$	**Tyr α44**	CE2	4.00	αB820	$C8^1$	**Phe α44**	CD2	4.07
αB850	$C8^2$	**Ile α34**	CD1	3.98	αB820	$C8^1$	**Val α34**	CG1	3.88
αB850	$C13^4$	Leu β25	CB	3.56	αB820	-	No contact		-

Table 6.10: The contacts made to the α-coordinated Bchl *a* molecules which differ in the two LH complexes.

The **Highlighted** residues also contact the β coordinated molecules (see below).

The αB850 data was taken from Prince et al. 97.[48]

Mol.	Atom	Residue	Atom	Dist. (Å)	Mol.	Atom	Residue	Atom	Dist (Å)
βB850	$C7^1$	**Trp α45**	CD1	3.54	βB820	$C7^1$	**Leu α45**	CD2	3.94
βB850	$O3^1$	**Tyr α44**	OH	2.64	βB820	$C8^1$	**Phe α44**	CZ	3.25
βB850	C10	**Ile α34**	CD1	3.63	βB820	-	No contact		-
βB850	$C13^4$	Ile α26	CG2	4.12	βB820	$C13^3$	Thr α26	OG1	3.5

Table 6.11: The contacts made to the β-coordinated Bchl *a* molecules which differ in the two LH complexes.

The **Highlighted** residues also contact the α coordinated molecules (see above).

The βB850 data was taken from Prince et al. 97.[48]

found in the B820 molecules, it is obvious that these H-bonds no longer exist in the B800-820 LH complex, and it was this loss of H-bonding that was proposed to be primarily responsible for the observed blue-shift in the absorption maxima of the molecules[47] (see Section 1.7.2). However, what was not accounted for was the presence of an additional H-bond to the αB850 molecule from Tyrα41 (Phe in the B800-850 LH complex) to $O3^1$ on αB820. The change in hydrogen bonding patterns to the acetyl groups on ring A of the B850 molecules is shown in Figure 6.17.

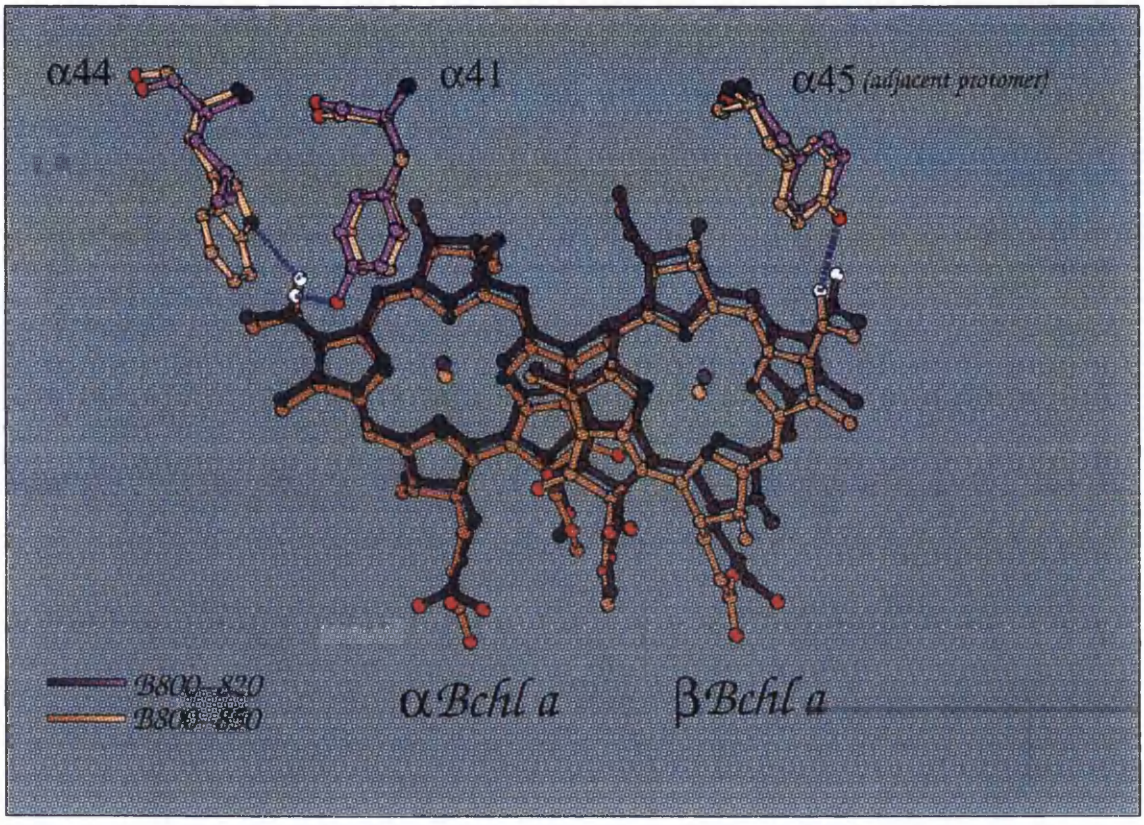

Figure 6.17: Comparison of the H-bonding patterns to the acetyl oxygens (white) from the αBchl *a* and βBchl *a* molecules.

The strengthening of a H-bond to the keto group on ring E ($O13^1$) of the a bacteriochlorin ring was also thought to be (partly) responsible for the change in the absorption spectrum of the B850 molecules[47]. However, in the B800-850 LH complex there are no possible H-bonds to this group on either of the B850 molecules[48]. In the B800-820 LH complex the OG1 of Thr α26 (Ile in the

B800-850 LH complex) lies close to $O13^1$ of βB820. However, these atoms are ~3.8 Å apart and do not have the correct orientation for H-bond formation. Therefore, there are no H-bonds found to any of the Bchl *a* molecules in either complex.

The change in the primary sequence of the complexes at α26 was previously considered a possible reason for the observed shift in the αB820 phytyl chain, whilst the changes observed at positions α34 and β25 do not appear to have any noticeable effect on the system.

6.4.3 Environmental effects on Bchl a

As described previously, the local environment of Bchl *a* affects the absorption range of the molecule. In organic solvents such as acetone, monomeric Bchl *a* absorbs at a wavelength of 772 nm[27]. The major red-shift of the absorption maxima exhibited in the LH complexes is a consequence of their location in the complex. However, inter-pigment geometry cannot fully account for the absorption maxima of these molecules as local environments modify this "ideal" system[137].

The B850 absorption maximum of the B800-850 LH complex from *Rps. acidophila* strain 10050 occurs at 856 nm and the corresponding absorption maxima from the B800-820 LH complex from *Rps. acidophila* strain 7050 is at observed at ~824 nm. The local environment of the Bchl *a* molecules in both of the LH complexes has been described above and there are various parameters known to effect the absorption of these macrocycles. To suggest possible reasons for the differences in the absorption spectra of the two complexes, the effect that altering the local environment of Bchl *a* molecules must also be considered.

Bchl a distortion modes

Bchl *a* is a porphyrin-type molecule and the distortion modes of such molecules are typically well characterised (see Barkigia *et. al.*[138] for a review). The standard conformation of such molecules generally occurs when the molecules are slightly bowed. Distortion of this system generally takes three distinct forms: where the molecule has a saddle-like appearance, a convex bulge, or a planar system. Any distortion of the molecule can affect its absorption characteristics and these modes generally arise from the coordination of axial ligands or peripheral contacts to

the system[139]. Calculations suggest that these distortions can lead to red-shifts in the region of 100 nm in extreme cases[140].

Coordination of all three independent Bchl *a* molecules, in the B800-850 LH complex, occurs through the central Mg^{2+} ions and through the acetyl group of ring A ($O3^1$)[48]. The donor residues for the latter interaction are the residues Trp α45 for α B850, Tyr α44 for βB850, and Arg β20 for the B800 molecule. The βB850 is significantly more distorted with respect to the αB850 and the B800 molecules, and shows a saddle conformation along the long axis of the conjugated double bond system[48]. This long axis is coincident with the Q_y transition dipole which gives rise to the characteristic absorption maxima (~850 nm) and the interaction between βB850 and Tyr α44 was described as being associated with the molecular distortion[48].

In the B800-820 LH complex the coordination of B800, αB820 and βB820 through the central Mg^{2+} ions is the same as found in the B800-850 LH complex. However, for the B820 molecules their coordination through $O3^1$ differs (see Section6.4.2). Overlaying the Bchl *a* molecules in the B800-820 LH complex with those in the B800-850 LH complex the differences in the distortion of the molecules could be estimated. For the two B800 molecules no difference was observed in their conformations. A very slight distortion was observed in the conformations of the the α-coordinated Bchl *a* although this was difficult to quantify. Here, the C10 atoms of both molecules overlay precisely but the C20 atom of the αB820 molecule was elevated ~0.3 Å out of the plane of the head group, with respect to the equivalent atom in αB850. The distortion of βB850 into a saddle conformation appears to be slightly greater in theβB820 molecule, with the atoms of rings A and D being lifted ~0.5 Å out of the plane of the corresponding atoms of βB850 (see Figure 6.18).

This molecule still adopts a similar saddle conformation to that of β850, despite the loss of the interaction between the molecule and Tyr α44 which was reported to be responsible for this distortion[48]. The effect that these slight distortions may have on the absorption maxima of these molecules has not been calculated.

C3 Acetyl group rotation

Rotation of the acetyl group on ring A of the bacteriochlorin ring *i.e.* the torsion angle around the

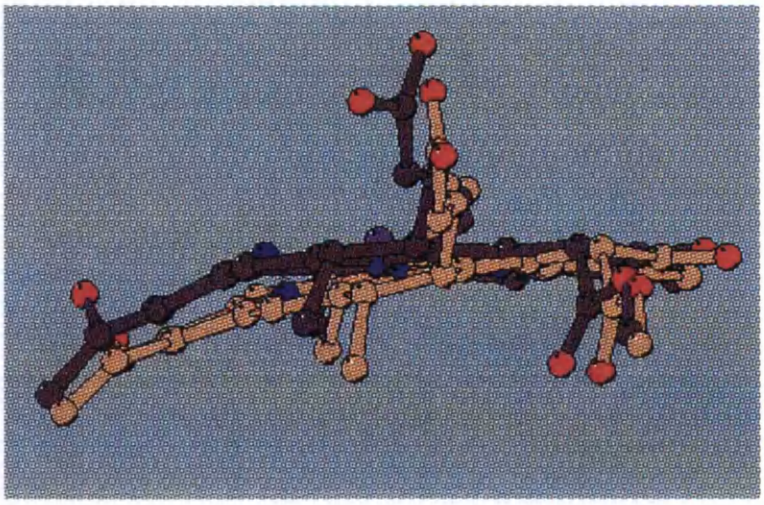

Figure 6.18: A comparison of the βB820 (purple) and βB850 (yellow).

bonds between C3 and $C3^1$, profoundly affects the absorption wavelength of the molecule. The influence of this group depends on its orientation to the ring and blue-shifts of up to 25 nm can be observed as this acetyl group is rotated out of the porphyrin plane[141]. For B850 molecules the acetyl group is effectively co-planar with the bacteriochlorin ring system and moves out of the plane by around 30° in the B800 molecule of this complex. Along with the rotation $O3^1$, the formation of H-bonds to this acetyl group and the keto group on ring E of the bacteriochlorin will also affect the absorption properties of the chromophore[142]. At the absorption wavelengths of the LH complexes red-shifts of around 6 nm for the Q_y transition dipole can occur when the C3 acetyl group ($O3^1$) accepts a H-bond and, the corresponding blue-shifts occur if the $O13^1$ keto group accepts a H-bond. In the B800-850 LH complex all of the acetyl groups accept a H-bond, whilst none of the $C13^1$ keto groups do.

In the B800-820 LH complex two H-bonds to $O3^1$ are broken and another is formed (see Section 6.4). Therefore, the actual loss of the H-bonds would only contribute to a blue-shift of up to 6 nm, whereas the actual blue-shift observed between these two complexes is 32 nm. However, the effect of the new H-bonding pattern on the system is most obvious when the orientation of the C3 acetyl group with respect to the conjugated ring system is considered. In the αB820 molecule

this group is rotated 42° out of the plane (as it turns to form a H-bond with Tyrα41), which is equivalent to a 58° rotation from its adopted position in the B800-850 LH complex (Figure 6.19)

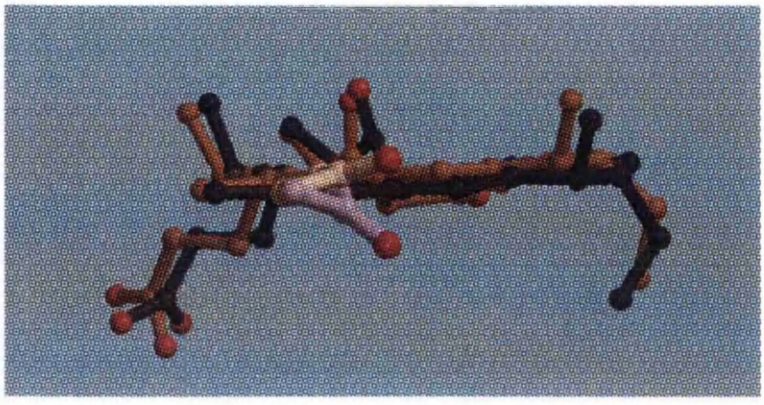

Figure 6.19: A comparison of the movement of the acetyl groups out of the bacteriochlorin plane of αB820 (purple) and αB850 (yellow).

In the βB820 molecule the rotation is 50° out of the plane and this represents a 26° rotation from the equivalent group of the βB850 molecule (Figure 6.20

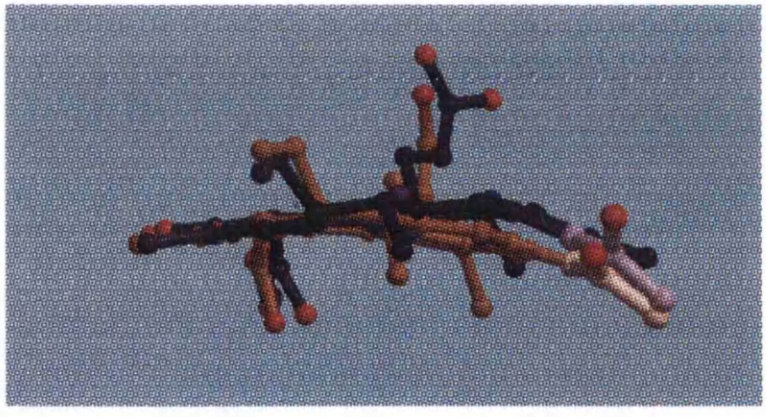

Figure 6.20: A comparison of the movement of the acetyl groups out of the bacteriochlorin plane of βB820 (purple) and βB850 (yellow).

According to a graph published by Nowak-Gudowaska *et al.*[141] the differences in the positions of the acetyl groups could be responsible for blue shifts of ~15 nm and ~10 nm, respectively.

Additionally, an effect similar to this was exhibited within the "special pair" of Bchl *a* molecules in a mutant (RM197) of the reaction centre from *Rhodobacter sphaeroides*[143]. Here the acetyl group within RM197 is rotated 20° with respect to its position in the wild type complex (Figure 6.21) and the absorption maximum of the molecule is blue-shifted by 15 nm.

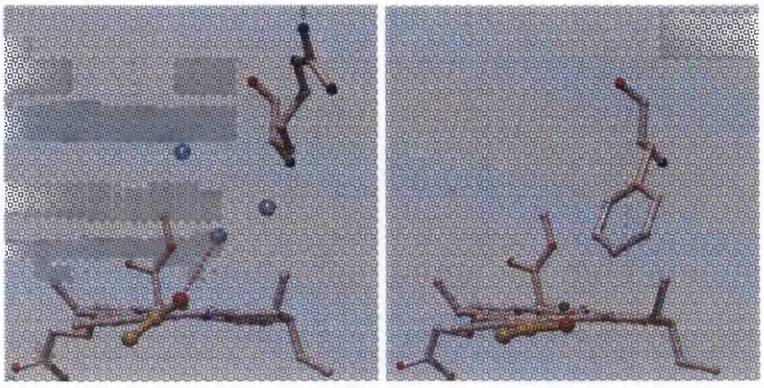

Figure 6.21: Bchl *a* molecules from RM197 (left) and wild type (right) reaction centre from *Rb. Sphaeroides*

Diagram courtesy of Dr. K. E. McAuley-Hecht

Polar species

Molecular orbital calculations have shown that point charges placed 3.5 Åaway from rings A and C on the bacteriochlorin can produce Q_y absorption shifts of the order of $\pm$100 nm depending on the position and polarity of the charge[142]. The optimal point charge orientation occurs when the group lies perpendicular to the plane of either ring A or ring C. In the B800-850 LH complex no such point charge is encountered with either of these rings for any of the Bchl *a* molecules and this is also the case in the B800-820 LH complex.

6.5 Conclusion

Overall, the two complexes described in this chapter are structurally very similar although the B800-820 LH complex is functionally more efficient than its counterpart. The differences found between the complexes are subtle and give an insight into the role that the protein plays in mod-

ulating the characteristics of this light harvesting system. From the comparisons made in this chapter, it may be fair to say that the conserved regions in the primary sequences of the two complexes have significant structural relevance; contributing to the secondary structure, pigment coordination, pigment arrangement and the oligomeric state of the complex.

It seems that several residues which are unconserved between the structures are indirectly responsible for the closer packing of the chromophores and the differences observed in their absorption spectra, thus allowing the bacteria to survive in extreme conditions *i.e.* when very little light is availible to them. The reason for the spectral blue-shift observed in the B800-820 LH complex is not a direct result of the breakage of the two predicted H-bonds to the $C13_1$ acetyl group[47]. Instead, it appears to be a secondary effect of the change in the H-bonding patterns to these groups, where $O13_1$ rotates out of the plane of the bacteriochlorin and the distortion modes of the molecules are affected.

The absorption maxima of the monomeric B800 molecules in the B800-850 LH complex is at the same position in the B800-820 LH complex ($\sim$804 nm) and comparing the B800-protein interactions within the two LH complexes, this appears to cohere.

7. EPILOGUE

The work contained in this thesis is relevant to the fields of membrane protein crystallogenisis and photosynthesis. Purification of the B800-850 LH complex from *Rps. acidophila* strain 10050 suggested that an increase in the reproducibility and quality of diffraction from crystals was a result of purifying the complex by methods based on charge rather than size[1]. While this was not found to be the case with the B800-820 LH complex from *Rps. acidophila* strain 7050, the work described in this thesis does emphasise the importance of an adequate purification protocol when working with membrane proteins, as neither this complex or the B800-820 LH complex from *Rps. cryptolactis* produced crystals until a method for monitoring the homogeneity of the complex was introduced.

The structure of the B800-820 LH complex reveals some of the finer details of the light harvesting system in photosynthetic bacteria and will eventually allow the interpretation of a large body of existing spectroscopic data, for which a high resolution structure is required. The reason for the observed spectroscopic shifts between the B800-820 and the B800-850 LH complexes can be attributed to differences in the apoproteins, which have secondary effects on the local environment, and certain conformational aspects of the bacteriochlorophyll molecules. The closer packing of the pigments and the increased efficiency of the energy transfer between them also appears to be a result of a change in the primary sequences of the apoproteins.

Although 2.0Ådata from crystals of the B800-850 LH complex from *Rps. acidophila* strain 10050 is now available[100], higher resolution data from the B800-820 LH complex will be required for a complete comparison of the more subtle diffrences between the complexes. However, the work contained in this thesis does begin to show the role that the protein plays in modulating the characteristics of the light harvesting system.

APPENDIX

A. GROWTH OF *RPS. CRYPTOLACTIS*

This is a summary of observations made when attempting to produce cells of *Rps. cryptolactis* which synthesised the B800-820 LH complex. This summary is a mixture of personal experience and information given to me by Dr. Anna Lawless (personal communication) who has worked extensively with photosynthetic bacteria for a number of years. The following points apply to both the B800-850 and the B800-820 complexes unless otherwise specified.

- *Rps. cryptolactis* does not grow above 46°C or below 36°C. The most effective temperatures were found to be 42°C for the growth of cells containing the B800-850 LH complex and 38°C for the cells whic produced a B800-820 LH complex.

- The temperature should remain consistent through out cell growth as changing the temperature during cell growth was found to be detrimental to the production of a homogeneous complex.

- The composition of growth media is an important parameter that should be considered, both for effective cell growth and for the production of a homogeneous complex. It appears that variations in the media, especially in the carbon source, can dramatically effect the cell growth.

- The amount of bacteria used to inoculate fresh media should be around 3 parts media to 1 part grown cells; anything less causes the cells to loose their colour and die. This is contrary to what is known for other species of purple bacteria, *e.g.*, *Rps. acidophila.*

- Growing the cells at HL conditions and then down-shifting the cells to the optimal low light intensity was the only way found to produce the stable growth of the B800-820 complex.

B. MASS SPECTROMETRY RESULTS FROM *RPS. CRYPTOLACTIS*

The primary sequence of the apoproteins of the light harvesting complexes from *Rps. cryptolactis* have not been determined. However, mass spectrometry was used to determine the number and molecular weight (MW) of the apoproteins present in the sample. Mass spectrometry was carried out using a MALDI (Matrix Assisted Laser Desorption Ionization) mass spectrometer at Arizona State University (MAr) and the Aberdeen University (MAab) and an electrospray mass spectrometer at Strathclyde University (EMs). Several purified forms of the B800-850 and the B800-820 LH complexes were analysed and the results obtained are given in Table B.1.

LH Complex	MW	MW	MW	MW	MW	Machine
B800-820 (A)	5255.8	**5348.8**	5468.6	**6508.9**	**6665.4**	MAr
B800-820 (B)	5256.6	**5349.9**	5470.2	**6507.4**	**6664.4**	MAr
B800-820 (C)	5256.8	5352.3	-	**6513.8**	**6670.1**	MAab
B800-820 (D)	5255.7	5348.0	-	**6512.9**	**6670.6**	MAab
B800-820 (E)	5256.8	5352.3	-	6513.8	6670.1	MAab
B800-850 (A)	**5163.4**	**5536.1**	5599.6	-	-	EMs
B800-850 (B)	**5163.8**	**5536.8**	5600.1	-	-	EMs
B800-850 (C)	**5177.0**	-	**5614.8**	5657.6	-	MAab
B800-850 (D)	**5163.1**	-	**5601.6**	-	-	MAab

Table B.1: Mass spectrometry results from different sources

The two largest peaks from a run are highlighted in **bold**.

MW = molecular weight in Daltons (D)

From these preliminary results it appears that both complexes contain multiple polypeptides. However, there does not seem to be any overlapping of the molecular weights suggesting that there was no cross contamination in the purified complexes.

C. AMINO ACID SYMBOLS

ALA	Alanine	A
ARG	Arginine	R
ASN	Asparagine	N
ASP	Aspartic Acid	D
CYS	Cystine	C
GLN	Glutamine	Q
GLU	Glutamic Acid	E
GLY	Glycine	G
HIS	Histidine	H
ILE	Isoleucine	I
LEU	Leucine	L
LYS	Lysine	K
MET	Methionine	M
PHE	Phenylalanine	F
PRO	Proline	P
SER	Serine	S
THR	Threonine	T
TRP	Tryptophan	W
TYR	Tyrosine	Y
VAL	Valine	V

Table C.1:

References

1. McDermott, G. *et al. Nature* **374**, 517–521 (1995).

2. van Grondelle, R. V., Dekker, J. P., Gilbro, T. & Sdstrom, V. *Biochimica et Biophysica Acta* **1187**, 1–65 (1994).

3. Wilmotte, A. in *The molecular biology of the cyanobactria,* (Bryant, D., ed), 1–25. Kluwer Academic, Netherlands (1994).

4. van Neil, C. B. *Advanced Enzymology* **1**, 263–328 (1941).

5. Zuber, H. & Bruinisholz, R. A. in *The Chlorophylls,* (Scheer, H., ed), 493–528. CRC Boca Raton.

6. Whitmarsh, J. & Govindjee. in *Encyclopedia of Applied Physics,* (Immergut, D. E., ed), volume 13, 513–532. VCH Publishers (1995).

7. Imhoff, J. F., Trouper, N. G. & Pfennig, N. *Int. J. Syst* **34**(340-343) (1984).

8. Clayton, R. K. *The photosynthetic bacteria.* Plenum press, (1978).

9. Deisenhofer, J., Epp, O., Miki, K., Huber, R. & Michel, H. *Nature* **318**, 618–624 (1985).

10. Deisenhofer, J. & Michel, H. *EMBO Journal* **8**(8), 2149–2170 (1989).

11. Clayton, R. K. & Haselkorn, R. *Journal of molecular biology* **68**, 97–105 (1972).

12. Chory, J., Donohue, T. J., Varga, A. R., Staehelin, L. A. & Kaplan, S. *Journal of Bacteriology* **159**(2), 540–554 (1984).

13. Deisenhofer, J. & Michel, H. *EMBO Journal* **8**, 2149–2169 (1989).

14. Zuber, H. & Cogdell, R. J. in *Anoxygenic Photosynthetic bacteria,* (Blankenship, R. E., Madigan, M. T. & Bauer, C. E., eds), volume 2. Kluwer Academic, Netherlands (1995).

15. Zuber, H. 233. (1987).

16. Guthrie, N. *et al. Journal of Molecular Biology* **224**, 527–528 (1992).

17. Zuber, H. *TiBS* **11**, 414–419 (1986).

18. Cogdell, R. J. & Scheer, H. *Photochemistry and Photobiology* **42**(669-678) (1985).

19. Wasielewski, M. R., Liddell, P. A., Barrett, P., Moore, T. A. & Gust, D. *Nature* **332**, 570–574 (1986).

20. Foote, C. S. *Science* **162**(963-970) (1968).

21. Foote, C. S. *Acc. Chem. Res.* **1**(104-110) (1968).

22. Griffiths, M., Sistrom, W. R., Cohen-Bazire, G. & Stainer, R. Y. *Nature* **176**, 1211–1214 (1955).

23. Cogdell, R. J. & Hawthornethwaite, A. M. *The Photosynthetic Reaction Center*, volume 1, chapter 2, 23–42. Academic Press, London. (1993).

24. Lang, H. P. & Hunter, C. N. *Biochemical Journal* **298**, 197–205 (1994).

25. Aagaard, J. & Sistrom, W. R. *Photochemistry and photobiology* **15**, 209–225 (1972).

26. Angerhofer, A., Cogdell, R. J. & Hipkins, M. F. *Biochimica et Biophysica Acta* **848**, 333–341 (1986).

27. Weigl, J. W. *Journal of American Chemical society* **75**, 999–1000 (1953).

28. Clayton, R. K. in *Bacterial photosythesis,* (Gest, H., Pietro, A. S. & Vermon, L. P., eds), 495–500. Antioch Press, Ohio (1963).

29. Hawthornthwaite, A. M. & Cogdell, R. J. in *The Chlorophylls,* (Scheer, H., ed), 493–528. CRC, Boca Raton.

30. Koepke, J., Hu, X., Muenke, C., Schulten, K. & Michel, H. *Structure* **4**, 581–597 (1996).

31. Cogdell, R. J. *et al. Photosynthesis Research* **48**, 55–63 (1996).

32. Papiz, M. Z. *et al. Trends in Plant Science* **1**, 198–206 (1996).

33. Hu, X. C., Ritz, T., A, D. & Schulten, K. *Journal of Physical Chemistry* **101**(19), 3854–3871 (1997).

34. Miller, K. R. *Nature* **300**, 53–55 (1982).

35. Stark, W. *EMBO Journal* **3**, 777–783 (1984).

36. Ghosh, R., Hauser, H. & Bachofen, R. *Biochemistry* **27**, 1004–1014 (1988).

37. Karrasch, S., Bullough, P. A. & Ghosh, R. *The EMBO Journal* **14**, 631–638 (1995).

38. Walz, T. & Ghosh, R. *Journal of molecular biology* **265**, 107–111 (1997).

39. Pullerits, T. & Sundstrom, V. *Accounts of Chemical Research* **29**(8), 381–389 (1996).

40. Allen, J. P., Feher, G., Yeates, T. O., Komiya, H. & Rees, D. C. *Proceedings of the National Academy of Science (USA)* **84**(17), 6162–6166 (1987).

41. Robert, B. & Lutz, M. *Biochimica et Biophysica Acta* **807**, 10–23 (1985).

42. Kramer, H. *et al. Biochimica et Biophysica Acta* **1231**, 33–40 (1995).

43. Deinum, G. *et al. Biochimica et Biophysica Acta* **1060**, 125–131 (1991).

44. Cogdell, R. J. *et al.* in *Molecular Biology od Membrane-Bound Complexes in Phototropic Bacteria,* (Drews, G. & Dawes, E. A., eds). Plenum Press, New York (1990).

45. Brunisholtz, R. A. & Zuber, H. 103–114. Walter de Gruyter and Co, New York (1988).

46. Fowler, G. J. S., Visschers, R. W., Greif, G. G., van Grondelle, R. & Hunter, C. N. *Nature* **355**(848-850), 848–850 (1992).

47. Fowler, G. J. S., Sockalingum, G. D., Robert, B. & Hunter, C. N. *Journal of Biochemistry* **299**, 695–700 (1994).

48. Prince, S. M. *et al. Journal of molecular biology* **268**, 1–12 (1997).

49. Garavito, R. M. & Rosenbush, J. P. *Journal of cell biology* **86**, 327 (1980).

50. Michel, H. & Oesterhelt, D. *Proceedings of the National Academy of Science (USA)* **81**, 6014–6018 (1980).

51. McPherson, A. *Preparation and Analysis of Protein Crystals.* Wiley, New York., (1982).

52. Garavito, R. M. & Picot, D. *Methods: A companion to Methods in Enzymology* **1**, 57–69 (1990).

53. Iawata, S., Ostermeir, C., Ludwig, B. & Michel, H. *Nature* **376**, 660–669 (1995).

54. Tsukihara, T. *et al. Science* **269**(5227), 1069–1074 (1995).

55. Song, L. Z. *et al. Science* **274**(5294), 1859–1866 (1996).

56. Landau, E. M. & Rosenbusch, J. P. *Proceedings of the National Academy of Science (USA)* **93**, 14532–14535 (1996).

57. Doyle, D. A. *et al. Science* **280**(5360), 69–77 (1998).

58. Singer, S. J. & Nicholson, G. L. *Science 175* **175**, 720–731 (1972).

59. Hjelmeland, L. M. *Methods in Enzymology* **182**, 253–264 (1990).

60. Lemaire, B., Bothorel, P. & Roux, D. *Journal of Physical Chemistry* **87**(6), 1023–1028 (1983).

61. Geige, R. & Ducruix, A. *Crystallization of Nucleic Acids and Proteins: A practical approach*, chapter 1, 1–18. IRL Press, Oxford University Press (1992).

62. Rosenberger, F. & Meehan, E. J. *Journal of Crystal Growth* **90**, 74–78 (1988).

63. Boistelle, R. & Astier, J. P. *Journal of crystal growth* **90**(1-3), 14–30 (1988).

64. Feigelson, R. S. *Journal of crystal growth* **90**(1-3), 14–30 (1988).

65. McPherson, A., Malkin, A. J. & Kuznetsov, Y. G. *Structure* **3**, 759–768 (1995).

66. Carter, C. W. *Crystallization of Nucleic Acids and Proteins: A practical approach*, chapter 3, 47–71. IRL Press, Oxford University Press (1992).

67. Reis-Kaut, M. & Ducruix, A. *Crystallization of Nucleic Acids and Proteins: A practical approach*, chapter 9, 195–218. IRL Press, Oxford University Press (1992).

68. McPherson, A. in *Crystallisation of Membrane proteins.,* (Michel, H., ed), 1–52. CRC Press, Boca Raton, Florida (1990).

69. Ducruix, A. & Geige, R. *Crystallization of Nucleic Acids and Proteins: A practical approach*, chapter 4, 73–98. IRL Press, Oxford University Press (1992).

70. Weber, P. C. *Methods in Enzymology* **276**, 13–22 (1997).

71. Popot, J. L. & Saraste, M. *Current Opinion in Structural Biology* **6**(4), 394–402 (1995).

72. Miroux, B. & Walker, J. E. *Journal of Molecular Biology* **260**(3), 289–298 (1996).

73. Varghese, J. N., Laver, W. G. & Coleman, P. M. *Nature* **303**, 35–40 (1983).

74. M., T. *Proceedings of the National Academy of Science (USA)* **81**, 6014–6018 (1984).

75. Henderson, R. & Shotten, D. *Journal of molecular biology* **139**, 99–109 (1980).

76. Nollert, P. Personal communication.

77. Garavito, R. M. & Karlin, A. *Current opinion in Structural Biology* **5**, 489–490 (1995).

78. Michel, H. *Trends in Biochemical Sciences* **8**, 56–59 (1983).

79. Roth, M. *et al. Nature* **340**, 659–662 (1989).

80. Pebay-Peroula, E., Garavito, R. M., Rosenbusch, J. P., Zulaf, M. & Timmins, P. A. *Structure* **3**, 1051–1059 (1995).

81. Ostermeier, C. & Michel, H. *Current Opinion in Structural Biology* **7**(5), 697–701 (1997).

82. Howard, T. D., McAuley-hecht, K. E. & Cogdell, R. J. *Membrane Transport: A Practical Approach*, chapter Crystallization of membrane proteins. Oxford University Press (In Press).

83. Findlay, J. B. C. & Evans, W. H. *Biological membranes - A practical approach.* IRL Press, Oxford, (1987).

84. Michel, H. in *Crystallisation of membrane proteins,* (Michel, H., ed), chapter 3, 89–106. CRC Press, Boca Raton (1991).

85. Hjelmeland, L. M. *Proceedings of the National Academy of Science (USA* **77**, 6368 (1980).

86. Rosenbusch, P. *Biological Chemistry Hoppe-Seyler* **368**(10), 1268 (1987).

87. Zulauf, M. *Crystallisation of membrane proteins*, chapter 2, 73–88. CRC Press, Boca Raton (1991).

88. Garavito, R. M., Markovic-Housley, Z. & Jenkins, J. A. *Journal of crystal growth* **776**, 701–709 (1986).

89. Welte, W. & Wacker, T. in *Crystallization of membrane-proteins,* (Michel, H., ed), volume 5, 107–124. CRC Press, Boca Raton (1991).

90. Wennerstrom, H. & Lindman, B. *Phys. Rep* **52**, 1–86 (1979).

91. Garavito, R. M. in *Crystallisation of Membrane proteins.,* (Michel, H., ed), 89–106. CRC Press, Boca Raton, Florida (1990).

92. Timmins, P. A., Leonard, M., Weltzien, H. U., Wacker, T. & Welte, W. *FEBS Letters* **238**, 361–368 (1988).

93. Thiyagarajan, P. & Tiede, D. M. *Journal of Physical Chemistry* **98**, 10343–10351 (1994).

94. Pfennig, N. *Journal of Bacteriology* **99**, 597–602 (1969).

95. Stadtwald-Demchick, R., Turner, R. F. & Gest, H. *FEBS Microbiology Letters* **71**(117-122) (1990).

96. McDermott, G. *Structural studies on an integral membrane light-harvesting complex.* PhD thesis, University of Glasgow, (1997).

97. McDermott, G. Personal communication.

98. Halloren, E. *et al. Photosynthesis research* **44**(1-2), 149–155 (1995).

99. McLuskey, K., Prince, S. M., Cogdell, R. J. & Isaacs, N. W. *Submitted to Acta Crystallographica D* .

100. Prince, S. M. Personal communication.

101. Gardiner, A. T. *Peripheral antenna complexes from* Rps. acidophila*: Structure, Function and Genetic Manipulation.* PhD thesis, University of Glasgow, (1993).

102. Schindler, P. A., Dorsselaer, A. V. & Falick, A. M. *Analytical Biochemistry* **213**, 256–263 (1993).

103. Papiz, M. Z. *et al. Journal of Molecular Biology* **209**, 833–835 (1989).

104. Guthrie, N. *Characterisation and crystallisation of a bacterial light-harvesting complex.* PhD thesis, University of Glasgow, (1992).

105. Cogdell, R. J. Personal communication.

106. Stryer, L. *Biochemistry.* W. H. Freeman, New York, (1988).

107. Zuber, H. in *Molecular biology of membrane-bound complexes in phototrophic bacteria.,* (Drews, G. & Dawes, E. A., eds), chapter 161-180. Plenum Press New York. (1990).

108. Collaborative Computing Project, Number 4. *Acta Crystallographica D* **50**, 760–763 (1994).

109. Otwinowski, Z. & Minor, W. in *Methods in Enzymology,* (Carter, C. W. & Sweet, R. M., eds), volume 276. Academic Press (1996).

110. Otwinowski, Z. in *Proceedings of the CCP4 Study Weekend January 1992,* (Sawyer, L., Isaacs, N. W. & Bailey, S., eds), 56–62 (Science and Engineering Research Council, Daresbury Laboratory, Warrington, UK, 1992).

111. French, G. S. & Wilson, K. S. *Acta Crystallographica A* **34**, 517–525 (1978).

112. Wilson, A. J. C. *Nature* **150**, 152 (1942).

113. Navaza, J. *Acta Crystallographica A* **46**, 619–620 (1990).

114. Navaza, J. *Acta Crystallographica A* **50**, 157–163 (1994).

115. Kabsch, W. *Acta Crystallographica A* **32**, 522–523 (1976).

116. Driessen, H. *et al. Journal of Applied Crystallography* **22**, 510–516 (1989).

117. Cowtan, K. D. & Main, P. *Acta crystallographica D* **49**, 148–157 (1993).

118. Zhang, K. Y. & Main, P. *Acta crystallogr. A* **46**, 377–381 (1990).

119. K. Cowtan in *Joint CCP4 and ESF-EACBM Newsletter on Protein Crystallography,* **31**, 34 – 38, (1994).

120. Murshudov, G. N., Dodson, E. J. & Vagin, A. A. in *Proceedings of the CCP4 Study Weekend January 1996,* (Dodson, E. J., Sawyer, L., Ralph, A. & Bailey, S., eds), 93–104 (Science and Engineering Research Council, Daresbury Laboratory, Warrington, UK, 1996).

121. Watson, D. G. *Journal of Research of the National Institute of Standards and Technology* **101**(3), 227–229 (1996).

122. Barkigia, K. M., Gottfried, D. S., Boxer, S. G. & Fajer, J. *Journal of American Chemical Society* **111**(16), 6444–6446 (1989).

123. Stocker, A. *et al. Helvetica Chimica Acta* **77**(7), 1721–1737 (1994).

124. Senge, M. O., Hope, H. & Smith, K. M. Private communication, Cambridge Structural Database, (1994).

125. Jeffrey, G. A. & Yeo, Y. *Carbohydrate Research* **237**, 45–52 (1992).

126. Jones, T. A., Cowan, S., Zou, J. Y. & Kjeldgaard, M. *Acta Crystallographica A* **47**, 110–119 (1991).

127. Brunger, A. T. *Nature* **355**, 472–475 (1992).

128. Brunger, A. T. *Acta Crystallographica D* **49**, 24–36 (1993).

129. Laskowski, R. A., MacArthur, M. W., Moss, D. S. & Thorton, J. M. *Journal of Applied Crystallography* (26), 283–291 (1993).

130. Ramakrishnan, C. & Ramachandran, G. N. *Biophysics Journal* **5**, 909 – 933 (1965).

131. Freer, A. A. *et al. Structure* **4**, 449–462 (1996).

132. Hutchinson, E. G. & Thornton, J. M. *Protein Science* **5**(2), 212–220 (1996).

133. Kabsch, W. & Sander, C. *Biopolymers* **22**, 2577–2637 (1893).

134. Gillbro, T., Cogdell, R. J. & Sundstrom, V. *FEBS Lett.* **235**, 169–172 (1988).

135. H. A. Frank, R. J. C. *Photochemistry and Photobiology* **63**(3), 257–264 (1996).

136. Young, A. & Britton, G. *Carotenoids in Photosynthesis*. Chapman and Hall, London, (1993).

137. Sauer, K. *et al. Photochemistry and Photobiology* **64**(3), 564–576 (1996).

138. Barkigia, K. M. & Fajer, J. in *The Photosynthetic reaction centre,* (Deiesenhofer, J. & Norris, J., eds), volume 2, 513–539. Academic Press, New York.

139. Scheidt, W. R. & Lee, Y. J. in *Structure and Bonding,* (Buchler, J. W., ed), volume 64, 1–70. Springer Verlag, Berlin. (1987).

140. Barkigia, K. M., Chantranupong, L., Smith, K. M. & Fajer, J. *Journal of American Chemical Society* **110**, 7566–7567 (1988).

141. Gudowska-Nowak, E. & Fajer, M. D. N. . J. *Journal of Physical Chemistry* **94**, 5795 (1990).

142. Hanson, L. K., Thompson, M. A. & Fajer, J. in *Progress in Photosynthesis Research,* (Biggins, J., ed), 311–314. Martinus Nihoff, Dordrecht (1987).

143. McAuley-Hecht, K. *et al. Biochemistry* **37**, 4740–4750 (1998).